Electronic Thesis and Dissertation Repository

8-10-2017 12:00 AM

Design and Synthesis of Hyaluronan:RHAMM Interaction Inhibitors

Emily Rodrigues
The University of Western Ontario

Supervisor
Dr. Len Luyt
The University of Western Ontario

Graduate Program in Chemistry
A thesis submitted in partial fulfillment of the requirements for the degree in Master of Science
© Emily Rodrigues 2017

Follow this and additional works at: https://ir.lib.uwo.ca/etd

Part of the Organic Chemistry Commons

Recommended Citation

Abstract

A major component of the extracellular matrix is hyaluronan, a regulator cell migration/survival and differentiation during response-to-injury processes. The receptor for hyaluronan-mediated motility (RHAMM) binds to HA and has limited constitutive expression but is upregulated during tissue injury. Blocking HA fragment:RHAMM interactions has therapeutic potential for treating cancer but truncation of RHAMM into peptides mimicking only the HA binding domains is predicted to lose their natural α-helical structure. The goal of this project is to explore the effects cyclizing each binding domain has on helicity and its biological effect. Eighteen peptides were synthesized and cyclized using lactam bridges. The peptides were analyzed by circular dichroism spectroscopy and one stapled peptide exhibited a 4-fold increase in helicity compared to the unstapled sequence and significantly decreased migration, inflammation, and fibrosis *in vitro*. This cyclic peptide is a novel protein-carbohydrate inhibitor and has the potential to be a therapeutic in the cancer treatment.

Keywords

Peptide, cyclization, lactam, alpha helix, receptor for hyaluronan mediated motility, hyaluronan, cancer, surface plasmon resonance, circular dichroism spectroscopy

Co-Authorship Statement

The author completed all synthesis, purification, characterization, CD spectroscopy, and SPR experiments. The peptide stability and trypsin assays were carried out and analyzed by Hilary Groom, a research assistant in the laboratory of Dr. Luyt (Section 2.2.3). The *in vitro* migration, inflammation, and fibrosis assays were carried out and analyzed by Dr. Teresa Peart, a research associate from the laboratory of Dr. Turley (Section 2.2.4).

All sections were written by the author with exception of Section 2.4.8 and 2.4.9 written by Hilary Groom, a research assistant in the laboratory of Dr. Luyt, as well as Section 2.4.10, 2.4.11, and 2.4.12 written by Dr. Teresa Peart, a research associate from the laboratory of Dr. Turley.

Acknowledgments

Table of Contents

List of Tables

List of Figures

List of Schemes

List of Abbreviations

Ac	Acetyl
CD	Circular dichroism
Da	Dalton
DMF	N,N-Dimethylformamide
DMSO	Dimethyl sulfoxide
ECM	Extracellular matrix
ELISA	Enzyme linked immnunosorbent assay
ESI-MS	Electrospray ionization mass spectrometry
Fmoc	9-fluorenylmethoxycarbonyl
GAG	Glycosaminoglycan
GPI	Glycosylphosphatidylinositol
HA	Hyaluronan
HABD	Hyaluronan binding domain
HABD1	First hyaluronan binding domain
HABD2	Second hyaluronan binding domain
HATU	2-(1H-7-azabenzotrial-1-yl)-1,1,33-tetramethyluronium hexafluorophosphate methanaminium
HCTU	O-(1H-6-chlorobenzotriazole-1-yl)-1,1,3,3-tetramethyluronium hexafluorophosphate
HPLC	High-performance liquid chromatography
LSPR	Localized surface plasmon resonance
MBHA	4-methylbenzhydrylamine
MW	Molecular weight
OAll	Allyl ester
PBS	Phosphate buffered saline
PCI	Protein-carbohydrate interaction
RHAMM	Receptor for hyaluronan mediated motility
RNS	Reactive nitrogen species
ROS	Reactive oxygen species
SPPS	Solid-phase peptide synthesis
SPR	Surface plasmon resonance
TBMe	Tertbutyl methyl ether
TFA	Trifluoroacetic acid
TFE	Trifluoroethanol
TIPS	Triisopropylsilane
UHPLC	Ultra-high performace liquid chromatography

Chapter 1

1   Introduction

1.1   Hyaluronan

The extracellular matrix (ECM) is a tissue component that provides structural and biochemical support to neighboring cells and that is constantly undergoing modifications to better suit the needs yof those cells. These changes are not always benign: during cancer metastasis, the regular ECM framework is disrupted and manipulated to facilitate tumor initiation and progression[1,2]. A major component of the ECM is hyaluronan (HA), a glycosaminoglycan (GAG) that contains repeating disaccharide units of N-acetyl-D-glucosamine and D-glucuronic acid (Figure 1.1).
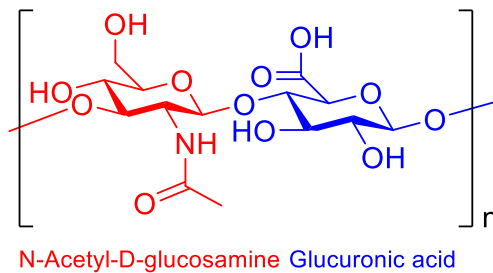
Figure 1.1 - Structure of hyaluronan.

HA has a variety of functions which include the regulation of proliferation, cell motility, and adhesion, all of which are factors in cancer metastasis[3–6]. It is important to note that the functions of HA are highly size-dependent. Native high molecular weight (MW) HA (>500 kDa) has the ability to reduce inflammation. In the case of tissue injury, HA can be fragmented by reactive oxygen and nitrogen species (ROS and RNS, respectively) such as hydroxyl radicals, peroxynitrite, or peroxynitrous acid[7]. HA can also be cleaved by hyaluronidases (Hyals), a family of proteins that are able to cleave the β-1,4-glycosidic bond of HA[8]. When HA fragments, the resulting lower MW HA (e.g. <200 kDa) aids in the promotion of inflammation and migration of cells (Figure 1.2).
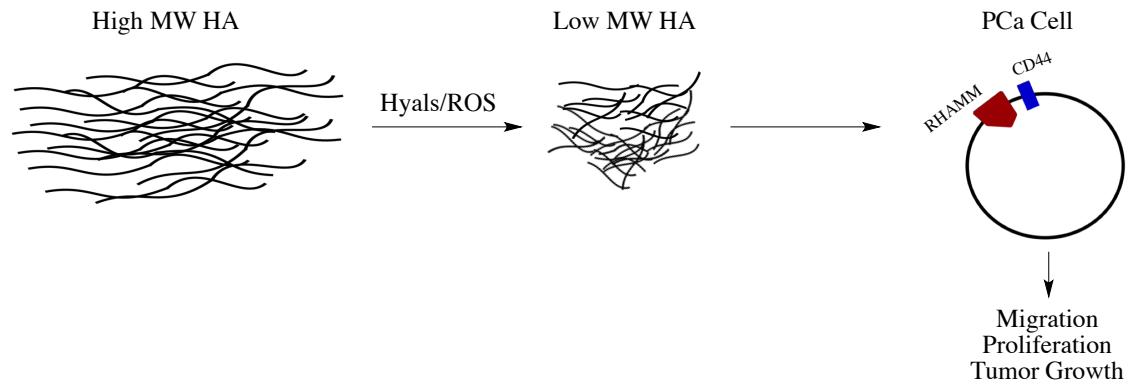
Figure 1.2 - HA can be fragmented by hyaluronidases (Hyals) or reactive oxygen species (ROS) in a tumor. When HA is fragmented, various cellular functions can occur due to interactions with the RHAMM/CD44 complex.

1.2   Receptor for Hyaluronan Mediated Motility (RHAMM)

Like many receptor ligands, HA is known to activate certain receptors, one of which is the receptor for hyaluronan mediated motility (RHAMM). RHAMM can be located on the cell surface as a glycosylphosphatidylinositol (GPI) linked protein, or it can be found internally within the cytoplasm[9]. On the cell surface, RHAMM is able to interact with other cell-surface receptors, such as CD44; this interaction is believed to activate the ERK1/2 MAP kinase pathway[10,11]. When RHAMM is located intracellularly, it acts as a mitotic spindle/centrosomal protein and can affect mitotic spindle integrity[11,12]. RHAMM mRNA expression in adult homeostatic tissue is tightly regulated; expression typically remains very low, but it transiently increases when tissue injury occurs[11]. When there are increased levels of RHAMM expression found in tumors, it is correlated with higher mortality rates [13]. For this reason, blocking the HA fragment:RHAMM interaction has therapeutic potential, as it could interrupt a vital facilitator of metastasis. In prostate cancer (PCa) specifically, elevated levels of RHAMM have been observed, as well as aberrant HA:RHAMM signaling in a metastatic cells line, PC3MLN4[14,15].

RHAMM is a 72 kDa protein that has been shown to be mainly α-helical by 2D nuclear magnetic resonance (NMR)[5]. Yang *et al*. observed that there are two HA binding domains (HABD) in RHAMM, located near the C-terminus of the protein, that are 10 and 11

amino acids in length respectively; these domains are separated by a 15 amino acid leucine zipper (Figure 1.3)[6].

| 518 RDSYAQLLG | 527 HQNLKQKIKH | 537 VVKLKDENSQ | 547 LKKSEVSKLRS | 557 QLVKRKQNEL | 567 RLQGELDKAL |
| CCCCCCCHH | HHHHHHHHHH | HHHHCCCCHH | HHHHHHHHHH | HHHHHHHHHH | HHHCCCEECC |

HABD1   HABD2
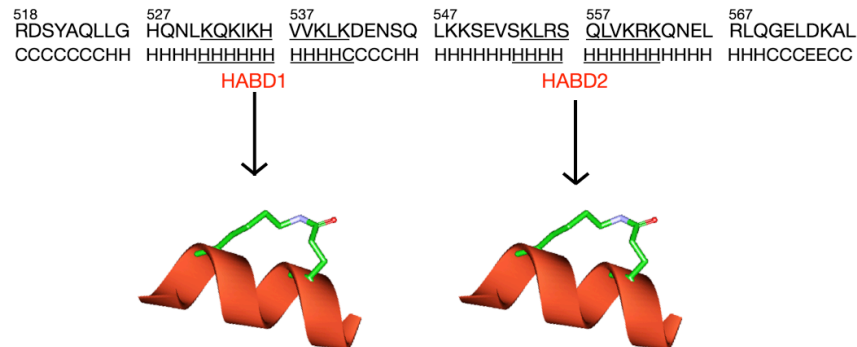
Figure 1.3 - Sequence of the C-terminal RHAMM(518-576) (top line) showing the two binding domains (underlined) and the secondary structure prediction by 2D NMR (bottom line). Depiction of the truncation of the sequence shows that it is possible to obtain a low molecular weight peptide with an α-helical characteristic. H = α-Helix; C = Random coil; E = Extended Coil

The HABDs are within two α-helical portions of RHAMM and have a BX_7B binding motif, where B is a basic residue (such as lysine or arginine) and X is any non-acidic residue (these are generally hydrophobic)[5,6]. The RHAMM HABDs have a positively charged surface due to the abundance of lysine and arginine residues that orient themselves such that they are exposed to solvent when in an α-helical confirmation. The positively charged surface binds through ionic interactions with the negatively charged carboxylate ions present in HA[5]. The regions surrounding the HABDs of RHAMM are thought to extend inward to form a hydrophobic core, which assists in stabilizing the secondary structure[5]; as such, this can contribute to the loss of secondary structure that occurs when the amino acid sequence is truncated to include just one of binding domains.

1.3 Peptides as Drugs

Proteins are stabilized by their natural biological environment and by binding to their endogenous target via one or more small regions in the amino acid sequence of the protein[16]. The biological activity of proteins is dependent on their three-dimensional structure,

including secondary structure, which is in turn governed by their amino acid sequence[16]. The secondary structure of a protein helps align the binding region properly for recognition of a specific ligand.

In drug design, the focus of pharmaceutical development is typically on either small molecules (compounds with a molecular weight less than 500 Da) or on large biologics (compounds with a molecular weight greater than 5000 Da)[17]. With these two classes taking the low and high molecular ranges, peptides fit nicely in between as they typically contain less than 50 amino acids and have molecular weights that fall between these two classes of drugs[17]. They are smaller than their larger protein biologic counterparts, meaning that they are often less expensive and easier to manufacture than biologics while still maintaining similar specificity and potency towards their intended target[17]. However, shortened unbound peptides have a propensity to lose their secondary structure under physiological conditions, mostly due to loss of side-chain interactions such as hydrogen bonding or electrostatic forces. These side-chain interactions facilitate the formation of the secondary structure needed for optimal binding[18,19], as greater affinity is observed when the ligand and receptor are both in their native conformation [16].

There are three main divisions of protein secondary structure: random coil, β-sheet, and α-helix that have been shown to be important for protein-peptide interactions. About 62 percent of protein-protein complexes in the Protein Data Bank include an α-helix interaction; this indicates that helical structures play a major role in mediating many biological processes, including those that involve therapeutic targets[16,19]. The helix-coil transition theory states that there is a high energy requirement needed for organizing three consecutive amino acids in a helical conformation, limiting the formation of helices and potentially the activity of shortened peptides[20]. This energy barrier is thought to be overcome by pre-folding shortened peptides, and would therefore enable truncated peptides to adopt the desired α-helix conformation[21].

1.4   Synthetic Stapling Methods

One additional disadvantage of peptides as therapeutics, is that peptides suffer from protease hydrolysis *in vivo*, and therefore have limited biological stability[16]. To overcome

this problem, strategies such as capping, amidation, and the addition of unnatural amino acids have been used. Another approach is the cyclization of peptides, which results in a constrained structure with limited flexibility and less rotatable bonds. Cyclization increases a peptide's resistance to protease degradation *in vivo,* as the α-helix diameter of the cyclized peptide is too large to fit into protease active sites[16]. Moreover, membrane permeability improves when a molecule has a less polar surface and fewer rotatable bonds. Therefore, cyclic peptides may have an improved ability to move across the epithelial barrier of the gastrointestinal tract, indicating greater potential for oral bioavailability compared to their noncyclic counterparts[17]. Peptide cyclization is a method of pre-folding shortened peptides, as it promotes α-helix formation prior to target binding, and may therefore increase the biological activity of these shortened peptides[19]. Synthesis of cyclic helical peptides does require that the sequence has the natural propensity to fold into an α-helix; without this, cyclization may not force the peptide into the desired conformation[18].

Cyclization can be introduced to a peptide by modifying the side chains of its amino acid residues. α-helical peptides have 3.6 amino acids per turn, which results in residues at positions *i*, *i+4*, and *i+7* occurring on the same face of the helix when the peptide is folded correctly[19]. It is ideal to join *i, i+4/i+7* residues by synthetically introducing covalent bonds, referred to as 'staples', to stabilize the α-helical conformation[22]. To identify the optimal location for a staple, a form of structure-activity relationship study termed a 'staple scan' is performed. This is achieved by introducing a covalent bond between every *i* and *i+4* pair of residues that are not essential for target binding and subsequently evaluating the structure for helicity and biological acitivty[18].

Currently there are four prevalent stapling techniques capable of promoting a helical structure are reported in the literature: a lactam bridge between side chains, a hydrocarbon linker between side chains, a metal-ion clip, or a hydrogen bond surrogate (Figure 1.4)[17,19].
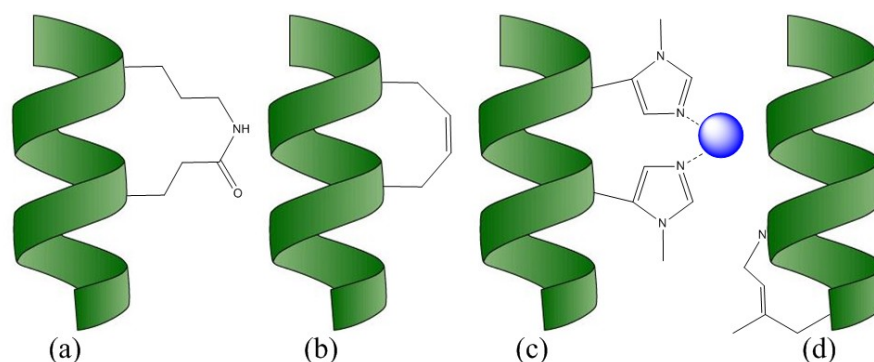
Figure 1.4 - The four methods of constraining a peptide into an α-helix: (a) lactam bridge; (b) hydrocarbon staple; (c) metal-ion clip; (d) hydrogen bond surrogate.

Different stapling strategies have different propensities to induce α-helical effects, as some staples produce peptides are optimally helical in water, while others may require secondary structure stabilizing solvents, such as trifluoroethanol (TFE), to increase the helicity of the peptide for analysis[16]. Hydrocarbon and lactam bridges tend to be more flexible, though this depends on the lengths of the side chain linkers[18]. Shorter staples have been hypothesized to create more rigid and stable helices[22], but ring size in cyclized peptides is also dependent on the sequence and confirmation[23]. In all cases, the linker chain for cyclization should be large enough to overcome ring strain, which in turn will prevent the need for a high activation energy to complete the cyclization[23]. When designing a cyclic peptide, it is imperative to remember that the side chains that are modified to create these linkers can no longer be involved in target recognition, so selection of position and amino acids to be replaced must be carefully considered. Cyclization steps are typically carried out on-resin as opposed to in-solution; this is due to the increased possibility of polymerization or dimerization during in-solution cyclization, as well as time-consuming dilution and purification leading to lower yields[24]. As these peptides are ultimately being designed as therapeutics, we decided to focus on lactam bridge cyclization due to its ease of synthesis and increased stability *in vivo* compared to the other techniques discussed.

1.5 Analysis of α-Helicity

Circular dichroism (CD) spectroscopy is a technique used to analyze the secondary structure of peptides and proteins. The optical technique of CD analyzes the extent to which exposed asymmetric molecules can absorb right and left handed circularly polarized light[25]. The chromophores of the amides in the peptide's primary amino acid sequence causes different excitation interactions that produce different features on the spectra depending on the amides' positioning (Figure 1.5a)[26]. Due to the differences in secondary structure, it has been observed that the CD spectrum for an α-helix is unique compared to those of other secondary structures. For a protein with an α-helix, two negative bands are observed at 222nm and 208nm and one positive band is observed at 193nm, while linear disordered proteins show one negative band around 195nm and shallow maxima at 210nm[25]. However, when comparing α-helical proteins and peptides to linear sequences, it is important to consider that macromolecules are able to adopt varying degrees of each conformation, depending on the environment surrounding each section. This will change the appearance of the CD spectrum, as the absorbance will be a mixture of the conformations present in the peptide or protein (Figure 1.5b)[26].
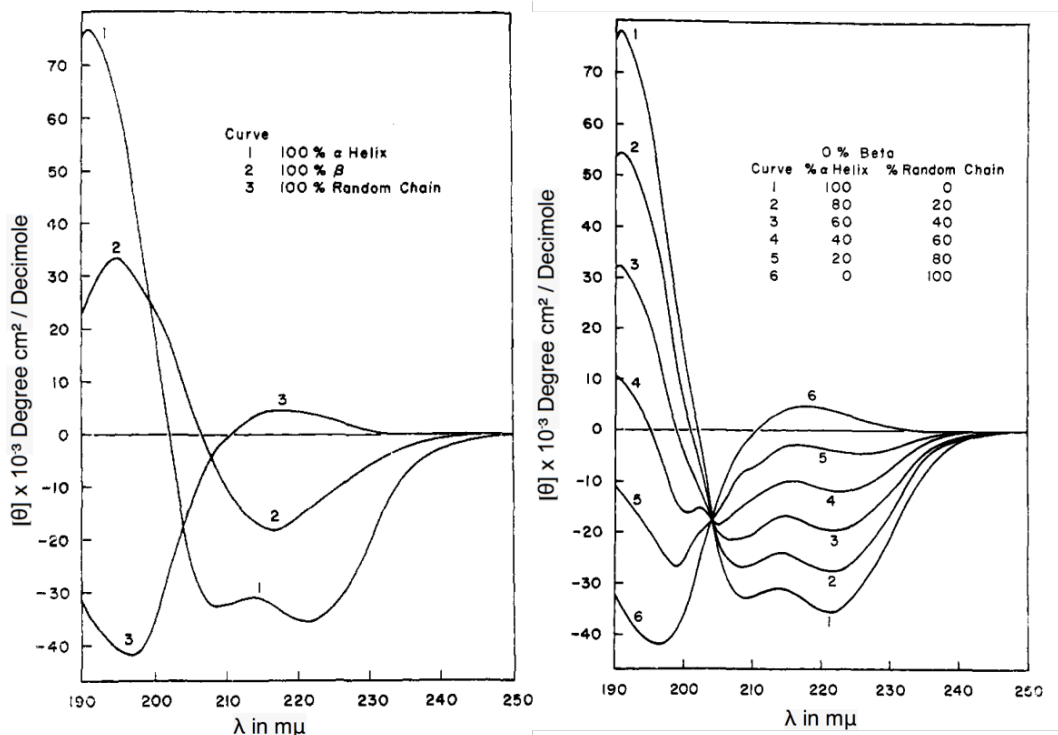
Figure 1.5 - (a) Experimental circular dichroism spectra of poly-L-lysine in the α-helical, β, and random conformation; (b) Calculated circular dichroism of poly-L-lysine containing 0% β and varying percentages of α-helix and random coil[26].

As this project deals with stapling a small region out of the whole sequence, it is assumed that the conformation of the entire peptide will not be 100 percent helical, as the termini of the peptide will have decreased stabilizing support. This may result in a combination of a random coil and α-helix, depending on how well the staple is able to induce helicity in areas of the peptide not contained within the cyclic region.

1.6   Surface Plasmon Resonance (SPR)

To be able to test the ability of synthesized peptides to bind to their natural ligand (i.e. HA), surface plasmon resonance (SPR) will be used. The technique of SPR has been used and continuously improved since its inception in 1977[27]. There have been many refinements to the base technology over the years, but its appeal – the ability to test the binding of unmodified compounds to a target bound to a surface (e.g. a chip) – has always remained the

same. SPR works upon the basis of measuring the mass change of a surface in real time. This mass change can contain kinetic and equilibrium (steady state) information[28]. The surface of the SPR chip can be composed of a variety of different metals, but gold is typically used as it is chemically inert and highly stable[28]. This gold surface can be readily modified with a ligand, and then an unmodified analyte can be released onto the surface (Figure 1.6).
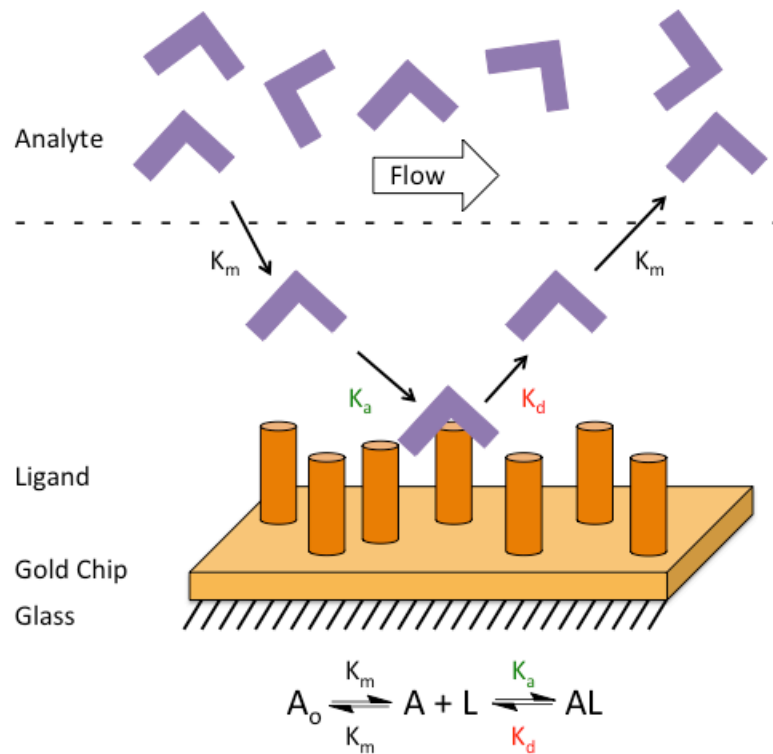
Figure 1.6 - How the binding of an analyte to a bound ligand is able to be measured using SPR.

In this thesis, a localized surface plasmon resonance (LSPR) was used instead of traditional SPR. LSPR differs from SPR by using gold nanoparticles instead of the continuous film that is traditionally used in SPR. To calculate analyte binding, LSPR measures the small change in the absorption of light of the nanoparticles, as opposed to the conventional measurement of change in reflected angle of light. Absorbance can be used in LSPR as nanoparticles produce a strong absorbance peak in the visible light range; a shift in this peak reflects the change in the refractive index of the nanoparticles when a binding event occurs (Figure 1.7).
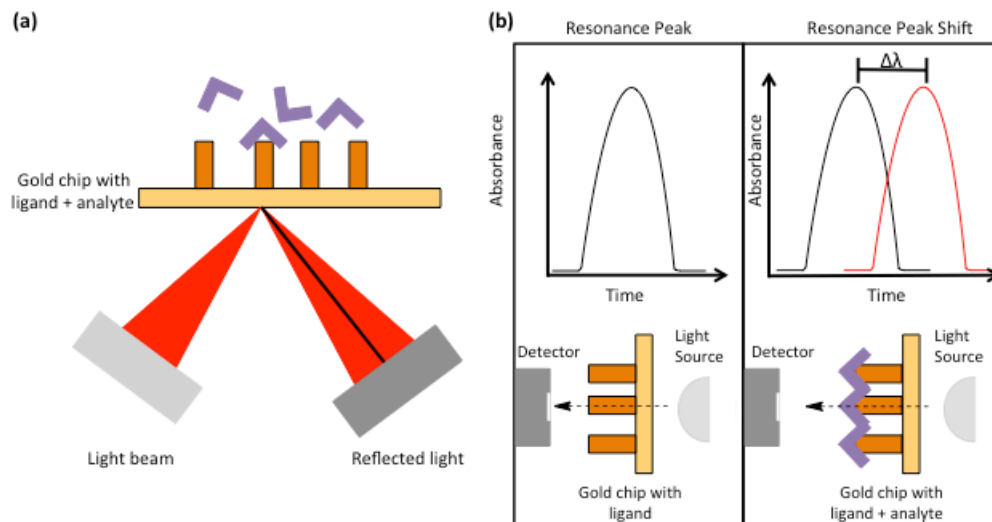
Figure 1.7 - The difference in how kinetic information is obtained in (a) traditional SPR and (b) localized SPR.

1.7 Objectives of Thesis

The purpose of this thesis is to create a potential peptide therapeutic that is able to prevent the RHAMM:HA fragment interaction from occurring. This will be done by synthesizing both HABDs and performing an *i, i+4* lactam staple scan to identify the optimal staple position. These peptides will be analyzed by CD spectroscopy to quantify the degree of α-helicity, and by SPR to determine binding to HA. It is hypothesized that the formation of a lactam bridge will increase both the helicity of the peptide and its binding towards HA. The cyclized peptide that shows the best α-helical conformation will become the lead compound for an alanine scan in order to identify the most essential residues for binding. This lead cyclized peptide candidate will then undergo *in vitro* assays to assess its ability to inhibit migration of cells and the release of inflammatory markers. This will indicate its potential for disrupting the RHAMM:HA fragment interaction that allows cancer cells to display increased migration and proliferation.

1.8 References

(1) Ween, M. P., Oehler, M. K., and Ricciardelli, C. (2011) Role of versican, hyaluronan and

CD44 in ovarian cancer metastasis. *Int. J. Mol. Sci. 12*, 1009–1029.

(2) Hamilton, S. R., Fard, S. F., Paiwand, F. F., Tolg, C., Veiseh, M., Wang, C., Mccarthy, J. B., Bissell, M. J., Koropatnick, J., and Turley, E. A. (2007) The hyaluronan receptors CD44 and RHAMM (CD168) form complexes with ERK1,2, which sustain high bassal motility in breast cancer cells. *J. Biol. Chem. 282*, 16667–16680.

(3) Yang, B., Yang, B. L., Savani, R. C., and Turley, E. A. (1994) Identification of a common hyaluronan binding motif in the hyaluronan binding proteins RHAMM, CD4 and link protein. *EMBO J. 1*, 286–296.

(4) Hirose, Y., Saijou, E., Sugano, Y., Takeshita, F., Nishimura, S., Nonaka, H., Chen, Y.-R., Sekine, K., Kido, T., Nakamura, T., Kato, S., Kanke, T., Nakamura, K., Nagai, R., Ochiya, T., and Miyajima, A. (2012) Inhibition of Stabilin-2 elevates circulating hyaluronic acid levels and prevents tumor metastasis. *Proc. Natl. Acad. Sci. U.S.A. 109*, 4263–4268.

(5) Ziebell, M. R., and Prestwich, G. D. (2004) Interactions of peptide mimics of hyaluronic acid with the receptor for hyaluronan mediated motility (RHAMM). *J. Comput. Aided. Mol. Des. 18*, 597–614.

(6) Yang, B., Zhang, L., and Turley, E. A. (1993) Identification of two hyaluronan-binding domains in the hyaluronan receptor RHAMM. *J. Biol. Chem. 268*, 8617–8623.

(7) Schwertfeger, K. L., Cowman, M. K., Telmer, P. G., Turley, E. A., and McCarthy, J. B. (2015) Hyaluronan, inflammation, and breast cancer progression. *Front. Immunol. 6*, 1–12.

(8) Jedrzejas, M. J., and Stern, R. (2005) Structures of Vertebrate Hyaluronidases and Their Unique Enzymatic Mechanism of Hydrolysis. *Proteins: Struct., Funct., Bioinf. 61*, 227–238.

(9) Fieber, C., Plug, R., Sleeman, J., Dall, P., Ponta, H., and Hofmann, M. (1999) Characterisation of the murine gene encoding the intracellular hyaluronan receptor IHABP (RHAMM). *Gene 226*, 41–50.

(10) Hall, C. L., Yang, B., Yang, X., Zhang, S., Turley, M., Samuel, S., Lange, L. A., Wang, C., Curpen, G. D., Savani, R. C., Greenberg, A. H., and Turley, E. A. (1995) Overexpression of the hyaluronan receptor RHAMM is transforming and is also required for H-ras

transformation. *Cell 82*, 19–28.

(11) Tolg, C., McCarthy, J. B., Yazdani, A., and Turley, E. A. (2014) Hyaluronan and RHAMM in Wound Repair and the "Cancerization" of Stromal Tissues. *Biomed Res. Int. 2014*, 1–18.

(12) Maxwell, C. A., McCarthy, J., and Turley, E. (2008) Cell-surface and mitotic-spindle RHAMM: moonlighting or dual oncogenic functions? *J. Cell Sci. 121*, 925–932.

(13) Veiseh, M., Kwon, D. H., Borowsky, A. D., Tolg, C., Leong, H. S., Lewis, J. D., Turley, E. A., and Bissell, M. J. (2014) Cellular heterogeneity profiling by hyaluronan probes reveals an invasive but slow-growing breast tumor subset. *Proc. Natl. Acad. Sci. U.S.A. 111*, E1731–E1739.

(14) Korkes, F., Castro, M. G. De, Zequi, S. D. C., Nardi, L., Giglio, A. Del, and Pompeo, A. C. de L. (2014) Hyaluronan-mediated motility receptor (RHAMM) immunohistochemical expression and androgen deprivation in normal peritumoral , hyperplasic and neoplastic prostate tissue. *BJU Int. 113*, 822–829.

(15) Rizzardi, A. E., Rosener, N. K., Koopmeiners, J. S., Vogel, R. I., Metzger, G. J., Forster, C. L., Marston, L. O., Tiffany, J. R., Mccarthy, J. B., Turley, E. A., Warlick, C. A., Henriksen, J. C., and Schmechel, S. C. (2014) Evaluation of protein biomarkers of prostate cancer aggressiveness. *BMC Cancer 14*, 1–14.

(16) Hill, T. A., Shepherd, N. E., Diness, F., and Fairlie, D. P. (2014) Constraining cyclic peptides to mimic protein structure motifs. *Angew. Chemie - Int. Ed. 53*, 2–24.

(17) Craik, D. J., Fairlie, D. P., Liras, S., and Price, D. (2013) The Future of Peptide-based Drugs. *Chem. Biol. Drug Des. 81*, 136–147.

(18) Walensky, L. D., and Bird, G. H. (2014) Hydrocarbon-stapled peptides: Principles, practice, and progress. *J. Med. Chem. 57*, 6275–6288.

(19) Estieu-Gionnet, K., and Guichard, G. (2011) Stabilized helical peptides: overview of the technologies and therapeutic promises. *Expert Opin. Drug Discov. 6*, 937–963.

(20) Poland, D., and Scheraga, H. A. (1970) Theory of Helix-Coil Transitions in Biopolymers: Statistical Mechanical Theory of Order-Disorder Transitions in Biological Macromolecules. Academic Press, New York.

(21) Wang, D., Chen, K., Kulp, J. L., and Arora, P. S. (2006) Evaluation of biologically relevant short α-helices stabilized by a main-chain hydrogen-bond surrogate. *J. Am. Chem. Soc. 128*, 9248–9256.

(22) Henchey, L. K., Jochim, A. L., and Arora, P. S. (2008) Contemporary strategies for the stabilization of peptides in the α-helical conformation. *Curr. Opin. Chem. Biol. 12*, 692–697.

(23) Fang, W. (2008) Design and Synthesis of Novel Linear and Cyclic Peptide Ligands for Kappa Opioid Receptors. University of Kansas.

(24) Grieco, P., Gitu, P. M., and Hruby, V. J. (2001) Preparation of `side-chain-to-side-chain' cyclic peptides by Allyl and Alloc strategy : potential for library synthesis. *J. Pept. Res. 57*, 250–256.

(25) Greenfield, N. J. (2009) Using circular dichroism spectra to estimate protein secondary structure. *Nat. Protoc. 1*, 2876–2890.

(26) Greenfield, N., and Fasman, G. D. (1969) Computed Circular Dichroism Spectra for the Evaluation of Protein Conformation. *Biochemistry 8*, 4108–4116.

(27) Pockrand, I., Swalen, J. D., Gordon II, J. G., and Philpott, M. R. (1977) Surface plasmon spectroscopy of organic monolayer assemblies. *Surf. Sci. 74*, 237–244.

(28) de Mol, N. J., and Fischer, M. J. E. (2010) Surface Plamon Resonance Methods and Protocols. Springer.

Chapter 2

2   Design, synthesis, and evaluation of stapled peptides that mimic the hyaluronan binding domains of RHAMM

2.1   Introduction

Cancer is a growing concern worldwide, as mortality rates from cancer have the potential to surpass those of heart disease[1]. Metastatic tumors are especially problematic, as it is the metastases forming distant from the primary tumor site that are the main cause of death in patients[2]. In order for metastases to form, the extracellular matrix (ECM) must be modified to make the cancer cell movement favorable[3]. The ECM provides structural and biochemical support for its surrounding cells and contains many chemoattractants, thereby allowing it to regulate the migration of cells[3]. A main component of the ECM is hyaluronan (HA), a glycosaminoglycan consisting of repeating disaccharides units of N-acetyl-D-glucosamine and D-glucuronic acid[3,4]. HA has a variety of functions that have been shown to regulate proliferation, cell motility, and adhesion, all of which are important in cancer metastasis[5–8]. HA function depends on the carbohydrate's ability to activate certain receptors, such as the receptor for hyaluronan mediated motility (RHAMM).

RHAMM can be located on the cell surface as a glycosylphosphatidylinositol (GPI) linked protein, or it can be found intracellularly within the cytoplasm. On the cell surface, RHAMM is interacts with other cell-surface receptors, such as CD44, which is believed to activate the extracellular signal-regulated kinase (ERK1/2)/mitogen activated protein kinase (MAPK) pathway[9,10]. RHAMM expression is tightly regulated: typically, it remains very low in adult homeostatic tissue, but mRNA expression increases due to tissue injury[10]. Increased RHAMM expression found in tumors have a positive correlation with a poor outcome for the patient[11]. Due to this, blocking the HA fragment:RHAMM interaction could interrupt the vital role in metastasis, leading to a potential therapeutic.

RHAMM is a 72kDa protein that is mainly α-helical as determined by 2D NMR[7]. It has two HA binding domains (HABD) which are located towards the C-terminus region of

the protein within two α-helical regions that are 10 and 11 amino acids in length[7,12,13]. Using site-directed mutagenesis, Yang et al. discovered that RHAMM and other HA-binding proteins have a characteristic BX_7B motif, where B is a basic residue (such as lysine or arginine) and X is any non-acidic residue that is generally hydrophobic[5]. It was observed that in the first HABD, four Lys residues (K401, K411, K405, and K409) were found to be important for interaction with HA[5]. Mutation of the residues K430, R431, or K432 within the second binding domain saw a decrease in HA binding. Also within the second HABD, when K423 was changed to Asn, there was no interaction with HA observed, indicating that there is a need for proper spacing of the basic amino acids for binding to HA[5]. It is the positive charges on these basic residues that are able to interact with the negatively charged carboxylic acid on HA. This clustering of amino acid charges flanking non-acidic residues was observed when the peptide $RG_3RG_2R_2$ was shown to have similar binding to HA as the second HABD[5]. The regions that surround the HABDs of RHAMM are thought to extend inwards to form a hydrophobic core, which assists in stabilizing the secondary structure, allowing the basic residues to be properly aligned to bind to HA[7]. If these surrounding regions are lost, it could be a contributing factor to the loss of secondary structure when the amino acid sequence is truncated to include just one of the binding domains.

The identification of protein-carbohydrate inhibitors (PCI) has largely focused on identifying moieties that mimic the carbohydrate function. However, creating this type of PCI poses a difficulty, as designing a carbohydrate mimic containing the specific multivalences required to increase binding strength between two biological targets can be challenging[14]. However, the focus can be switched to the protein component of the PCI. In order to create a drug-like molecule, peptides can be used instead of their larger protein counterparts, as it makes them less expensive and often easier to manufacture while still having good specificity and potency to their endogenous ligand[15]. Previously, RHAMM mimicking peptides have been developed through the use of phage display libraries[4,16]. One peptide, peptide 15-1, was found to have a 40 percent homology with the linker region between the two HABDs of RHAMM and was able to decrease fibroblast migration and reduce inflammation and fibrosis[4]. Additionally, peptides have been developed that contain the *Mus musculus* sequence of the linker region between the two HABDs of RHAMM, and have been shown to increase adipogensis in mammary fat pads of mice[17]. However, a disadvantage of

peptides deriving from a protein sequence is that they are unlikely to retain their secondary structure under physiological conditions due to the absence of stabilizing residues that enable the protein to properly fold[15,18]. A lack of secondary structure in a recognition site-mimicking peptide increases the energy necessary for target binding, as the specific conformation must form upon binding. Due to this, promoting secondary structure formation (such as an α-helix) in these short peptides prior to binding, may overcome the energetic penalty and potentially increase biological activity[19].

One technique that can achieve this goal is the cyclization of peptides, which can induce helical formation within the cyclic portion. Cyclizing peptides results in a structure with limited flexibility and increased resistance to protease degradation, which can correlate to improved stability *in vivo* as the diameter of the α-helical cyclized peptide is larger than the protease active sites[18]. To aid in the synthesis of cyclic peptides, it is desirable for the linear peptide chain to have the propensity to fold into an α-helix. In order to identify the optimal location within a sequence for the cyclic region to promote helical formation while maintaining binding affinity to a specific target, a 'staple scan' can be performed. This is done by manipulating each residue that is not essential for target binding, and subsequently evaluating the ensuing structure[20]. In an α-helix, which contains 3.6 amino acid residues per turn, residues at positions *i, i+4*, and *i+7* occur on the same face of the helix when the peptide is folded correctly[19]; therefore, introducing covalent bonds via stapling at these positions can stabilize an α-helical conformation[21].

To investigate the effect that truncation has on the bioactivity and helicity of the RHAMM HABDs and the subsequent cyclization, a staple scan was performed for both the first HABD (HABD1) and the second HABD (HABD2). The focus was on creating *i, i+4* lactam staples throughout the HABDs, positioning the staples between the two basic residues that make up the essential BX_7B motif. After each staple was created, the helicity and bioactivity of the peptide was evaluated and compared to the linear, unstapled sequence. This was done in order to identify and assess any stapled RHAMM analogues that may have potential for therapeutic use for treating diseases that involve HA fragmentation such as prostate cancer.

2.2   Results and Discussion

2.2.1   Synthesis of peptides

The effect of synthetic bridging on the degree of α-helicity and the binding/bioactivity of the truncated binding domains was studied. All peptides were synthesized by Fmoc solid-phase peptide synthesis (SPPS). The linear sequences were synthesized using the native amino acid sequence from those portions of the protein (Scheme 2.1).
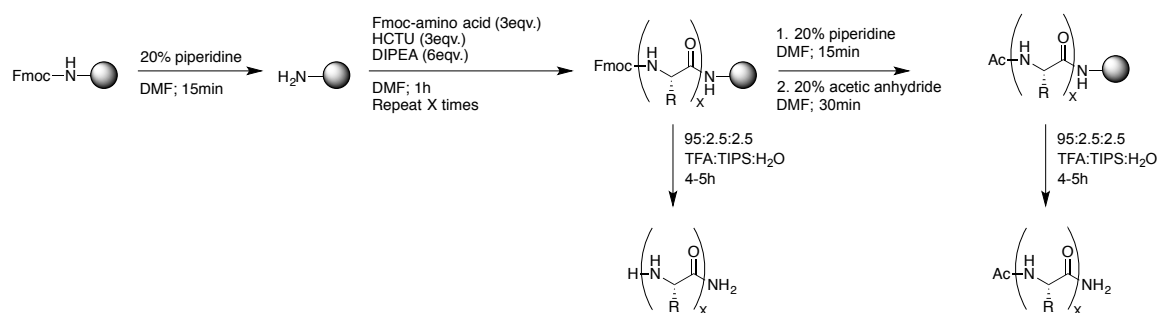
Scheme 2.1 - General Fmoc-SPPS method used to synthesize linear peptides to yield either the acetylated or non-acetylated sequences.

The staple scan was performed to identify the effect of synthetic bridging on the degree of α-helicity and resulting bioactivity of the truncated binding domains. Cyclization was carried out by replacing two amino acids within the sequence with glutamic acid and lysine and creating a lactam bridge between their side chains (Figure 2.1).
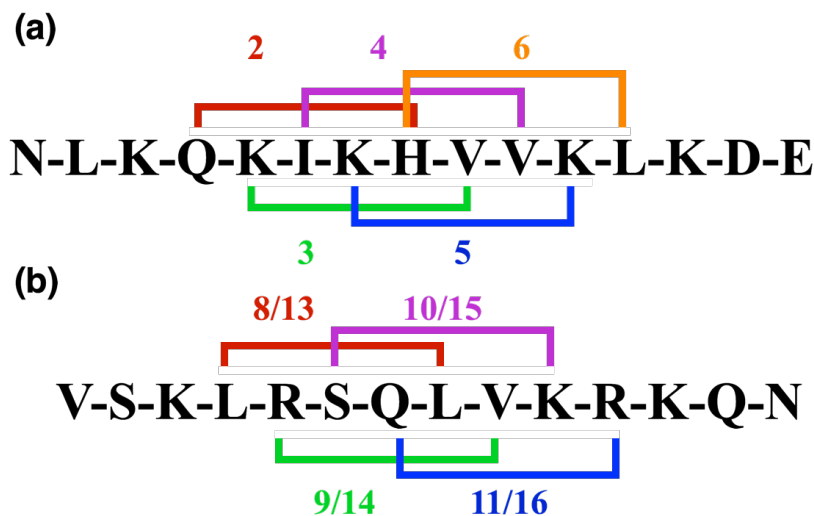
Figure 2.1 – Location for cyclization of peptides using lactam bridge staples (a) cyclic peptides derived from HABD1. Compound numbers indicated, see Table 2.1 for structure; (b) cyclic peptides derived from HABD2. Compound numbers indicated, see Table 2.2 for structure.

The sequences were synthesized by solid-phase peptide synthesis; however, the glutamic acid and lysine residues were protected by allylester and allyloxycarbonyl protecting groups respectively. These protecting groups allow for the selective deprotection of those amino acids using a palladium (0) catalyst so they can subsequently be coupled. The remaining protecting groups were removed and the lactam-bridged peptide was cleaved from the solid support to obtain the cyclized peptide sequences (Scheme 2.2).
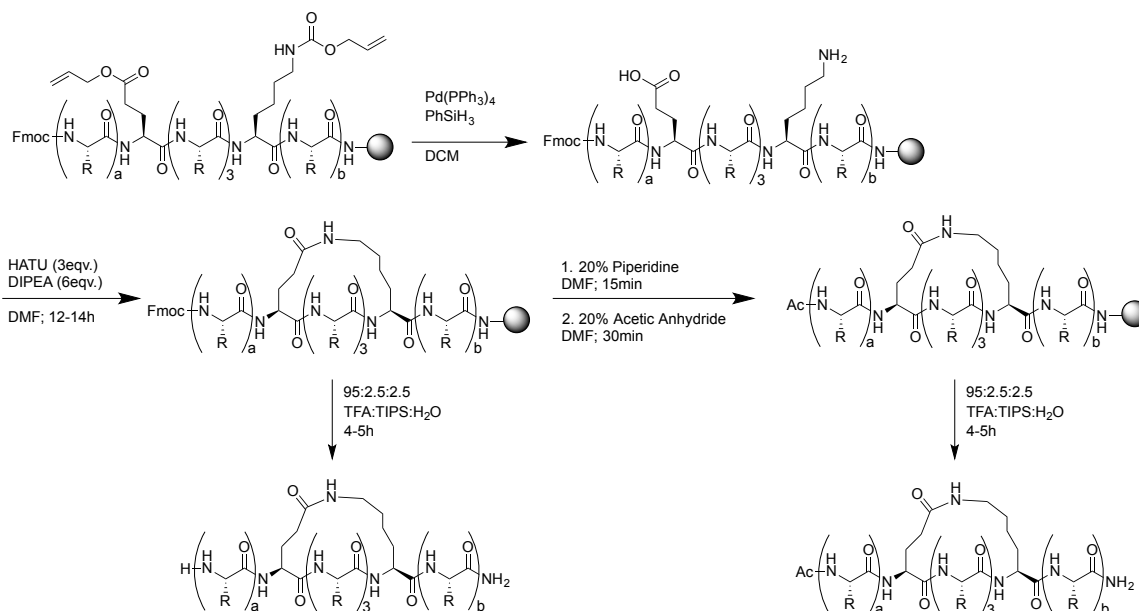
Scheme 2.2 - General method showing the formation of the lactam bridge between a glutamic acid residue and a lysine residue.

Linear and cyclized peptides were synthesized for HABD1, RHAMM(531-541) (Table 2.1) and the HABD2, RHAMM(553-562) (Table 2.2). All peptides (with the exception of compounds **7-11**) were carboxyamidated and N-terminal acetylated to maintain a neutral charge at the termini, allowing them to better mimic the native protein[22]. Compounds **7-11** have a free, charged N-terminus in order to study the effects of this charge on helicity and binding. All peptides were purified and characterized by LC-MS.

Table 2.1 - Sequences of binding domain one (HABD1) where (*i, i+4*) staples were placed in cyclized versions. Mean residue ellipticity values at 222 nm, ratios of mean residue ellipticities at 222/208 nm and percentage helicity that were determined at 20°C.

	Sequence	Water			40% TFE/Water		
		$[\theta]_{222}$ x10^3 (deg cm^2/dmol)	$[\theta]_{222}$/ $[\theta]_{208}$	% Helicity	$[\theta]_{222}$ x10^3 (deg cm^2/dmol)	$[\theta]_{222}$/ $[\theta]_{208}$	% Helicity
1	Ac-NLKQKIKHVVKLKDE-NH$_2$	-1.14	0.11	6.3	-12.42	0.74	40.3
2	cyclo-4,8(Ac-NLK[EKIKK]VVKLKDE-NH$_2$)	-2.45	0.38	6.9	-12.49	0.80	44.5
3	cyclo-5,9(Ac-NLKQ[EIKHK]VKLKDE-NH$_2$)	-2.82	0.43	8.2	-12.43	0.84	38.0
4	cyclo-6,10(Ac-NLKQK[EKHVK]KLKDE-NH$_2$)	-2.61	0.44	7.8	-12.55	0.85	40.8
5	cyclo-7,11(Ac-NLKQKI[EHVVK]LKDE-NH$_2$)	-3.84	0.55	11.1	-14.22	0.86	42.5
6	cyclo-8,12(Ac-NLKQKIK[EVVKK]KDE-NH$_2$)	-1.79	0.31	19.1	-16.02	0.82	41.5

Table 2.2 - Sequences of binding domain two (HABD2) where (*i, i+4*) staples were placed in cyclized versions. Mean residue ellipticity values at 222 nm, ratios of mean residue ellipticities at 222/208 nm and percentage helicity that were determined at 20°C.

	Sequence	Water			40% TFE/Water		
		$[\theta]_{222}$ x10^3 (deg cm^2/dmol)	$[\theta]_{222}/$ $[\theta]_{208}$	% Helicity	$[\theta]_{222}$ x10^3 (deg cm^2/dmol)	$[\theta]_{222}/$ $[\theta]_{208}$	% Helicity
7	H-VSKLRSQLVKRKQN-NH$_2$	-1.07	0.21	16.5	-10.5	0.68	39.5
8	cyclo-4,8(H-VSK[ERSQK]VKRKQN-NH$_2$)	-2.26	0.45	15.8	-8.56	0.72	36.2
9	cyclo-5,9(H-VSKL[ESQLK]KRKQN-NH$_2$)	-4.40	0.57	21.7	-10.32	0.79	52.6
10	cyclo-6,10(H-VSKLR[EQLVK]RKQN-NH$_2$)	-4.34	0.58	22.6	-10.09	0.81	51.3
11	cyclo-7,11(H-VSKLRS[ELVKK]QN-NH$_2$)	-1.53	0.30	23.1	-9.52	0.69	33.3
12	Ac-VSKLRSQLVKRKQN-NH$_2$	-1.10	0.23	14.8	-11.4	0.72	40.9
13	cyclo-4,8(Ac-VSK[ERSQK]VKRKQN-NH$_2$)	-3.34	0.53	14.6	-9.75	0.81	37.0
14	cyclo-5,9(Ac-VSKL[ESQLK]KRKQN-NH$_2$)	-6.45	0.70	25.5	-13.33	0.82	51.2
15	cyclo-6,10(Ac-VSKLR[EQLVK]RKQN-NH$_2$)	-4.85	0.61	28.0	-11.86	0.79	44.8
16	cyclo-7,11(Ac-VSKLRS[ELVKK]QN-NH$_2$)	-2.96	0.54	16.3	-10.53	0.74	34.9
17	cyclo-5,9(Ac-VSKL[KSQLE]KRKQN-NH$_2$)	-0.97	0.20	5.5	-8.78	0.75	36.3
18	cyclo-6,10(Ac-VSKLR[KQLVE]RKQN-NH$_2$)	-1.98	0.37	8.2	-12.84	0.75	52.2

Cyclization of the HABDs was achieved though the formation of a lactam bridge between two amino acid side chains. Glutamic acid was placed in the *i* position and lysine in the *i+4* position in order to create a ring size of 21 atoms. These amino acids were used for creating the lactam bridge as it has been reported that lactam bridges forming 21-membered rings are α-helix-inducing, while 19-membered rings are α-helix destabilizing[23]. Therefore, cyclization in this way should allow the peptide to more easily overcome the high-energy barrier required to form an α-helix.

The composition of the staple has been reported to affect the properties of cyclized peptides; therefore the placement of the lysine and glutamic acid residues in the staple was evaluated. For cyclic lactams, peptides are most helical when the glutamic acid is in the *i* position and lysine is in the *i+4* position[24]. The composition of the staple was reversed in the two peptides from HABD2 that were found to have the greatest induced helicity (**14** and **15**). These peptides (**17** and **18**) contained a staple that was constructed by a lysine residue in the *i* position and a glutamic acid residue in the *i+4* position.

2.2.2   Helicity analysis of cyclization by circular dichroism spectroscopy

Cyclized sequences have been shown to have greater helicity and a corresponding increase in bioactivity[23,25–29]. The synthesized sequences were analyzed by CD spectroscopy in order to determine the degree of α-helicity present in each peptide. A mean residue ellipticity ratio ($[\theta]_{222}/[\theta]_{208}$) that is ~1.00 indicates high α-helical character, while a lower ratio implies that the conformation could contain a combination of an α-helix and a β–sheet or random coil[26,30]. The molar ellipticity ratios and the quantification of helicity for HABD1 and HABD2 can be found in Table 2.1 and Table 2.2, respectively.

The linear, unstapled peptides (1, 7, 12) show minimal α-helical character in water. This was expected, as there is a lack of residues that could contribute to a hydrophobic core, which would result in a stabilized secondary structure[7]. However, when the same sequences were tested in 40% TFE solution, a higher $[\theta]_{222}/[\theta]_{208}$ ratio was observed, with **1**, **7**, and **12** having values of around 0.75, suggesting the formation of an α-helical structure. This is due to the natural propensity of the sequence to adopt a helical shape, as the TFE facilitates the peptide's folding[18]. It is assumed that the $[\theta]_{222}/[\theta]_{208}$ ratio of the linear sequences in the

presence of 40% TFE is the theoretical maximum helicity that these synthetic sequences can possess.

The HABD1 did not achieve as substantial of an increase in helicity when the staples were introduced compared to the improvements seen when the staple was placed in HABD2 (Figure 2.2). This can be seen by the larger minima seen with the stapled peptides in HABD2 compared to that of their linear counterparts. This difference between binding domains could be due to the differences in their primary sequences. HABD2 has more leucine and glutamine residues in its primary sequence than HABD1, and those residues are proposed to be helix-stabilizing residues[26]. Without these residues in the sequence, the α-helical structure may become less stable and therefore result in a weaker α-helical signal.
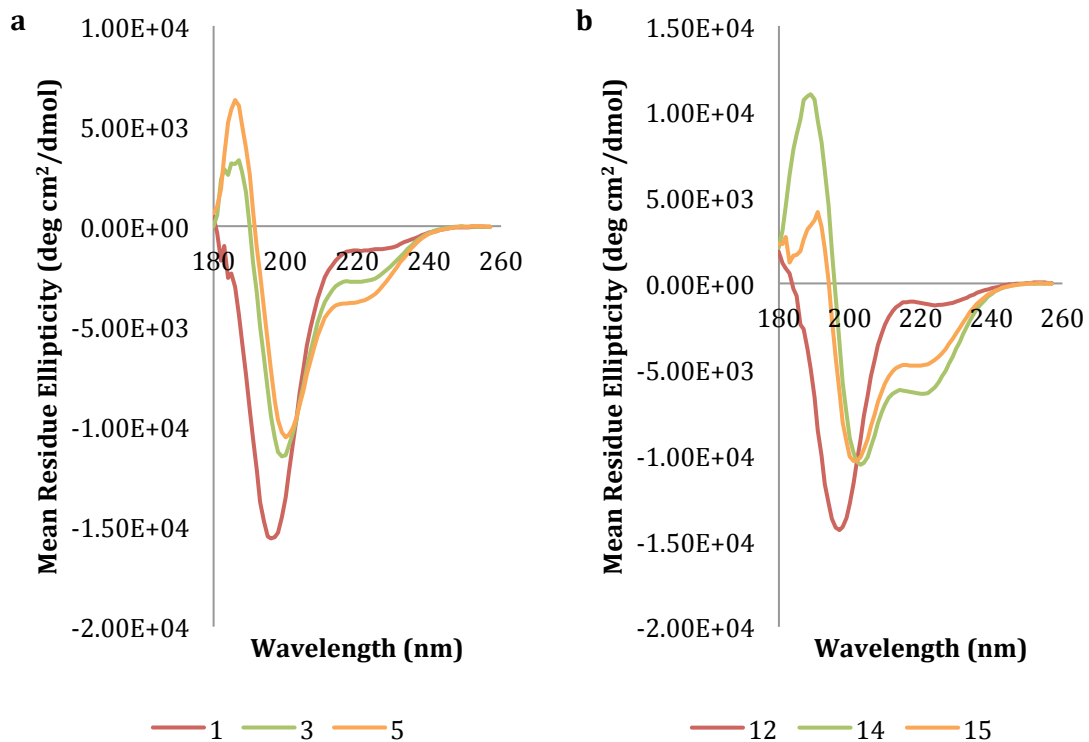
Figure 2.2 - (a) CD spectra of linear unstapled sequence of HABD1 (1) and the cyclic versions (3 and 5) that showed the greatest increase in helicity; (b) CD spectra of linear unstapled sequence of HABD2 (12) and the cyclic versions (14 and 15) that showed the greatest increase in helicity.

The stapled peptides of HABD1 resulted in an increase in helicity when compared to the linear sequence. This was determined by the increase in the molar ellipticity at 222 nm (Figure 2.3; a) and the minimum moving closer to 208 nm, which is characteristic of an α-helix. Comparing the molar ellipticity ratios demonstrates that the values of the stapled peptides (**2-6**) in water are greater than that of the unstapled sequence (**1**) (Figure 2.3; b). The greatest $[\theta]_{222}/[\theta]_{208}$ ratio for the cyclic peptides from HABD1 was compound **5**. The sequence has a $[\theta]_{222}/[\theta]_{208}$ ratio of 0.55 which approaches 0.74, which is the $[\theta]_{222}/[\theta]_{208}$ value of the unstapled sequence (**1**) in the presence of 40% TFE.
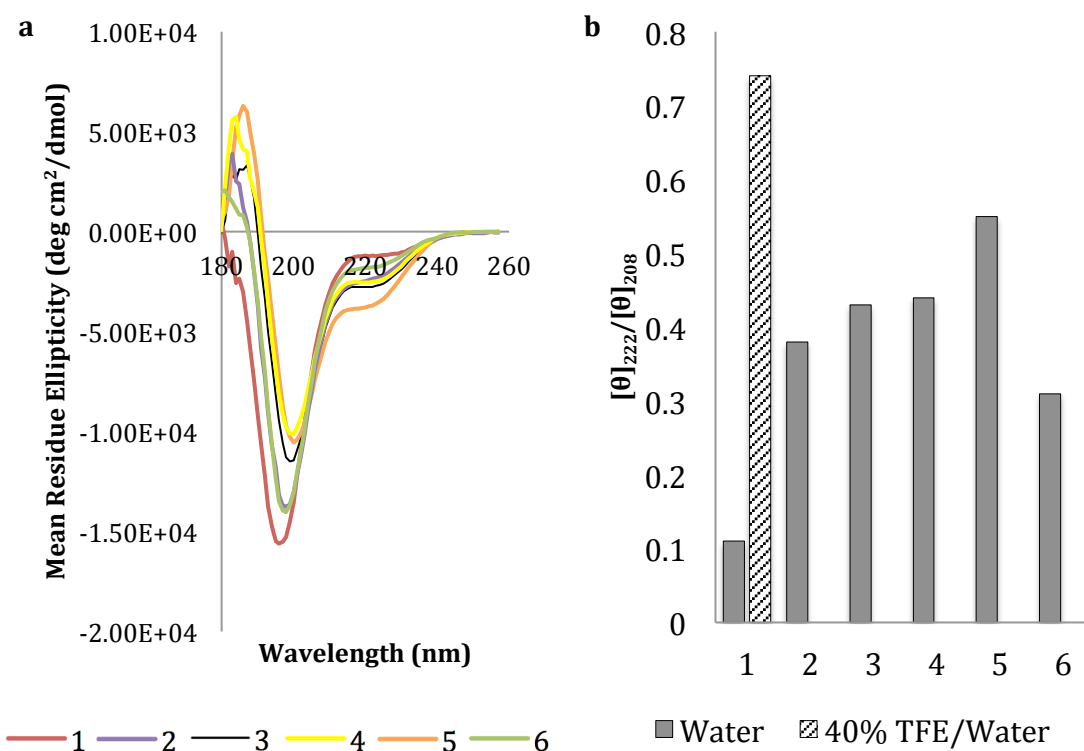
Figure 2.3 - (a) Comparison of CD spectra of the linear sequence of HABD1 (1) and the cyclized sequence (2-6) in water; (b) Comparison of $[\theta]_{222}/[\theta]_{208}$ values for the sequences (linear and cyclized) that derive from HABD1.

There was a greater increase in induced helicity of HABD2 when the stapled were introduced to the sequence (Figure 2.4; a) than seen in HABD1. Cyclizing this sequence creates a CD signal that has a greater minimum at 222nm, as well as a larger maximum at

192nm, both indicators of α-helicity. When the $[\theta]_{222}/[\theta]_{208}$ ratio from the linear peptide sequence is compared to the cyclized versions, the ratios for the cyclized sequences in water are comparable to the value of the linear counterpart in 40% TFE (Figure 2.4; b). The cyclized peptides in water alone achieve similar $[\theta]_{222}/[\theta]_{208}$ ratios as the theoretical maximum obtained by the linear counterpart in 40% TFE/water, indicating that the staple is helping induce the maximum helicity possible for this sequence.
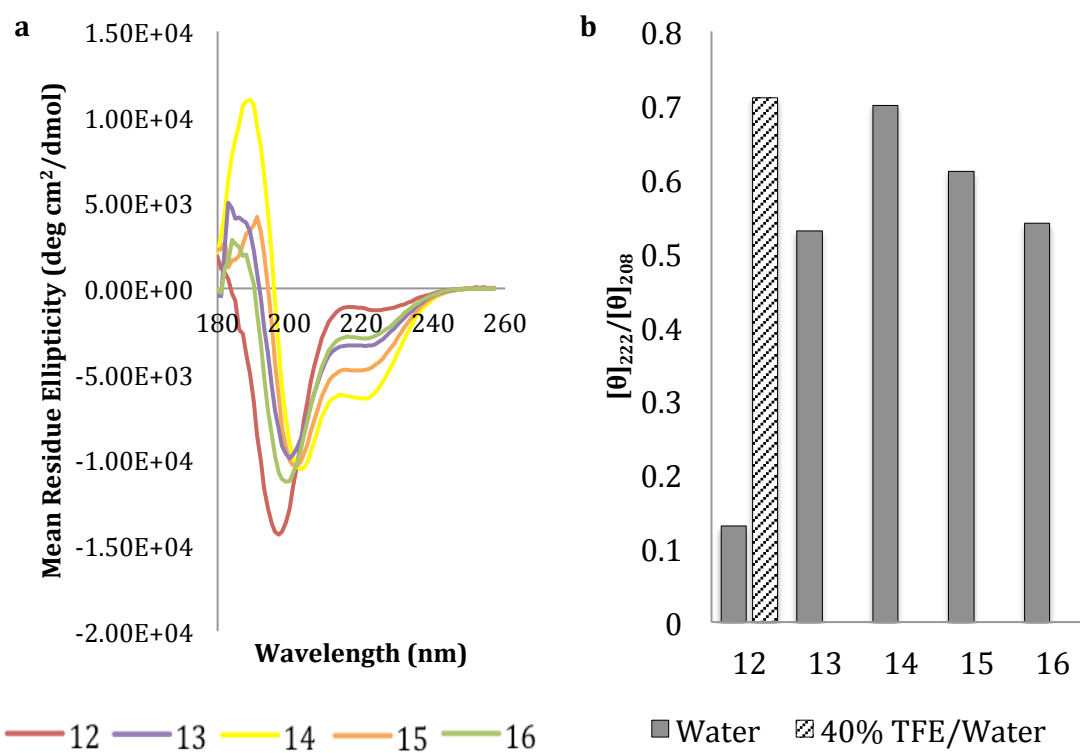
Figure 2.4 - (a) Comparison of CD spectra of the linear sequence of HABD (12) and the cyclized sequences (13-16) in water; (b) Comparison of $[\theta]_{222}/[\theta]_{208}$ values for the sequences (linear and cyclized) that derive from HABD2.

Staple placement within the peptide backbone is important for helicity, and a maximal increase in α-helical structure was observed in peptides where staples were introduced towards the center of the peptide (**14** and **15**). However, the staples placed near the termini of the peptides (**13** and **16**) do not stabilize the core of the peptide and do not facilitate the formation of a complete α-helical conformation. Differences in α-helicity

induced by the staples placed at different points within each peptide may be due to the changes made to their primary sequences, since two amino acids (in the i and $i+4$ positions) must be substituted in order to form the lactam bridge. In compound **13**, leucine was replaced at both the i and $i+4$ position, while in compound **16**, glutamine was replaced at the i position and arginine was replaced at $i+4$. Leucine and glutamine are proposed to be helix-stabilizing residues[26] and the loss of these amino acids may contribute to the lower helicity.

During the assessment of HABD2, the positioning of the amino acids that compose the staple were reversed in two instances to observe its effect on the formation of an α-helix. It was noted that when lysine was in the i position and glutamic acid in the $i+4$ position (**17** and **18**), their molar ellipticity ratios were 0.20 and 0.37 respectively. This ratio is greatly decreased compared compounds **14** and **15** (0.70 and 0.61, respectively), as these sequences have the same staple position, just different staple composition. Compound **14** was 3.5 times more helical than **17**, a trend that is also seen between **15** and **18**, as **15** was 1.6 times more helical than **18**.

2.2.3   *In vitro* stability of peptides

Peptides are susceptible to degradation *in-vivo* due to their natural composition; however, pre-forming the helix by introducing the lactam bridge can reduce exposure of the vulnerable amide backbone and increase resistance to protease cleavage[31]. For these reasons, all peptides were subjected to a human serum stability analysis to evaluate the effect of staple positions on the peptides' stability.

The shortest half-life was seen for Compound **7** at 220 minutes. This was expected, as it is a linear peptide with a free N-terminus. However, when the sequences were cyclized, but still had a free N-terminus (compounds **8-11**), no significant breakdown was observed after 24 hours. The remaining peptides studied were C and N-terminus capped, both linear and cyclized and these peptides displayed no degradation over 24 hours, regardless if they were cyclized. It has previously been reported that the combination of N-terminal acetylation and carboxyamidation increases a peptide's resistance to protease degradation[32].

To assess the effectiveness of the staple in interfering with trypsin degradation of the peptides, a trypsin assay was run on compounds **12** and **15**. As expected, hydrolysis was

found to preferentially occur at Arg and Lys residues near the C-terminus in peptides **12** and **15**. The major, initial trypsin hydrolysis sites of **12** were at the carboxyl-terminus of Lys-3 and Arg-5, and at Lys-10 to a lesser degree. The half-life of peptide **12** towards trypsin degradation was determined to be 0.5 minutes, while the introduction of the lactam bridge in **15** significantly improved the peptide's stability towards trypsin, as the half-life improved to 30 minutes. Hydrolysis of **15** differed from **12** such that digestion did not occur at Arg-5 or Lys-10, the latter of which forms a portion of the lactam bridge of **15**. The major, initial trypsin hydrolysis sites of **15** were at carboxy-terminus of Lys-3, and Arg-11 to a lesser degree.

2.2.4   Ability of peptides to bind hyaluronan

Due to α-helical character being important to the RHAMM protein for binding to HA, it was hypothesized that an improvement in helicity of the stapled peptides over their linear counterpart would also increase their ability to bind HA. To test the peptides' binding, either biochemical or biophysical assays can be used. Biochemical assays, such as ELISA, allow for a small amount of the protein target to be used and can be useful in a high-throughput assay[33]. However, direct binding measurement of these peptides to HA using an ELISA would require tagging of the HABD mimics with a tag molecule, such as biotin, to generate a signal. This has the potential to change how the peptide interacts with HA, which undesirable. The use of a biophysical screening method such as surface plasmon resonance (SPR) allows for a low to medium throughput screening[33], but is an ideal method of measuring binding, as it does not require modification of the peptides in order to test direct binding to HA. To use SPR, 5-10 kDa HA was modified by reductive amination of the anomeric carbon with cystamine following a published procedure[34] (Scheme 2.3).
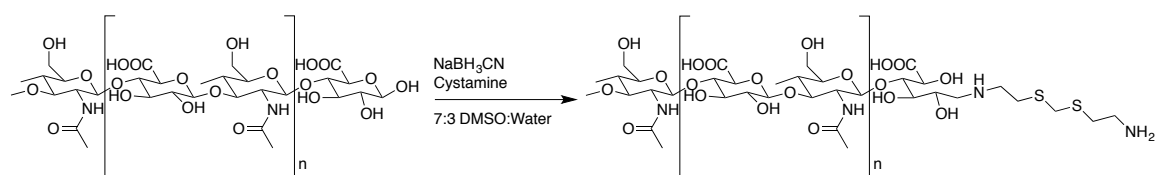
Scheme 2.3 - Modification of 5-10 kDa HA with cystamine.

Following modification, HA was bound to the surface of the gold chip to be used in the SPR experiments. Unmodified peptides were passed over the surface at varying concentrations in order to obtain the binding kinetics and the absorbance readings of each peptide were also plotted together to compare their signals intensities at identical concentrations (Figure 2.5).
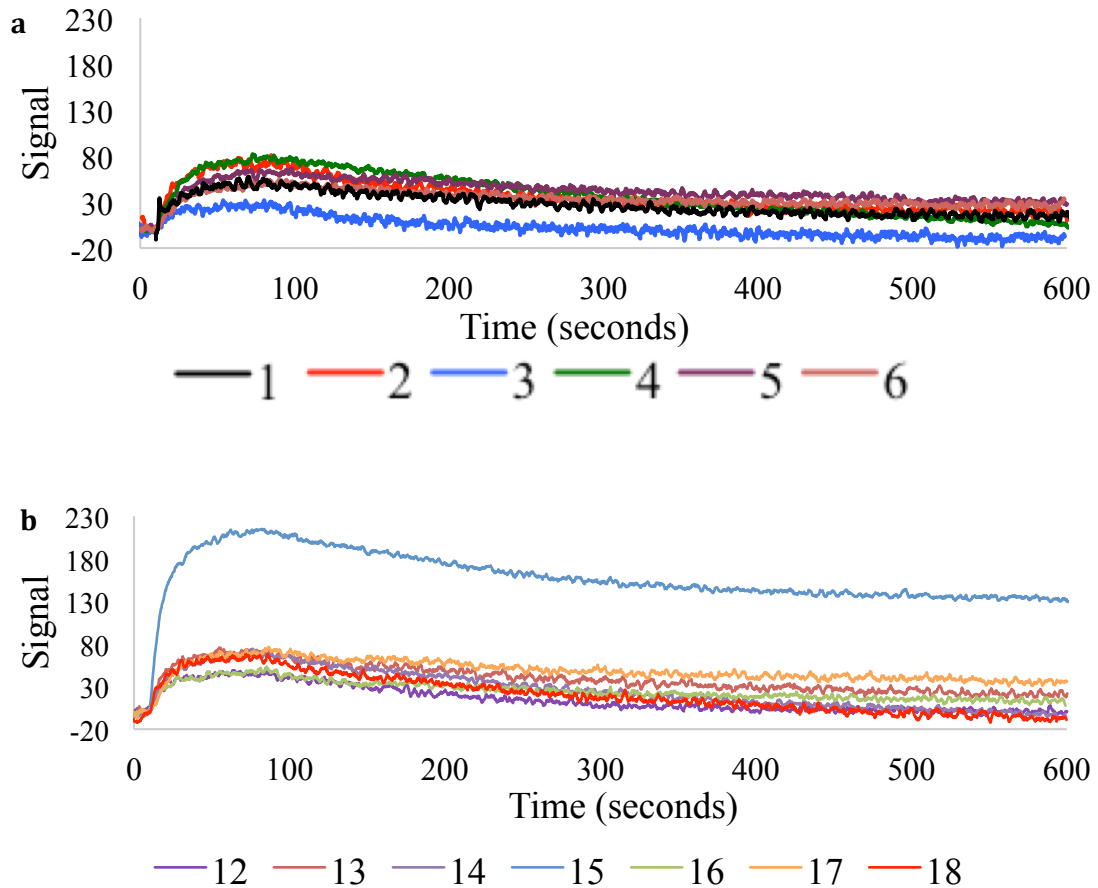
Figure 2.5 - SPR binding curves for peptides from (a) HABD1 or (b) HABD2 that were passed over HA-coated gold chip at a concentration of 25 μM.

The K_D values were obtained for all of the peptides mimicking HABD1, all acetylated peptides from HABD2, and the non-acetylated peptides **7** and **10**, in order to determine the effect of acetylation on the peptide's binding to HA (Table 2.3).

Table 2.3 - Sequences from both HABD1 and HABD2 and the calculated K_D values determined by SPR.

Cmpd	Binding Domain	Sequence	K_D (μM)
1	1	Ac-NLKQKIKHVVKLKDE-NH$_2$	59.8
2		cyclo-4,8(Ac-NLK[EKIKK]VVKLKDE-NH$_2$)	29.6
3		cyclo-5,9(Ac-NLKQ[EIKHK]VKLKDE-NH$_2$)	6.2
4		cyclo-6,10(Ac-NLKQK[EKHVK]KLKDE-NH$_2$)	158
5		cyclo-7,11(Ac-NLKQKI[EHVVK]LKDE-NH$_2$)	332
6		cyclo-8,12(Ac-NLKQKIK[EVVKK]KDE-NH$_2$)	15.7
7	2	H-VSKLRSQLVKRKQN-NH$_2$	3030
10		cyclo-6,10(H-VSKLR[EQLVK]RKQN-NH$_2$)	1.9
12		Ac-VSKLRSQLVKRKQN-NH$_2$	1076
13		cyclo-4,8(Ac-VSK[ERSQK]VKRKQN-NH$_2$)	144
14		cyclo-5,9(Ac-VSKL[ESQLK]KRKQN-NH$_2$)	4.7
15		cyclo-6,10(Ac-VSKLR[EQLVK]RKQN-NH$_2$)	1.0
16		cyclo-7,11(Ac-VSKLRS[ELVKK]KQN-NH$_2$)	22.2
17		cyclo-5,9(Ac-VSKL[KSQLE]KRKQN-NH$_2$)	158
18		cyclo-6,10(Ac-VSKLR[KQLVE]RKQN-NH$_2$)	156

The linear sequence from HABD1 (**1**) bound to HA more strongly than the linear sequences from HABD2 (**7** and **12**). However the introduction of the staples in HABD1 decreased binding to HA in some cases (**4** and **5**). Compound **3**, however, showed a significant increase in binding. This might be because the residues that were switched out to allow formation of the lactam bridge in **4** and **5** were essential for binding, where the modified amino acids in compound **3** were not important for HA-RHAMM interactions.

The introduction of the staples to HABD2 caused an improvement in binding in all cases. In this binding domain, a positive correlation was seen between the mean residue ellipticity ratio and the peptide's ability to bind to HA. Compounds **14** and **15** showed the greatest induction of helicity, as well as the greatest increase in binding compared to the linear sequence. Also, when the Lys and Glu residues were reversed (compounds **17** and **18**), the binding to HA decreased compared to their similar sequences **14** and **15**. This was a trend that followed what was seen via CD spectroscopy, as the helicity was also decreased when the lactam bridge was switched from a Glu – Lys to a Lys – Glu. It was also observed that the N-terminally acetylated sequences (**12** and **15**) had better binding compared to those that had a free N-terminus (**7** and **10**).

2.2.5   *In vitro* bioactivity

It has been established that RHAMM regulates cell motility and stem cell differentiation[10]. These functions have been linked to HA binding capability of RHAMM, and to its intracellular association with proteins such as ERK and tubulin. For this reason, all peptides were tested *in vitro* to evaluate their biological activity and identify any correlation between bioactivity and helicity. High expression levels of RHAMM has been shown to be positively correlated with cellular migration, inflammation, and fibrosis[35]. Therefore, we evaluated our peptides in functional assays relating to these cellular responses. The stapled peptides have been designed to mimic RHAMM, and therefore should interact with HA and prevent the RHAMM:HA fragment interaction from occurring. The stapled sequence from each binding domain that showed the highest binding to HA according to SPR analysis for both binding domains were analyzed for their ability to inhibit cellular migration (Figure 2.6).
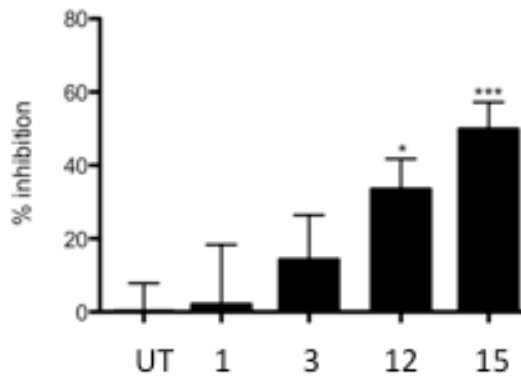
Figure 2.6 – The inhibition of cellular migration of LR21 cells overexpressing RHAMM assessed by a Boyden Chamber assay. Assay was performed at a 10 μg/mL concentration of the linear and best cyclic peptides from each binding domain. The positive control (no added peptide), which showed minimal inhibition of cellular migration, was also measured (UT). (*p<0.05; ***p<0.001)

LR21 cells overexpressing RHAMM were used in a Boyden Chamber assay to assess the ability of cells to migrate through pores to the chemoattractant below. When only serum is present, cells can actively migrate through the pores. However, in the presence of bioactive peptides, there is an inhibitory effect on the cell, resulting in a decrease in migration. Compound **15** had a greater inhibitory effect on cell migration than **12**, as seen in Figure 2.6, which may be linked to its propensity to form an α-helix compared to other peptides studied, indicating a direct correlation between HABD2's helicity and bioactivity. Based on these results, HABD1 did not have a significant inhibition of cellular migration while compound **15** did (p<0.001). For this reason, all inflammation and fibrosis assays were carried out on the HABD2 linear and cyclic sequences. The ability of **15** to reduce inflammation and fibrosis relative to the linear sequence **12** was then assessed (Figure 2.7).
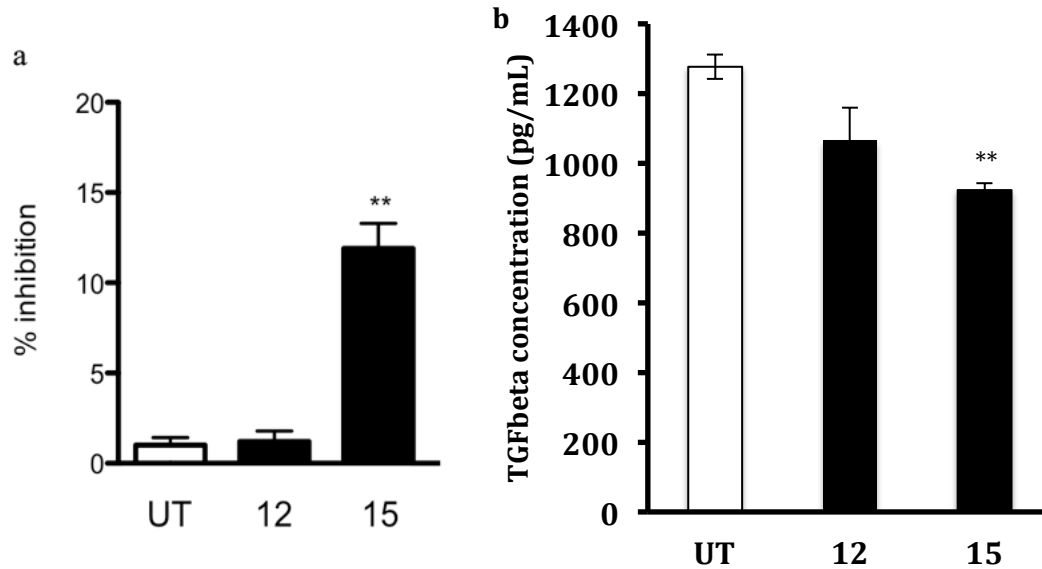
Figure 2.7 - (a) Inflammation assay run with RAW 264.7 macrophages carrying a SEAP reporter to assess the inhibition of release of inflammatory markers; (b) Fibrosis assay performed with IMR90 human fetal lung fibroblasts to assess the inhibition of fibrosis markers. The positive control (no added peptide), which showed minimal response in both assays, was also measured (UT). (**p<0.01)

Inflammation plays a key role in cancer, as it has been shown that cancer growth and spread can be accelerated through the intrusion of lymphocytes[36]. NF-κB is an inflammatory response that is released from macrophages when they are stimulated with pro-inflammatory signals such as PAM3CSK4. It has been observed that there is increased RHAMM expression in macrophages when there is tissue injury[35]. The results have shown a significant increase in inhibition of inflammation when **15** is added (p<0.01), while there is not a significant inhibitory effect with **12**. This indicates that the cyclic RHAMM mimetic (**15**) is able to inhibit the release of NF-κB (Figure 2.7; a), signifying it may be possible for this peptide to decrease the accumulation of macrophages, and thus inflammation, within injured tissue (i.e. a tumor).

There is an increase in TGF-β_1 production from fibroblasts when there is an injury to the tissue. This increase in TGF-β_1 can also up-regulate the production and deposition of HA,

leading to increased fibrosis[35]. However, RHAMM:HA interactions are needed in order for there to be TGF-β_1-stimulated cell locomotion, which would allow for this increase in HA production. The fibrosis assay showed that there is a significant decrease in production of fibrosis markers upon introduction of **15** ($p<0.01$), indicating there is less *in vitro* fibrosis occurring. Through comparison of the *in vitro* assays, peptide **15**, which has a 3-fold increase in helicity compared to the linear sequence, was able to inhibit a wide range of cellular functions.

2.3 Conclusion

Peptides containing either HABD1 or HABD2 of RHAMM were synthesized and chemically modified in order to stabilize the compounds' α-helicity. These peptides were stapled at various *i* and *i+4* positions along the peptide's primary sequence as a means of constraining the peptide, thus limiting the number of possible conformations that it could adopt. Fifteen cyclic peptides were designed and synthesized to mimic the HA binding domains of RHAMM. CD spectroscopy was used to analyze and quantify the degree of α-helicity that the staples introduced in comparison to their unstapled counterpart. It was observed that the unstapled peptide had minimal α-helicity in water, as was expected, and that compounds **14** and **15** from HABD2 had a greatly improved degree of α-helical conformation. It was seen that these stapled peptides had improved serum stability and increased resistance to trypsin compared to the unstapled sequence. There was a positive correlation between helicity of the cyclic peptides from HABD2 and their ability to bind to HA, but the same trend was not observed with HABD1. The best cyclic compound, **15**, has the potential to be a cancer therapeutic, as it is able to decrease cell migration, inflammation, and fibrosis. It has the potential to help decrease the metastases of a primary tumor, leading to the potential reduction in the mortality of cancer. We will continue optimize these lead compounds and will develop additional *in vivo* assays for further evaluation.

2.4 Experimental

2.4.1   General information

All Fmoc-protected amino acids were obtained from ChemImpex. HCTU, HATU, and Rink

Amide MBHA Resin (4-(2',4'-dimethoxyphenyl-(9-fluorenylmethoxycarbonyl)-aminomethyl)-phenoxy-acetamidonorleucyl-4-methyl benzhydrylamine resin) were obtained from ChemImpex. Tetrakis(triphenylphosphine)palladium(0), phenylsilane, Fmoc-AEEA spacer, and NHS-Biotin were obtained from Sigma-Aldrich. All solvents were obtained from Fischer Thermo-Scientific.

2.4.2 Solid-phase peptide synthesis

Fmoc-based solid-phase synthesis was carried out by either manual synthesis using a fritted glass peptide vessel or by automated synthesis using a Biotage® Syro *Wave*™ automated peptide synthesizer. Synthesis was performed on a 0.1 mmol scale with 0.52 mmol/g Fmoc-Rink amide MBHA resin and a 3-fold excess of the protected amino acids. The resin was swelled in CH_2Cl_2 (2.0 mL, 15 minutes) then rinsed with DMF (1.0 mL, 1 min). Fmoc deprotection was performed with a solution of 20% piperidine/DMF (1.5 mL) 5 minutes, then washed with three times with DMF (2.0 mL, vortex 30 seconds) and then again for 15min with 20% piperidine/DMF (1.5 mL). The resin was further washed with DMF six times (2.0 mL, vortex 30 seconds). A Kaiser test was performed after the Fmoc removal to verify the presence of a free primary amino group. Fmoc-protected amino acid (0.3 mmol) and HCTU (0.3 mmol) was dissolved in DMF (1.5 mL) and added to the resin. The mixture was vortexed for 30 seconds and then DIPEA (0.6 mmol) was added to the mixture and vortexed for 1 hour. The deprotection/amino acid coupling cycle was repeated until the desired amino acid sequence was obtained. After the final amino acid was coupled, the resin was washed with DMF (3x) and CH_2Cl_2 (3x) and then dried under vacuum and stored in the freezer (-20 °C). Removal of the N-terminal Fmoc protecting group was achieved using the previously described deprotection procedure. Cleavage of the peptide from the resin and side chain protecting groups was performed by adding a solution of 95% trifluoroacetic acid/2.5% triisopropylsilane/2.5% water (3 mL) to the resin and vortexing for 4-5 hours. After filtration, the peptide was precipitated with cold *tert*-butyl methyl ether (TBME) (20 mL) and collected by centrifugation. The mother liquor was decanted, the pellet dissolved in water (20mL) and lyophilized to obtain the crude fully deprotected peptide.

2.4.3 Deprotection of the allyloxycarbonyl (Alloc) and allylester (OAll) protecting groups

Selective deprotection of the allyloxycarbonyl and the allylester protecting groups was accomplished by adding CH_2Cl_2 (4.5 mL) to the resin-bound peptide and shaking gently for 10 minutes. After addition of phenylsilane (24 eq), the peptide vessel was flushed with nitrogen for 5 minutes. Tetrakis(triphenylphosphine) palladium (0) (0.1 eq) was then added to the mixture and the peptide vessel was again flushed with nitrogen, and the reaction was allowed to proceed for 10 minutes. The peptide-resin was washed with CH_2Cl_2 (4 x 30 seconds), followed by a series of washings with CH_2Cl_2, DMF, MeOH, DMF, and CH_2Cl_2 (30 seconds each).

2.4.4 Lactam bridge formation

After selective deprotection of alloc and allyl ester groups, HATU (3 eq) was dissolved in DMF (1.5 mL), added to the resin and vortexed for 30 seconds. DIPEA (6 eq) was then added and the reaction was vortexed for 2 hours. The resin was rinsed with DMF and CH_2Cl_2 (2.0 ml, 3 x 30 seconds each) to remove any residual reactants.

2.4.5 Purification by RP-HPLC/ESI-MS

Peptides were analyzed using a reverse-phase analytical HPLC column (Agilent Zorbax SB-C18 column 4.6 x 150 mm, 3.5 μm). This system was equipped with a Waters 600E Multisolvent Delivery System, Waters 600 controller, Waters inline degasser, and Waters Masslynx software (version 4.1). Employed mobile phases were 0.1% TFA in Milli-Q water (eluent A) and 0.1% TFA in acetonitrile (eluent B). The flow rate was set at 1.5 mLmin^{-1} with a gradient elution over a 12 minute gradient. The column eluent was monitored using a Waters 2998 Photodiode array detector. Peptides were purified using a reversed-phase preparative HPLC column (Agilent Zorbax SB-C18 column 21.2 x 150 mm, 5 μm) on the same system described above. The detection method and eluents were the same as the analytical system, with the flow rate was set at 20 mLmin^{-1}. The collected fractions were then lyophilized to a solid and analyzed by ESI-MS. Purity of final products was determined by an Acquity UHPLC-MS (220 nm).

2.4.6   Circular dichroism (CD) spectroscopy

CD spectra were obtained on a Jasco J-810 spectropolarimeter and recorded in the range of 180-260 nm. Peptide solutions were prepared with a 0.1 M phosphate buffer solution to a concentration of 0.5 mM. The measurements were performed in quartz cuvettes with a path length of 1 mm and a scanning speed of 10-50 nm/min. Five individual data points were averaged by the instrument in order to obtain the reported CD spectrum. The measurements were carried out at 20 $^{\circ}$C. A blank solution of 0.1 M phosphate buffer solution was run before every measurement in order to baseline correct for any UV-interference observed from the buffer. Deconvolution of CD spectra were obtained using the CONTINLL program, which is part of the web-based program CdPro (http://lamar.colostate.edu/~sreeram/CDPro/).

2.4.7   Surface plasmon resonance

HA was modified using a literature procedure, with some modifications[34]. 5-10kDa HA (40 mg) was dissolved in DMSO/H_2O (7/3, v/v) with an excess amount of sodium cyanoborohydride added. This solution was allowed to stir for 12 hours at room temperature, 10 eq of cystamine was added and the mixture was allowed to stir for a further 24 hours. The solution was then added to a dialysis membrane (MWCO 3.5-5 kDa) where the by-products were removed by dialysis for 3 days followed by lyophilization until a white powder was obtained. SPR experiments were performed with an openSPR (Nicoya Lifesciences, Waterloo, Canada) at 25°C with a 100 μL loading loop and a constant flow rate of 50 μL/min. The cystamine-modified HA was added to a functionalized gold chip by dissolving HA-cystamine (1 mg/mL) in water and incubating for 24 hours at 4°C. Binding of the HABD mimics and the linear sequences were tested in a 10mM solution of phosphate buffered saline (137 mM NaCl, 2.7 mM KCl, 10mM Na_2HPO_4, 2 mM KH_2PO_4). The peptides were injected over the bound HA in concentrations from 1 μM to 1 mM for 2 min to allow association. 10 mM PBS was passed over the sensor for 8 min to allow dissociation. After each peptide injection, 1 mM NaCl was injected to completely dissociate the complex and regenerate the HA surface. Data analysis was performed using Trace Drawer software (Ridgeview Instruments AB) as recommended by the manufacturer. Kinetic parameters were calculated using global analysis, fitting the data to a simple 1:1 model.

2.4.8   Serum stability

Each peptide (1 mM final concentration) was incubated in a mixture of 25% human serum (Sigma-Aldrich, Male type AB cat# H4522) in PBS (Phosphate buffer saline, pH 7.4, 450 μL final volume, DMSO final concentration 0.5%) at 37°C. At various time intervals, aliquots of peptide solution were removed and mixed with either acidic solutions (4% phosphoric acid, pH 1-2) or basic (4% ammonium hydroxide, pH 11-13) to dissociate peptide interactions with components of human serum. Peptide was isolated from human serum by column separation on Oasis® sorbent 96-well μElution plates (HLB- amphiphilic resin and MCX-cation exchange resin) and manifold. The extracted peptide was quantified on an Acquity UHPLC-MS system, by measuring the peak area of a peptide specific M^{+n} ion peak (average of 3 replicates). Percent abundance of peptide peak area relative to peptide peak abundance at T0 was plotted as a function of time. Peptide half-life was calculated by optimized curve fitting (linear, 2-parameter or 3-parameter exponential decay curve) on SigmaPlot™ and solving for time at 50% peptide peak abundance.

2.4.9   Trypsin assay

Human trypsin was purchased from Sigma-Aldrich (EC# 3.4.21.4). Lyophilized trypsin was reconstituted in a solution of 1 mM HCl, 10% glycerol, 1 mM 2-mercaptoethanol, aliquoted and frozen until future use. Assays were carried out with 25 nM trypsin, 250 μM peptide in 67 mM Sodium Phosphate Buffer, pH 7.6 at 37°C. Periodically, aliquots were taken and trypsin activity quenched with equal volume 50:50 methanol:water, 1 M HCl. Peptide was quantified on an Acquity UHPLC, combined with a Xevo QTof mass spectrometer (Waters, Milford, MA.) The UPLC system was equipped with a Waters Acquity UHPLC BEH C18 2.1 x 50 mm, 1.7 μm column; samples were run with a gradient of 5 to 40% water + 0.1% formic acid : acetonitrile + 0.1% formic acid for four minutes. Mass analysis was carried out in electro-spray ionization positive (ESI+) mode. Peptide and trypsin digest products were quantified by M/Z peak area analysis. Data was normalized to peptide abundance at T_0, and half-life was measured by curve-fitting and solving for 50% abundance. Trypsin assays were carried out in triplicate. Trypsin activity towards a control substrate, 250 μM Nα-benzoyl-L-Arginine Ethyl Ester (BAEE), was run before each test to confirm enzyme activity.

2.4.10   Cell migration assay

Cell migration assay was performed using Chemicon Assay Kits (ECM510, ECM555; Billerica, MA, USA) according to manufacturer's protocol. Briefly, sub-confluent cultures of RHAMM-overexpressing (LR21) cells were serum-starved overnight before plating $7.5x10^4$ cells in the upper chamber of the Boyden chamber either in the presence or absence of 10 ng/mL of peptide. 30% fetal bovine serum in DMEM was used as the chemo-attractant in the lower chamber. The number of cells that had crossed the membrane after 20 hours was assessed using the CyQUANT® GR Dye and lysis buffer solution provided in the kit. Fluorescence was measured with a fluorescent plate reader using a 480/520 nm filter set.

2.4.11   RAW-blue macrophage reporter assay

To determine the effect of various peptides on inflammation, commercially available murine RAW 264.7 macrophages carrying a SEAP reporter that is inducible by NF-κB (RAW-Blue; InvivoGen, San Diego, CA, USA) were used. Cells were grown to 80% confluence in DMEM containing 4.5 g/L glucose, 10% heat-inactivated fetal bovine serum, 2 mM L-glutamine, 50μg/mL penicillin/streptomycin, 100 μg/mL Normocin (InvivoGen) at 37°C in 5% CO_2. For peptide screening experiments, cells were scraped in growth medium, counted, and plated to flat-bottom 96-well plates at a density of $5x10^4$ cells/well either in the presence or absence (control) of 200 ng/mL TLR1/TLR2 agonist PAM3CSK4 (InvivoGen). RHAMM peptides were added in 6 replicate wells at a dose of 10 ng/mL in the presence of PAM3CSK4. After 18 hours of stimulation, SEAP concentrations (indicating NF-κB activity) were measured in the supernatants collected from the RAW-Blue cells using QUANTI-Blue reagent (InvivoGen). After 20 minutes of incubation at 37°C, SEAP levels were determined using spectrophotometry at a wavelength of 630 nm.

2.4.12   TGF-β-induced fibrosis assay

IMR90 human fetal lung fibroblasts were obtained from ATCC and maintained in DMEM supplemented with 10% fetal bovine serum. In order to examine the effect of RHAMM peptides on myofibroblast differentiation, 80% confluent cultures were serum starved overnight prior to addition of TGF-β (2 ng/mL, R&D Systems). Cells were treated with TGF-β for 24 hours prior to addition of RHAMM peptides (10ng/mL). 48 hours after addition of

peptides, culture supernatants were collected and levels of active TGF-β measured using commercially available TGF-β ELISA (Quantikine, R&D Systems).

2.5 References

(1) Siegel, R. L., Miller, K. D., and Jemal, A. (2015) Cancer Statistics, 2015. *CA Cancer J. Clin. 65*, 5–29.

(2) Weigelt, B., Peterse, J. L., and van't Veer, L. J. (2005) Breast cancer metastasis: markers and models. *Nat. Rev. 5*, 591–602.

(3) Ween, M. P., Oehler, M. K., and Ricciardelli, C. (2011) Role of versican, hyaluronan and CD44 in ovarian cancer metastasis. *Int. J. Mol. Sci. 12*, 1009–1029.

(4) Tolg, C., Hamilton, S. R., Zalinska, E., McCulloch, L., Amin, R., Akentieva, N., Winnik, F., Savani, R., Bagli, D. J., Luyt, L. G., Cowman, M. K., McCarthy, J. B., and Turley, E. A. (2012) A RHAMM mimetic peptide blocks hyaluronan signaling and reduces inflammation and fibrogenesis in excisional skin wounds. *Am. J. Pathol. 181*, 1250–1270.

(5) Yang, B., Yang, B. L., Savani, R. C., and Turley, E. A. (1994) Identification of a common hyaluronan binding motif in the hyaluronan binding proteins RHAMM, CD4 and link protein. *EMBO J. 1*, 286–296.

(6) Hirose, Y., Saijou, E., Sugano, Y., Takeshita, F., Nishimura, S., Nonaka, H., Chen, Y.-R., Sekine, K., Kido, T., Nakamura, T., Kato, S., Kanke, T., Nakamura, K., Nagai, R., Ochiya, T., and Miyajima, A. (2012) Inhibition of Stabilin-2 elevates circulating hyaluronic acid levels and prevents tumor metastasis. *Proc. Natl. Acad. Sci. U.S.A. 109*, 4263–4268.

(7) Ziebell, M. R., and Prestwich, G. D. (2004) Interactions of peptide mimics of hyaluronic acid with the receptor for hyaluronan mediated motility (RHAMM). *J. Comput. Aided. Mol. Des. 18*, 597–614.

(8) Yang, B., Zhang, L., and Turley, E. A. (1993) Identification of two hyaluronan-binding domains in the hyaluronan receptor RHAMM. *J. Biol. Chem. 268*, 8617–8623.

(9) Hall, C. L., Yang, B., Yang, X., Zhang, S., Turley, M., Samuel, S., Lange, L. A., Wang,

C., Curpen, G. D., Savani, R. C., Greenberg, A. H., and Turley, E. A. (1995) Overexpression of the hyaluronan receptor RHAMM is transforming and is also required for H-ras transformation. *Cell 82*, 19–28.

(10) Tolg, C., McCarthy, J. B., Yazdani, A., and Turley, E. A. (2014) Hyaluronan and RHAMM in Wound Repair and the "Cancerization" of Stromal Tissues. *Biomed Res. Int. 2014*, 1–18.

(11) Veiseh, M., Kwon, D. H., Borowsky, A. D., Tolg, C., Leong, H. S., Lewis, J. D., Turley, E. A., and Bissell, M. J. (2014) Cellular heterogeneity profiling by hyaluronan probes reveals an invasive but slow-growing breast tumor subset. *Proc. Natl. Acad. Sci. U.S.A. 111*, E1731–E1739.

(12) Fieber, C., Plug, R., Sleeman, J., Dall, P., Ponta, H., and Hofmann, M. (1999) Characterisation of the murine gene encoding the intracellular hyaluronan receptor IHABP (RHAMM). *Gene 226*, 41–50.

(13) Ziebell, M. R., Zhao, Z.-G., Luo, B., Luo, Y., Turley, E. A., and Prestwich, G. D. (2001) Peptides that mimic glycosaminoglycans: high-affinity ligands for a hyaluronan binding domain. *Chem. Biol. 8*, 1081–1094.

(14) Holgersson, J., Gustafsson, A., and Breimer, M. E. (2005) Characteristics of protein-carbohydrate interactions as a basis for developing novel carbohydrate-based antirejection therapies. *Immunol. Cell Biol. 83*, 694–708.

(15) Craik, D. J., Fairlie, D. P., Liras, S., and Price, D. (2013) The Future of Peptide-based Drugs. *Chem. Biol. Drug Des. 81*, 136–147.

(16) Mummert, M. E., Mohamadzadeh, M., Mummert, D. I., Mizumoto, N., and Takashima, A. (2000) Development of a Peptide Inhibitor of Hyaluronan-mediated Leukocyte Trafficking. *J. Exp. Med. 192*, 769–779.

(17) Bahrami, S. B., Tolg, C., Peart, T., Symonette, C., Veiseh, M., Umoh, J. U., Holdworth, D. W., McCarthy, J. B., Luyt, L. G., Bissell, M. J., Yazdani, A., and Turley, E. A. (2017) Receptor for hyaluronan mediated motility (RHAMM/HMMR) is a novel target for

promoting subcutaneous adipogenesis. *Integr. Biol. 9*, 223–237.

(18) Hill, T. A., Shepherd, N. E., Diness, F., and Fairlie, D. P. (2014) Constraining cyclic peptides to mimic protein structure motifs. *Angew. Chemie - Int. Ed. 53*, 2–24.

(19) Estieu-Gionnet, K., and Guichard, G. (2011) Stabilized helical peptides: overview of the technologies and therapeutic promises. *Expert Opin. Drug Discov. 6*, 937–963.

(20) Walensky, L. D., and Bird, G. H. (2014) Hydrocarbon-stapled peptides: Principles, practice, and progress. *J. Med. Chem. 57*, 6275–6288.

(21) Henchey, L. K., Jochim, A. L., and Arora, P. S. (2008) Contemporary strategies for the stabilization of peptides in the α-helical conformation. *Curr. Opin. Chem. Biol. 12*, 692–697.

(22) Arispe, N., Diaz, J. C., and Flora, M. (2008) Efficiency of Histidine-Associating Compounds for Blocking the Alzheimer's A b Channel Activity and Cytotoxicity *95*, 4879–4889.

(23) Felix, A. M., Wang, C.-T., Campbell, R. M., Toome, V., Fry, D. C., and Madison, V. S. (1992) Biologically active cyclic (lactam) analogs of growth hormone-releasing factor: Effect of ring size and location on confirmation and biological activity, in *Peptides: Chemistry and Biology*, pp 77–79. ESCOM Science Publishers B. V., Cambridge.

(24) Houston, M. E., Gannon, C. L., Kay, C. M., and Hodges, R. S. (1995) Lactam Bridge Stabilization of a-Helical Peptides : Ring Size , Orientation and Positional Effects. *J. Pept. Sci. 1*, 274–282.

(25) Nielsen, D. S., Hoang, H. N., Lohman, R. J., Hill, T. A., Lucke, A. J., Craik, D. J., Edmonds, D. J., Griffith, D. A., Rotter, C. J., Ruggeri, R. B., Price, D. A., Liras, S., and Fairlie, D. P. (2014) Improving on Nature: Making a Cyclic Heptapeptide Orally Bioavailable. *Angew. Chemie - Int. Ed. 53*, 12059–12063.

(26) Shepherd, N. E., Hoang, H. N., Abbenante, G., and Fairlie, D. P. (2005) Single Turn Peptide Alpha Helices with Exceptional Stability in Water. *J. Am. Chem. Soc. 127*, 2974–2983.

(27) Hu, K., Geng, H., Zhang, Q., Liu, Q., Xie, M., Sun, C., Li, W., Lin, H., Jiang, F., Wang, T., Wu, Y., and Li, Z. (2016) An In-tether Chiral Center Modulates the Helicity, Cell Permeability, and Target Binding Affinity of a Peptide. *Angew. Chemie - Int. Ed. 55*, 8013–8017.

(28) Speltz, T. E., Fanning, S. W., Mayne, C. G., Fowler, C., Tajkhorshid, E., Greene, G. L., and Moore, T. W. (2016) Peptides with γ -Methylated Hydrocarbon Chains for the Estrogen Receptor/Coactivator Interaction. *Angew. Chemie - Int. Ed. 55*, 4252–4255.

(29) Hilinski, G. J., Kim, Y., Hong, J., Kutchukian, P. S., Crenshaw, C. M., Berkovitch, S. S., Chang, A., Ham, S., and Verdine, G. L. (2014) Stitched α - Helical Peptides via Bis Ring-Closing Metathesis. *J. Am. Chem. Soc. 136*, 12314–12322.

(30) Pelton, J. T., and Mclean, L. R. (2000) Spectroscopic Methods for Analysis of Protein Secondary Structure. *Anal. Biochem. 176*, 167–176.

(31) Schafmeister, C. E., Po, J., and Verdine, G. L. (2000) An All-Hydrocarbon Cross-Linking System for Enhancing the Helicity and Metabolic Stability of Peptides. *J. Am. Chem. Soc. 122*, 5891–5892.

(32) Nguyen, L. T., Chau, J. K., Perry, N. A., de Boer, L., Zaat, S. A. J., and Vogel, H. J. (2010) Serum Stabilities of Short Tryptophan- and Arginine-Rich Antimicrobial Peptide Analogs. *PLoS One 5*, 11–18.

(33) Mashalidis, E. H., Sledz, P., Lang, S., and Abell, C. (2013) A three-stage biophysical screening cascade for fragment-based drug discovery. *Nat. Protoc. 8*, 2309–2324.

(34) Park, H., Lee, S. J., Oh, J., Lee, S., Jeong, Y., and Lee, H. C. (2015) Smart Nanoparticles Based on Hyaluronic Acid for Redox-Responsive and CD44 Receptor-Mediated Targeting of Tumor. *Nanoscale Res. Lett. 10*, 1–10.

(35) Zaman, A., Cui, Z., Foley, J. P., Zhao, H., Grimm, P. C., Delisser, H. M., and Savani, R. C. (2005) Expression and Role of the Hyaluronan Receptor RHAMM in Inflammation after Bleomycin Injury. *Am. J. Cell Mol. Biol. 33*, 447–454.

(36) Balkwill, F., and Mantovani, A. (2001) Inflammation and cancer: back to Virchow?

Lancet 357, 539–545.

Chapter 3

3 Structure activity relationship studies of cyclic peptides comprised of the second hyaluronan binding domain of RHAMM

3.1 Introduction

3.1.1 Difference between *Mus musculus* and *Homo sapiens* sequences

The use of *Mus musculus* in research is a practice that dates back to 1910[1]. This is because *M. musculus* and *Homo sapiens* share a common ancestor, allowing for a high degree of homology between the genomes[2]. Approximately 80% of genes within the *M. musculus* sequence have a single homologue in the *H. sapiens* genome, with both genomes encoding for approximately 30,000 proteins[2]. This homology allows for the translation of results from mouse models to humans. In the previously described work, in which the secondary structure of the hyaluronan binding domains (HABDs) of the receptor for hyaluronan mediated motility (RHAMM) were stabilized by cyclization, the RHAMM sequences that were used were drawn from the genome of *M. musculus*. The *M. musculus* and *H. sapiens* sequences of full length RHAMM have 85 percent homology, with HABD1 having 100 percent homology and HABD2 having 71 percent homology with two conservative changes[3] (Figure 3.1).

633 NLKQKIKHVVKLKDENSQLKSEVSKLRCQLAKKKQS **669**
NLKQKIKHVVKLKDENSQLKSEVSKLR QL K+ KQ+
716 NLKQKIKHVVKLKDENSQLKSEVSKLR SQLVKRKQN **752**

Figure 3.1 - Sequences of RHAMM from *Homo sapiens* (top) and *Mus musculus* (bottom). HABD1 is highlighted in red and HABD2 is highlighted in green. The homologous sequences are seen (middle) with non-conserved changes seen as a blank and a conserved change as a +.[3]

The *H. sapiens* sequence was not originally used for the HABD modifications, as the second hyaluronan binding domain (HABD2) sequence contains a cysteine residue (position 744). Cysteine can cause issues during solid-phase peptide synthesis due to racemization during coupling steps or formation of intermolecular disulfide bonds via oxidation[4]. These problems can be avoided by using alternative coupling reagents or by removing the cysteine residue from the sequence. Therapeutics containing free thiols can result in oxidation before or after administration of the drug, therefore changing its composition and potential effects[5]. Changing the cysteine to another amino acid (such as serine in the *M. musculus* sequence) would eliminate this problem and would provide a more stable drug for *in vivo* use. In order to identify the impact that this sequence change to *H. sapiens* would have on binding to hyaluronan (HA), its effect on helicity and binding was investigated.

3.1.2   Identifying essential residues for binding

The hyaladherin group of proteins, which all bind HA, have a conserved binding region that can provide insight on how these proteins interact with this polysaccride[6]. The binding regions of the hyaladherins include the previously mentioned BX_7B binding motif, where seven non-acidic residues separate two basic residues in order to provide adequate spacing[6]. There are four basic residues within HABD2; if helicity can be introduced in this sequence via cyclization of two amino acid side chains, the basic residues are likely to be positioned more optimally, facilitating interaction with HA. However, if only two basic residues are needed to provide the proper BX_7B motif remains, it would allow for further peptide modifications and ultimately an improved sequence with increased affinity to HA. Reducing the number of positively charged residues may also be beneficial for future development of this cyclic peptide as a therapeutic.

Alanine scans are a method used to identify the necessary residues for functional activity of a peptide, such as target binding or bioactivity. An alanine scan involves creating a series of peptides in which one amino acid in the sequence is replaced with alanine, and comparing the activity of the alanine-containing sequences to the parent sequence. This has been used to yield important functional information and can provide insight into how the parent sequence can be further modified to increase activity[7–9]. Alanine is utilized because its side chain does not continue past the β-carbon, and therefore determines whether the side

chain of the replaced amino acid is important for bioactivity[7]. Alanine is a helix-stabilizing residue; however, the loss of the side chain functionality may disrupt the secondary structure[10]. An alanine scan was completed on the lead helical lactam-bridged peptide (**15**) to identify which basic residues were essential for binding to HA, as well as to determine how the positioning of those positive charges in the sequence affects binding to HA.

3.2 Results and Discussion

3.2.1 *H. sapiens* sequence

The linear and the cyclized version of the *H. sapiens* RHAMM sequence were synthesized to compare them to the *M. musculus* sequence reported in Chapter 2 (Table 3.1). These peptides were synthesized as previously mentioned through solid phase peptide synthesis. However, when cleaving the linear peptide from the resin, dithiothritol (DTT) was employed due to the presence of cysteine. DDT is a redox reagent that will help reduce the chance of the oxidation of the thiol or the formation of intermolecular bonds during the reaction.

Table 3.1 - *H. sapiens* linear and cyclized (*i, i+4*) sequences of HABD2. Both sequences were amidated on the C-terminus and acetylated on the N-terminus. Mean residue ellipticity values at 222 nm, ratios of mean residue ellipticities at 222/208 nm and percentage helicity at 25°C are reported.

Cmpd	Sequence	Species	Water		Water/40% TFE	
			$\theta_{222}/\theta_{208}$	% Helicity	$\theta_{222}/\theta_{208}$	% Helicity
12	Ac-VSKLRSQLVKRKQN-NH$_2$	*M. musculus*	0.23	14.8	0.72	40.9
15	cyclo-6,10(Ac-VSKLR[EQLVK]RKQN-NH$_2$)		0.61	28.0	0.79	44.8
19	Ac-VSKLRCQLLAKKKQS-NH$_2$	*H. sapiens*	0.22	22.9	0.75	79.6
20	cyclo-6,10(Ac-VSKLR[EQLAK]KKQS-NH$_2$)		0.79	82.5	0.86	91.6

The helicity of the *H. sapiens* sequences (**19** and **20**) was evaluated and compared with their *M. musculus* equivalents (**12** and **15**). The *H. sapiens* linear sequence (**19**) has comparable percent helicity to the linear sequence of *M. musculus* (**12**). However, the cyclized version of *H. sapiens* (**20**) has an increase in helicity over the *M. musculus* (**15**), which might be due to the non-conserved amino acids aiding in helical formation. When examining the CD spectra of the compounds, the *H. sapiens* sequence (**20**) has greater minima at 222 nm and 208 nm than compound **15** (the *M. musculus* sequence), which is indicative of greater α-helical character (Figure 3.2).
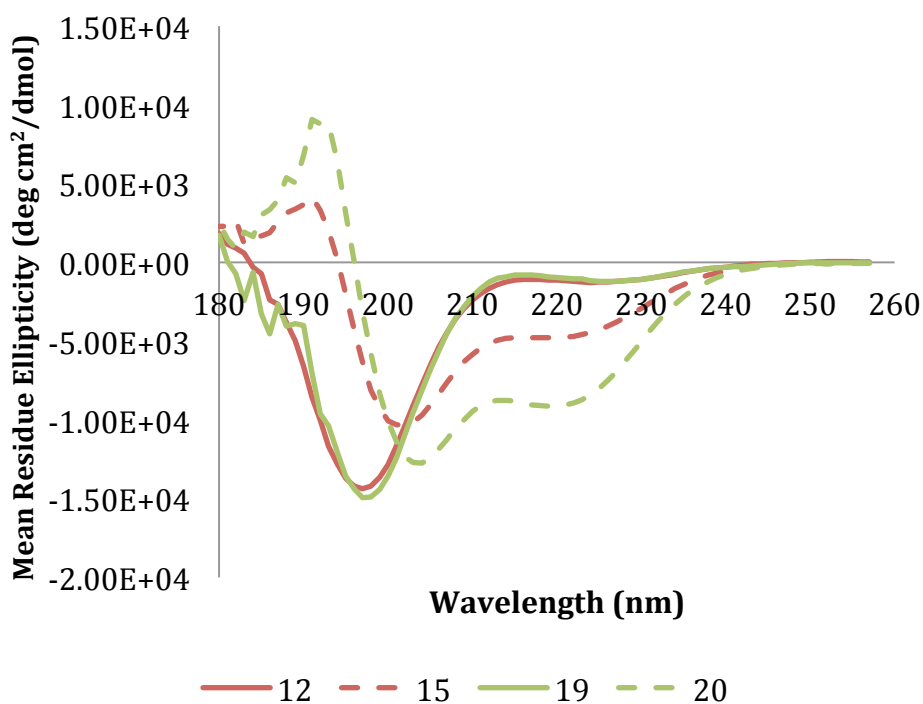
Figure 3.2 - CD spectra of the linear and cyclized sequences from *M. musculus* (12 and 15) compared with the linear and cyclized sequences from *H. sapiens* (19 and 20).

The peptides were evaluated for their ability to bind HA, as it was hypothesized that an increase in helicity would correlate to an increase in binding affinity. Both linear sequences (**12** and **19**) showed comparable binding to HA, while the cyclized peptide from *M. musculus* (**15**) still exhibited the strongest binding interaction (Figure 3.3).
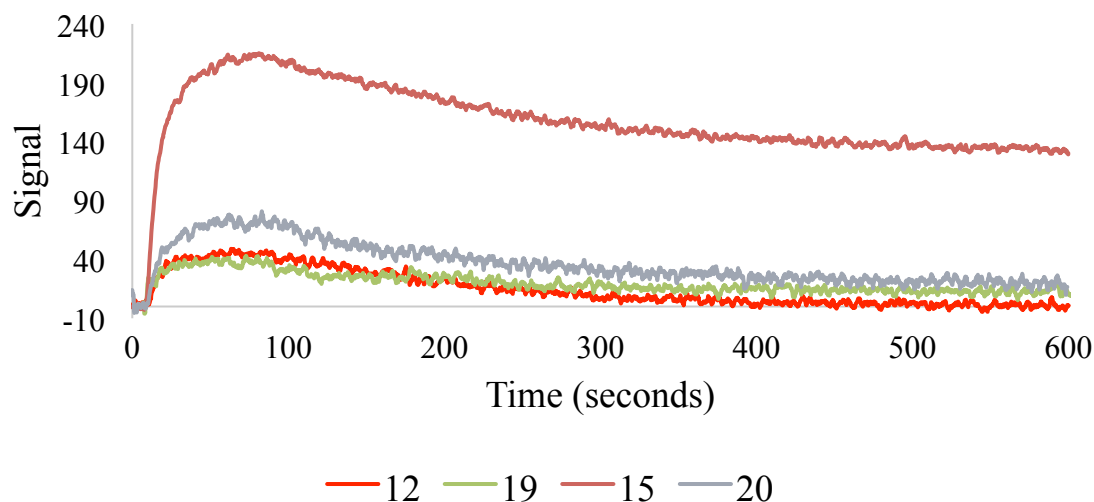
Figure 3.3 - SPR binding curves for both *M. musculus* sequences (12 and 15) and *H. sapiens* sequences (19 and 20) that was passed over HA-coated gold chip at a concentration of 25 μM.

The binding affinities were determined from the SPR data, and it can be observed that cyclizing the *H. sapiens* sequence (**20**) did improve the binding when compared to the linear counterpart (**19**), but affinity was not as the cyclized peptide derived from *M. musculus* (**15**) (Table 3.2).

Table 3.2 - The calculated K_D values determined by SPR for the *M. musculus* and *H. sapiens* sequences from HABD2.

Cmpd	Species	K_D (μM)
12	*M. musculus*	1076
15		1.0
19	*H. sapiens*	1660
20		16.2

The HABD2 sequences of *H. sapiens* and *M. musculus* are 71 percent homologous, but the differences have an effect upon binding to HA. Despite there being an increase in helicity, the conformation of the *H. sapiens* sequence might not permit for the proper

orientation of the binding residues; for instance, these residues might not be solvent exposed, causing a decrease in binding.

3.2.2 Alanine scan to identify essential binding residues

An alanine scan was completed in order to identify the essential binding residues within compound **15**. This involved the replacement of two of the four basic residues in the sequence with alanine residues, resulting in only one basic residue on either side of the staple (Table 3.3). If only one basic residue at a time was replaced with alanine, then there is the potential for the remaining basic residues to mask the contribution of the lost residue.

Table 3.3 - Comparison of the helicity of compound 15 and the resulting sequences resulting from the alanine scan of its basic residues (21-24). All sequences were amidated on the C-terminus and acetylated on the N-terminus. Mean residue ellipticity values at 222 nm, ratios of mean residue ellipticities at 222/208 nm and percentage helicity that were determined at 20°C.

Cmpd	Sequence	Water		Water/40% TFE	
		$\theta_{222}/\theta_{208}$	% Helicity	$\theta_{222}/\theta_{208}$	% Helicity
15	cyclo-6,10(Ac-VSKLR[EQLVK]RKQN-NH$_2$)	0.61	55.9	0.79	75.7
21	cyclo-6,10(Ac-VSKLA[EQLVK]RAQN-NH$_2$)	0.84	88.0	0.84	87.9
22	cyclo-6,10(Ac-VSKLA[EQLVK]AKQN-NH$_2$)	0.82	80.9	0.84	86.5
23	cyclo-6,10(Ac-VSALR[EQLVK]RAQN-NH$_2$)	0.60	58.1	0.82	81.0
24	cyclo-6,10(Ac-VSALR[EQLVK]AKQN-NH$_2$)	0.72	69.8	0.83	84.3

The CD spectra and resulting percentage helicity of the alanine scan peptides showed that three of the four peptides had increased α-helical character (**21**, **22**, and **24**) (Figure 3.4). It was hypothesized that the same degree of helicity would be introduced in each sequence, as the same two helix-stabilizing residues were introduced in all cases. However, when a basic residue immediately preceding or following the staple is replaced with an alanine there

is an increase in helicity, suggesting that the charged side chain of these basic residues may have had a negative impact on the helicity of the sequences. This indicates that the placement of basic residues is important in determining the optimal helicity, as compound **23** has the basic residues surrounding the staple within the sequence and it contains the least amount of helicity.
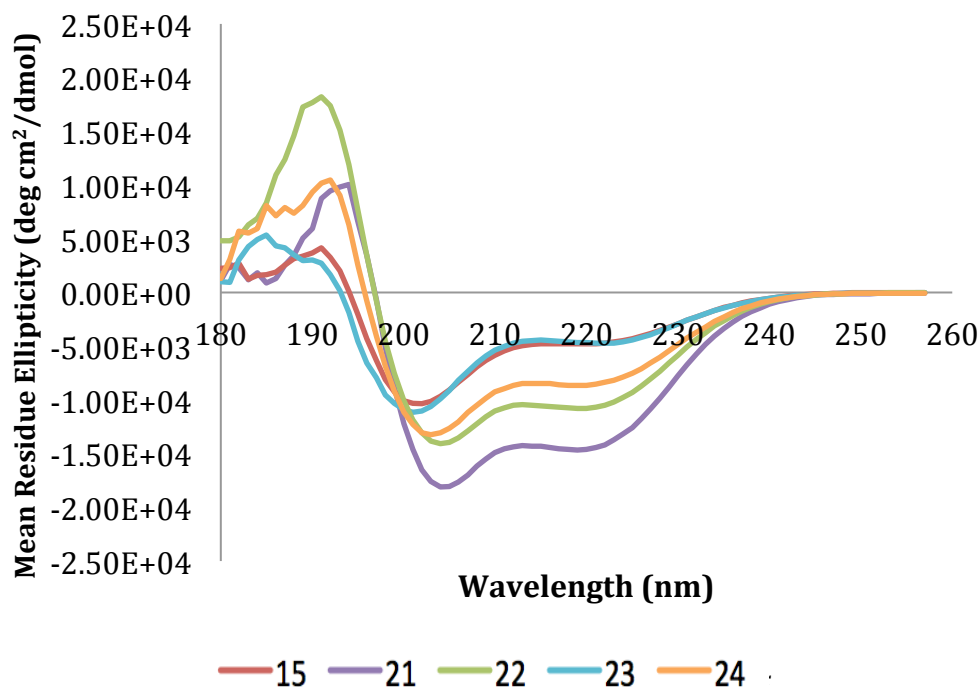
Figure 3.4 - CD spectra from the lead cyclic peptide from HABD2 (15) compared with the alanine scan sequences (21-24).

Of the alanine scan compounds, compound **21** has the greatest increase in helicity compared to compound **15,** and has a 4-fold increase in helicity compared to the linear sequence of HABD2 (compound **12**).

The alanine scan peptides were next analyzed by SPR to identify the peptides' binding to HA compared to the lead sequence (**15**). These peptides were passed over the 5-10 kDa HA-coated chip at various concentrations as previously described in order to determine their binding kinetics; the absorbance readings of each peptide were also plotted together to compare their signals intensities at identical concentrations (Figure 3.5).
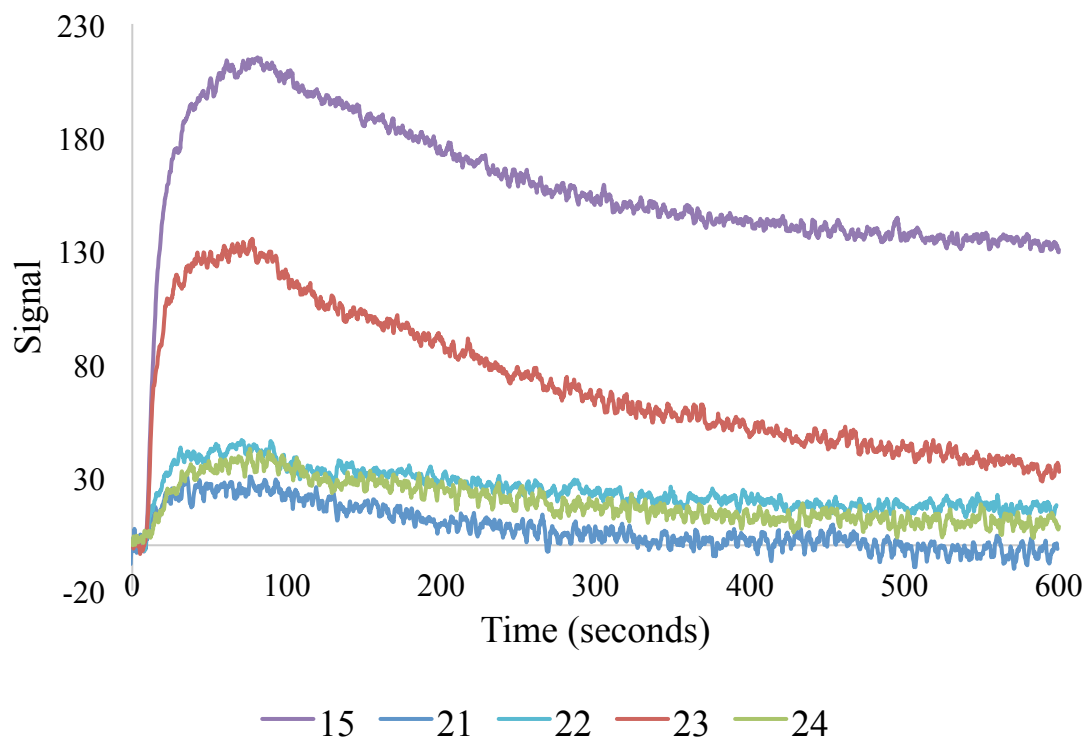
Figure 3.5 - SPR binding curves for the lead cyclic peptide from HABD2 (15) and the alanine scan sequences (21-24) that were passed over HA-coated gold chip at a concentration of 25 μM.

Compound **15** still had the greatest signal intensity and the strongest binding affinity (1.01 μM) towards HA, but peptide **23** showed comparable binding to HA with a K_D of 3.08 μM. Compound **21**, which had the greatest increase in helicity, actually had diminished binding, with a K_D that was higher than the linear sequence (Table 3.4). The other sequences that had improved helicity (**22** and **24**), had worse binding compared to that of **15** and **23**. Site-directed mutagenesis of the HABDs of RHAMM discovered that the removal of the basic residue at the beginning of HABD2 (K3 in the cyclic peptides mimicking HABD2) was critical for binding of the RHAMM protein to HA[6]. Compounds **23** and **24** have this K3 residue replaced with an alanine, but have greater affinity to HA compared to **21** and **22** (where K3 is present). This highlights one of the differences between the properties of these cyclic peptides mimicking RHAMM and the full-length protein.

Table 3.4 - The calculated K_D values determined by SPR for the alanine scan sequences

Cmpd	K_D (μM)
21	4058
22	11
23	3.0
24	8.5

Compound **21** has the proper BX_7B binding motif that was previously hypothesized to be essential for binding to HA. However, these results show compound **21** has worse binding to HA when compared to the other alanine sequences (**22-24**), and yet these sequences do not have the exact BX_7B motif. The diminished binding of compound **21** despite the large increase in helicity may be due to the positioning of the remaining basic residues in the sequence when folded. This can be determined using a helical-wheel projection, which shows the position of the amino acids in a sequence assuming that this sequence allows for the formation of a perfect helix[11]. Helical wheel projections can be used to gain an approximate understanding of where these basic residues fall in relation to the staple; as these sequences do not form a perfect α-helix, the reported positions are understood not to be the exact locations of the residues (Figure 3.6).
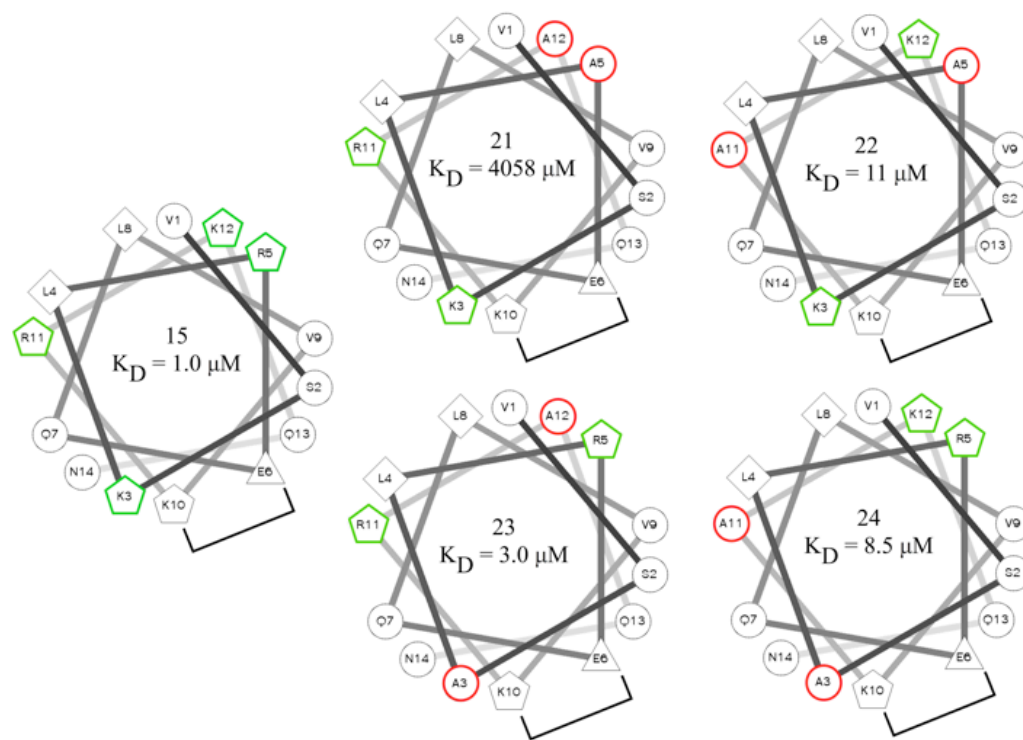
Figure 3.6 - Helical wheel projection of the best cyclized sequence of HABD2 (15) and the sequences resulting from the alanine scan of the basic residues (21-24). The basic residues are highlighted in green and the alanine residues are in red.

When the Lys-12 and Arg-5 are both replaced by an alanine residue (as in compound **21**), only Arg-11 and Lys-3 remain available for binding. These two residues are close to the lactam bridge and are separated by Asn-14 and Gln-7. Asn and Gln both have long side chains that could interfere with the binding of Lys/Arg to HA. All other sequences have improved binding to HA when compared to **21**, and this might be due to the presence of a basic residue on the opposite face of the helix to the staple. The placement of residues away from the staple appears to be imperative for binding, as compound **21** shows that a lack of residues placed opposite to the staple results in a loss of binding. Compound **23** is seen to have comparable binding to that of the best cyclic sequence (**15**), and this might be because of an optimal spacing in the helical wheel of the basic residues. In addition, the amino acids separating the basic residues in **23** (Leu and Val) have short, nonpolar side chains, which are less likely to interact with HA than amino acids that have longer, polar side chains.

3.3   Conclusions

As the cyclized peptide with the best binding to HA, compound **15** remains the lead sequence across both HABD1 and HABD2 of RHAMM. The cyclic peptide derived from the *H. sapiens* RHAMM sequence had improved helicity over the original *M. musculus* sequence but did not bind HA as strongly. The replacement of two basic residues with alanine residues also did not result in the positive correlation between helicity and binding to HA that was previously seen in the HABD2 staple scan. In these instances, the specific residue replaced by alanine appeared to be of importance: the placement of the positive residues on the opposite face of the helix than to staple was required in order to bind HA. This was modeled by the helical-wheel projection, which demonstrated that the placement of the staple close to the two remaining basic residues within the sequence resulted in loss of binding.

It can also be seen that the there is not a need for the specific BX_7B binding motif for cyclic peptides that mimic HABD2. Compound **21,** the only alanine scan sequence that has the BX_7B motif, was not able to bind to HA ($K_D = 4058$ μM), while compound **23**, that has a BX_5B motif, had comparable binding to HA as the lead cyclic peptide (**15**) ($K_D = 3.0$ μM for **23**; $K_D = 1.0$ μM for **15**). It can be concluded that the positioning of the positive residues in three-dimensional space within these cyclic peptide sequences is the most important determinant for binding. This allows for a better understanding of how these cyclic peptides differ from that of the full protein sequence of RHAMM. This information on interactions between ligands and cyclic peptide mimics can assist in the design of more peptide therapeutics that inhibits protein-carbohydrate interactions.

3.4   Experimental

3.4.1   General information

All Fmoc-protected amino acids were obtained from ChemImpex. HCTU, HATU, and Rink Amide MBHA Resin (4-(2',4'-dimethoxyphenyl-(9-fluorenylmethoxycarbonyl)-aminomethyl)-phenoxy-acetamidonorleucyl-4-methyl benzhydrylamine resin) were obtained from ChemImpex. Tetrakis(triphenylphosphine)palladium(0), phenylsilane, Fmoc-AEEA spacer, and NHS-Biotin were obtained from Sigma-Aldrich. All solvents were obtained from

Fischer Thermo-Scientific.

3.4.2   Solid-phase peptide synthesis

Fmoc-based solid-phase synthesis was carried out by either manual synthesis using a fritted glass peptide vessel or by automated synthesis using a Biotage® Syro *Wave*™ automated peptide synthesizer. Synthesis was performed on a 0.1 mmol scale with 0.52 mmol/g Fmoc-Rink amide MBHA resin and a 3-fold excess of the protected amino acids. The resin was swelled in CH_2Cl_2 (2.0 mL, 15 minutes) then rinsed with DMF (1.0 mL, 1 min). Fmoc deprotection was performed with a solution of 20% piperidine/DMF (1.5 mL) 5 minutes, then washed with three times with DMF (2.0 mL, vortex 30 seconds) and then again for 15min with 20% piperidine/DMF (1.5 mL). The resin was further washed with DMF six times (2.0 mL, vortex 30 seconds). A Kaiser test was performed after the Fmoc removal to verify the presence of a free primary amino group. Fmoc-protected amino acid (0.3 mmol) and HCTU (0.3 mmol) was dissolved in DMF (1.5 mL) and added to the resin. The mixture was vortexed for 30 seconds and then DIPEA (0.6 mmol) was added to the mixture and vortexed for 1 hour. The deprotection/amino acid coupling cycle was repeated until the desired amino acid sequence was obtained. After the final amino acid was coupled, the resin was washed with DMF (3x) and CH_2Cl_2 (3x) and then dried under vacuum and stored in the freezer (-20 °C). Removal of the N-terminal Fmoc protecting group was achieved using the previously described deprotection procedure. Cleavage of the peptide from the resin and side chain protecting groups was performed by adding a solution of 95% trifluoroacetic acid/2.5% triisopropylsilane/2.5% water (3 mL) to the resin and vortexing for 4-5 hours. After filtration, the peptide was precipitated with cold *tert*-butyl methyl ether (TBME) (20 mL) and collected by centrifugation. The mother liquor was decanted, the pellet dissolved in water (20mL) and lyophilized to obtain the crude fully deprotected peptide.

3.4.3   Deprotection of the allyloxycarbonyl (Alloc) and allylester (OAll) protecting groups

Selective deprotection of the allyloxycarbonyl and the allylester protecting groups was accomplished by adding CH_2Cl_2 (4.5 mL) to the resin-bound peptide and shaking gently for 10 minutes. After addition of phenylsilane (24 eq), the peptide vessel was flushed with

nitrogen for 5 minutes. Tetrakis(triphenylphosphine) palladium (0) (0.1 eq) was then added to the mixture and the peptide vessel was again flushed with nitrogen, and the reaction was allowed to proceed for 10 minutes. The peptide-resin was washed with CH_2Cl_2 (4 x 30 seconds), followed by a series of washings with CH_2Cl_2, DMF, MeOH, DMF, and CH_2Cl_2 (30 seconds each).

3.4.4   Lactam bridge formation

After selective deprotection of alloc and allyl ester groups, HATU (3 eq) was dissolved in DMF (1.5 mL), added to the resin and vortexed for 30 seconds. DIPEA (6 eq) was then added and the reaction was vortexed for 2 hours. The resin was rinsed with DMF and CH_2Cl_2 (2.0 ml, 3 x 30 seconds each) to remove any residual reactants.

3.4.5   Purification by RP-HPLC/ESI-MS

Peptides were analyzed using a reverse-phase analytical HPLC column (Agilent Zorbax SB-C18 column 4.6 x 150 mm, 3.5 μm). This system was equipped with a Waters 600E Multisolvent Delivery System, Waters 600 controller, Waters inline degasser, and Waters Masslynx software (version 4.1). Employed mobile phases were 0.1% TFA in Milli-Q water (eluent A) and 0.1% TFA in acetonitrile (eluent B). The flow rate was set at 1.5 mLmin^{-1} with a gradient elution over a 12 minute gradient. The column eluent was monitored using a Waters 2998 Photodiode array detector. Peptides were purified using a reversed-phase preparative HPLC column (Agilent Zorbax SB-C18 column 21.2 x 150 mm, 5 μm) on the same system described above. The detection method and eluents were the same as the analytical system, with the flow rate was set at 20 mLmin^{-1}. The collected fractions were then lyophilized to a solid and analyzed by ESI-MS. Purity of final products was determined by an Acquity UHPLC-MS (220 nm).

3.4.6   Circular dichroism (CD) spectroscopy

CD spectra were obtained on a Jasco J-810 spectropolarimeter and recorded in the range of 180-260 nm. Peptide solutions were prepared with a 0.1 M phosphate buffer solution to a concentration of 0.5 mM. The measurements were performed in quartz cuvettes with a path length of 1 mm and a scanning speed of 10-50 nm/min. Five individual data points were

averaged by the instrument in order to obtain the reported CD spectrum. The measurements were carried out at 20 $^{\circ}$C. A blank solution of 0.1 M phosphate buffer solution was run before every measurement in order to baseline correct for any UV-interference observed from the buffer. Deconvolution of CD spectra were obtained using the CONTINLL program, which is part of the web-based program CdPro (http://lamar.colostate.edu/~sreeram/CDPro/).

3.4.7   Surface plasmon resonance

HA was modified using a literature procedure, with some modifications[12]. 5-10kDa HA (40 mg) was dissolved in DMSO/H$_2$O (7/3, v/v) with an excess amount of sodium cyanoborohydride added. This solution was allowed to stir for 12 hours at room temperature, 10 eq of cystamine was added and the mixture was allowed to stir for a further 24 hours. The solution was then added to a dialysis membrane (MWCO 3.5-5 kDa) where the by-products were removed by dialysis for 3 days followed by lyophilization until a white powder was obtained. SPR experiments were performed with an openSPR (Nicoya Lifesciences, Waterloo, Canada) at 25°C with a 100 µL loading loop and a constant flow rate of 50 µL/min. The cystamine-modified HA was added to a functionalized gold chip by dissolving HA-cystamine (1 mg/mL) in water and incubating for 24 hours at 4°C. Binding of the HABD mimics and the linear sequences were tested in a 10mM solution of phosphate buffered saline (137 mM NaCl, 2.7 mM KCl, 10mM Na$_2$HPO$_4$, 2 mM KH$_2$PO$_4$). The peptides were injected over the bound HA in concentrations from 1 µM to 1 mM for 2 min to allow association. 10 mM PBS was passed over the sensor for 8 min to allow dissociation. After each peptide injection, 1 mM NaCl was injected to completely dissociate the complex and regenerate the HA surface. Data analysis was performed using Trace Drawer software (Ridgeview Instruments AB) as recommended by the manufacturer. Kinetic parameters were calculated using global analysis, fitting the data to a simple 1:1 model.

3.5   References

(1) Morse III, H. C. (2007) Building a better mouse: one hundred years of genetics and biology, in *The Mouse in Biomedical Research* (Fox, J. G., Davisson, M. T., Quimby, F. W., Barthold, S. W., Newcomer, C. E., and Smith, A. L., Eds.) 2nd ed., pp 1–11. Academic Press, Burlington, MA.

(2) Waterston, R. H. (2002) Initial sequencing and comparative analysis of the mouse genome. *Nature 420*, 520–562.

(3) Altschul, S. F., Madden, T. L., Schäffer, A. A., Zhang, J., Zhang, Z., Miller, W., and Lipman, D. J. (1997) Gapped BLAST and PSI-BLAST: a new generation of protein database search programs. *Nucleic Acids Res. 25*, 3389–3402.

(4) Kaiser, T., Nicholson, G. J., Kohlbau, H. J., and W., V. (1996) Racemization Studies of Fmoc-Cys(Trt)-OH during Stepwise Fmoc-Solid Phase Peptide Synthesis. *Tetrahedron Lett. 37*, 1187–1190.

(5) Craik, D. J., Fairlie, D. P., Liras, S., and Price, D. (2013) The Future of Peptide-based Drugs. *Chem. Biol. Drug Des. 81*, 136–147.

(6) Yang, B., Yang, B. L., Savani, R. C., and Turley, E. A. (1994) Identification of a common hyaluronan binding motif in the hyaluronan binding proteins RHAMM, CD4 and link protein. *EMBO J. 1*, 286–296.

(7) Cunningham, B. C., and Wells, J. A. (1989) High-Resolution Epitope Mapping of hGH-Receptor Interactions by Alanine-Scanning Mutagenesis. *Science (80-.). 244*, 1081–1085.

(8) Blaber, M., Baase, W. A., Gassner, N., and Matthews, B. W. (1995) Alanine scanning mutagenesis of the α-Helix 115-123 of phage T4 lysozyme: effects on structure , stability and the binding of solvent. *J. Mol. Biol. 246*, 317–330.

(9) Ashkenazi, A., Prestat, L. G., Marsters, S. A., Camerato, T. R., Rosenthalf, K. A., Fendlyt, B. M., and Capon, D. J. (1990) Mapping the CD4 binding site for human immunodeficiency virus by alanine-scanning mutagenesis. *Proc. Natl. Acad. Sci. USA 87*, 7150–7154.

(10) Shepherd, N. E., Hoang, H. N., Abbenante, G., and Fairlie, D. P. (2005) Single Turn Peptide Alpha Helices with Exceptional Stability in Water. *J. Am. Chem. Soc. 127*, 2974–2983.

(11) Schiffer, M., and Edmundson, A. B. (1967) Use of helical wheels to represent the structures of proteins and to identify segments with helical potential. *Biophys. J. 7*, 121–135.

(12) Park, H., Lee, S. J., Oh, J., Lee, S., Jeong, Y., and Lee, H. C. (2015) Smart Nanoparticles Based on Hyaluronic Acid for Redox-Responsive and CD44 Receptor-Mediated Targeting of Tumor. *Nanoscale Res. Lett. 10*, 1–10.

Chapter 4

4 Conclusions

4.1 Outlooks and Conclusions

An elevated level of the receptor for hyaluronan mediated motility (RHAMM) has been observed in malignant prostate cancer and is correlated with poor prognosis due to increased likelihood of metastases[1]. RHAMM can bind to hyaluronan (HA) to promote cell migration, inflammation, and fibrosis[2]. This interaction primarily occurs ionically between the basic residues present in the two hyaluronan binding domains (HABDs) of RHAMM and the carboxylic acids contained in HA[3,4]. The ability of the basic residues of RHAMM to bind to HA is facilitated by the highly α-helical secondary structure of the protein. To make a more drug-like molecule capable of interfering with RHAMM-HA interactions, truncating the RHAMM sequence to contain only one of the binding domains is more favorable. A truncated peptide would be a more drug-like molecule than the full-length protein, provided that it still maintained affinity for the polysaccharide HA. Also, there is an advantage for a shorter amino acid sequence than a large protein, due to ease of synthesis and lower production costs. However, when the sequence is truncated, the elimination of stabilizing residues causes loss of secondary structure; this would decrease interaction between the peptide and HA. To maintain the secondary structure of this shortened sequence, cyclization via stapling of two amino acid residues can be accomplished. This allows the peptide to overcome the high energetic barrier that is associated with α-helix formation[5]. In this thesis, both HABDs of the protein RHAMM were examined to determine whether a lactam bridge-cyclized peptide could mimic the native interactions of RHAMM towards its endogenous ligand HA.

A staple scan of both HABDs was performed to identify the cyclized sequence that had the best induced helicity and binding to HA. When helicity was examined, the linear sequences of the HABDs were tested in both water and a 40% trifluoroethanol (TFE)/water solution. TFE can act to stabilize secondary structure; therefore the measured helicity of the linear sequence in this solution can be viewed as the theoretical maximum helicity of the sequence. Because these sequences are truncated and do not have the support of stabilizing

residues in the native sequence, it is unlikely they will possess the same degree of helicity as the full protein sequence.

When examining the helicity of the peptides containing HABD1, none of the staples that were introduced achieved the same degree of helicity as the linear sequence in the 40% TFE solution. However, when the staples were introduced to HABD2, there were two sequences that acquired comparable helicity to that of the theoretical maximum helicity. This difference in the effect that the staples had on HABD2 compared to HABD1 could be due to the increased amount of helix stabilizing residues present in the HABD2 sequence.

The ability of all peptides to bind HA was also examined. The linear sequence of HABD1 had greater binding to HA compared to the linear sequence of HABD2. This is opposite of that was seen with the helicity, as HABD1 had a lower helical content than that of HABD2. The introduction of staples to HABD1 increased HA binding in three out of the five sequences tested, while the introduction of staples to HABD2 increased binding for all four sequences tested. The lack of improved binding in two of the HABD1 sequences might be due to the replacement of amino acids essential for binding in order to create the lactam bridge; whereas in HABD2, no such residues were removed.

Through these staple scans, one lead peptide (**15**) produced a significant improvement in helicity and binding to HA. This compound was cyclized between the amino acid residues in position 6 and 10 of HABD2. This cyclized peptide was observed to inhibit migration of cancer cells as well as the release of markers for inflammation and fibrosis. Peptide **15** also had increased stability towards degradation via both trypsin and human serum. Modification of this sequence to mimic the *H. sapiens* sequence was not possible; while the humanized sequence increased helicity, it diminished binding to HA. Results of an alanine scan showed that at least one basic residue must be on the opposite face of the helix relative to the staple location (Figure 4.1). This may be due to the staple blocking the basic residues when on the same face of the helix.
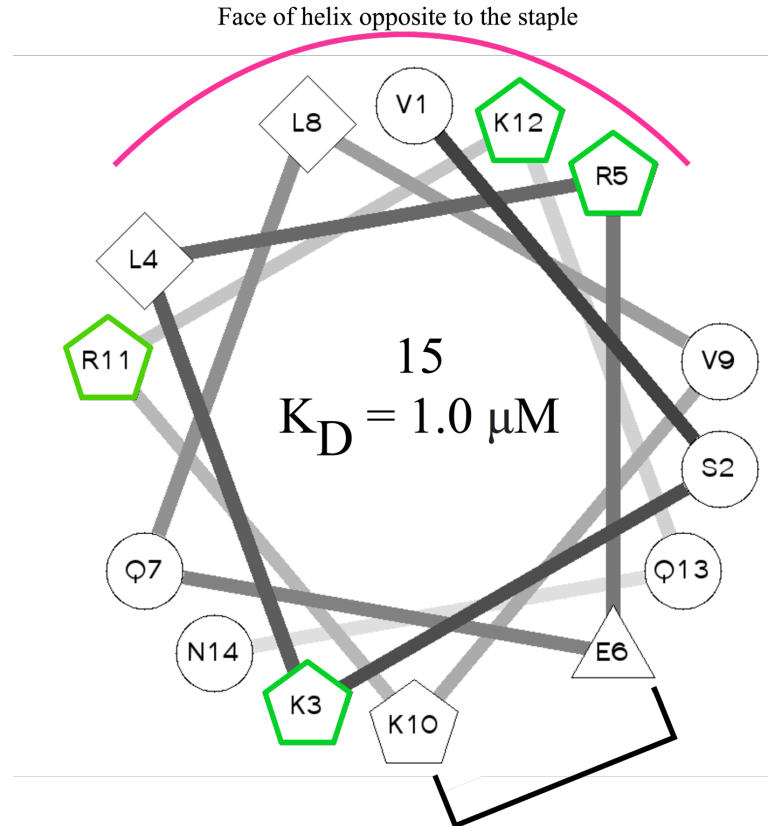
Figure 4.1 - Helical wheel projection of lead cyclic peptide (15). At least one basic residue must be present on the face of the helix that is opposite to the staple for binding to HA.

To create a better drug candidate, this lead cyclized sequence can be further modified to increase helicity while hopefully also improving binding to HA. While there was a positive correlation between helicity and binding to HA present in the HABD2 staple scan, this is not always the case. To further modify this sequence, helix-stabilizing residues could be introduced between the stapling residues as a means of avoiding potential interference with these amino acid side chains with binding to HA.

It is important to further evaluate the structure of this lead cyclized peptide. The secondary structure could be more accurately resolved through the use of crystallography and 2D NMR spectroscopy studies. This would clarify which segments of the sequence contain

an α-helical conformation, as the CD spectral data suggests a combination of secondary structural elements.

Compound **15** has therapeutic potential in the treatment of cancer, such as prostate or breast. Due to its ability to mimic RHAMM, compound **15** can bind to HA and block the native interaction between RHAMM and HA. This can decrease cell migration and the inflammation associated with cancer. Preventing the spread of a primary tumor through decreased cell migration would help to decrease the formation of metastatic tumors, a major cause of complications in cancer treatment[6]. Due to this and many other problems associated with treating metastases, it would be beneficial to stop the parental tumor from spreading. If a RHAMM-overexpressing tumor could be detected and diagnosed at an early stage, then a peptide such as compound **15** could be added to a patient's treatment regimen to prevent metastasis or to slow the tumor's ability to metastasize. This would be a novel therapeutic route for cancer treatment.

4.2 References

(1) Korkes, F., Castro, M. G. De, Zequi, S. D. C., Nardi, L., Giglio, A. Del, and Pompeo, A. C. de L. (2014) Hyaluronan-mediated motility receptor (RHAMM) immunohistochemical expression and androgen deprivation in normal peritumoral , hyperplasic and neoplastic prostate tissue. *BJU Int. 113*, 822–829.

(2) Zaman, A., Cui, Z., Foley, J. P., Zhao, H., Grimm, P. C., Delisser, H. M., and Savani, R. C. (2005) Expression and Role of the Hyaluronan Receptor RHAMM in Inflammation after Bleomycin Injury. *Am. J. Cell Mol. Biol. 33*, 447–454.

(3) Yang, B., Yang, B. L., Savani, R. C., and Turley, E. A. (1994) Identification of a common hyaluronan binding motif in the hyaluronan binding proteins RHAMM, CD4 and link protein. *EMBO J. 1*, 286–296.

(4) Yang, B., Zhang, L., and Turley, E. A. (1993) Identification of two hyaluronan-binding domains in the hyaluronan receptor RHAMM. *J. Biol. Chem. 268*, 8617–8623.

(5) Poland, D., and Scheraga, H. A. (1970) Theory of Helix-Coil Transitions in Biopolymers: Statistical Mechanical Theory of Order-Disorder Transitions in Biological Macromolecules.

Academic Press, New York.

(6) Fidler, I. J. (1999) Critical determinants of cancer metastasis: rationale for therapy. *Cancer Chemother. Pharmacol. 43*, 3–10.

5 Appendix

5.1 Characterization of synthesized peptides

Table 1 – Sequences of HABD1 where (*i, i+4*) staples were placed in cyclized versions. All sequences were amidated on the C-terminus and acetylated on the N-terminus.

Cmpd	Sequence	ESI-MS		Purity (%)*
		Expected	Observed	
1	Ac-NLKQKIKHVVKLKDE-NH$_2$	$[M+2H]^{2+}$ = 931.75 $[M+3H]^{3+}$ = 621.33	$[M+2H]^{2+}$ = 931.60 $[M+3H]^{3+}$ = 621.32	>98
2	cyclo-4,8(Ac-NLK[EKIKK]VVKLKDE-NH$_2$)	$[M+2H]^{2+}$ = 918.07 $[M+3H]^{3+}$ = 612.38	$[M+2H]^{2+}$ = 918.77 $[M+3H]^{3+}$ = 612.81	96.1
3	cyclo-5,9(Ac-NLKQ[EIKHK]VKLKDE-NH$_2$)	$[M+2H]^{2+}$ = 937.04 $[M+3H]^{3+}$ = 635.03	$[M+2H]^{2+}$ = 937.79 $[M+3H]^{3+}$ = 635.45	>98
4	cyclo-6,10(Ac-NLKQK[EKHVK]KLKDE-NH$_2$)	$[M+2H]^{2+}$ = 944.55 $[M+3H]^{3+}$ = 630.03	$[M+2H]^{2+}$ = 945.30 $[M+3H]^{3+}$ = 630.50	>98
5	cyclo-7,11(Ac-NLKQKI[EHVVK]LKDE-NH$_2$)	$[M+2H]^{2+}$ = 922.53 $[M+3H]^{3+}$ = 615.35	$[M+2H]^{2+}$ = 923.36 $[M+3H]^{3+}$ = 615.74	>98
6	cyclo-8,12(Ac-NLKQKIK[EVVKK]KDE-NH$_2$)	$[M+2H]^{2+}$ = 925.56 $[M+3H]^{3+}$ = 617.37	$[M+2H]^{2+}$ = 926.15 $[M+3H]^{3+}$ = 617.73	97.2

*Purity is determined by integrating the area under the LC curve

Table 2 – Sequences of HABD2 where (*i, i+4*) staples were placed in cyclized versions. All sequences were amidated on the C-terminus and either non-acetylated or acetylated the N-terminus.

Cmpd	Sequence	ESI-MS		Purity (%)
		Expected	Observed	
7	H-VSKLRSQLVKRKQN-NH$_2$	$[M+2H]^{2+}$ = 842.51 $[M+3H]^{3+}$ = 562.01	$[M+2H]^{2+}$ = 842.85 $[M+3H]^{3+}$ = 562.31	>98
8	cyclo-4,8(H-VSK[ERSQK]VKRKQN-NH$_2$)	$[M+2H]^{2+}$ = 848.99 $[M+3H]^{3+}$ = 566.33	$[M+2H]^{2+}$ = 848.80 $[M+3H]^{3+}$ = 566.13	>98
9	cyclo-5,9(H-VSKL[ESQLK]KRKQN-NH$_2$)	$[M+3H]^{3+}$ = 556.33 $[M+4H]^{4+}$ = 417.49	$[M+3H]^{3+}$ = 556.36 $[M+4H]^{4+}$ = 417.52	97.5
10	cyclo-6,10(H-VSKLR[EQLVK]RKQN-NH$_2$)	$[M+2H]^{2+}$ = 854.02 $[M+3H]^{3+}$ = 569.68	$[M+2H]^{2+}$ = 854.45 $[M+3H]^{3+}$ = 569.85	>98
11	cyclo-7,11(H-VSKLRS[ELVKK]KQN-NH$_2$)	$[M+2H]^{2+}$ = 819.50 $[M+3H]^{3+}$ = 546.67	$[M+2H]^{2+}$ = 819.93 $[M+3H]^{3+}$ = 546.63	>98
12	Ac-VSKLRSQLVKRKQN-NH$_2$	$[M+2H]^{2+}$ =863.75 $[M+3H]^{3+}$ = 575.92	$[M+2H]^{2+}$ = 863.50 $[M+3H]^{3+}$ = 575.92	>98
13	cyclo-4,8(Ac-VSK[ERSQK]VKRKQN-NH$_2$)	$[M+2H]^{2+}$ =869.89 $[M+3H]^{3+}$ = 580.33	$[M+2H]^{2+}$ = 870.28 $[M+3H]^{3+}$ = 580.25	>98
14	cyclo-5,9(Ac-VSKL[ESQLK]KRKQN-NH$_2$)	$[M+2H]^{2+}$ =855.43 $[M+3H]^{3+}$ = 570.62	$[M+2H]^{2+}$ = 855.45 $[M+3H]^{3+}$ = 570.59	>98
15	cyclo-6,10(Ac-VSKLR[EQLVK]RKQN-NH$_2$)	$[M+2H]^{2+}$ =876.10 $[M+3H]^{3+}$ = 583.91	$[M+2H]^{2+}$ = 876.24 $[M+3H]^{3+}$ = 583.56	96.3
16	cyclo-7,11(Ac-VSKLRS[ELVKK]KQN-NH$_2$)	$[M+2H]^{2+}$ = 840.51 $[M+3H]^{3+}$ = 560.67	$[M+2H]^{2+}$ = 840.88 $[M+3H]^{3+}$ = 560.81	>98
17	cyclo-5,9(Ac-VSKL[KSQLE]KRKQN-NH$_2$)	$[M+2H]^{2+}$ =855.43 $[M+3H]^{3+}$ = 570.62	$[M+2H]^{2+}$ = 855.51 $[M+3H]^{3+}$ = 570.72	>98
18	cyclo-6,10(Ac-VSKLR[KQLVE]RKQN-NH$_2$)	$[M+2H]^{2+}$ =876.10 $[M+3H]^{3+}$ = 583.91	$[M+2H]^{2+}$ = 876.11 $[M+3H]^{3+}$ = 584.49	>98

Table 3 – Sequences of HABD2 derived from *Homo sapiens* where (*i, i+4*) staples were placed in cyclized versions. All sequences were amidated on the C-terminus and acetylated on the N-terminus.

Cmpd	Sequence	ESI-MS		Purity (%)
		Expected	Observed	
19	Ac-VSKLRCQLLAKKKQS-NH$_2$	[M+2H]$^{2+}$ = 822.03 [M+3H]$^{3+}$ = 548.02	[M+2H]$^{2+}$ = 822.33 [M+3H]$^{3+}$ = 548.67	>98
20	cyclo-6,10(Ac-VSKLR[EQLAK]KKQS-NH$_2$)	[M+2H]$^{2+}$ = 833.5 [M+3H]$^{3+}$ = 556.00	[M+2H]$^{2+}$ = 834.35 [M+3H]$^{3+}$ = 556.64	>98

Table 4 – Sequences of the alanine scan of HABD2 where (*i, i+4*) staples were placed in cyclized versions. All sequences were amidated on the C-terminus and acetylated on the N-terminus.

Cmpd	Sequence	ESI-MS		Purity (%)
		Expected	Observed	
21	cyclo-6,10(Ac-VSKLA[EQLVK]RAQN-NH$_2$)	[M+2H]$^{2+}$ = 812.97 [M+3H]$^{3+}$ = 542.31	[M+2H]$^{2+}$ = 812.86 [M+3H]$^{3+}$ = 542.78	>98
22	cyclo-6,10(Ac-VSKLA[EQLVK]AKQN-NH$_2$)	[M+2H]$^{2+}$ = 803.96 [M+3H]$^{3+}$ = 536.31	[M+2H]$^{2+}$ = 804.96 [M+3H]$^{3+}$ = 537.01	>98
23	cyclo-6,10(Ac-VSALR[EQLVK]RAQN-NH$_2$)	[M+2H]$^{2+}$ = 817.97 [M+3H]$^{3+}$ = 545.64	[M+2H]$^{2+}$ = 818.62 [M+3H]$^{3+}$ = 546.31	>98
24	cyclo-6,10(Ac-VSALR[EQLVK]AKQN-NH$_2$)	[M+2H]$^{2+}$ = 803.96 [M+3H]$^{3+}$ = 536.31	[M+2H]$^{2+}$ = 804.85 [M+3H]$^{3+}$ = 536.99	>98

5.2 Trypsin degradation products

5.2.1 Trypsin Degradation Products of Compound 12
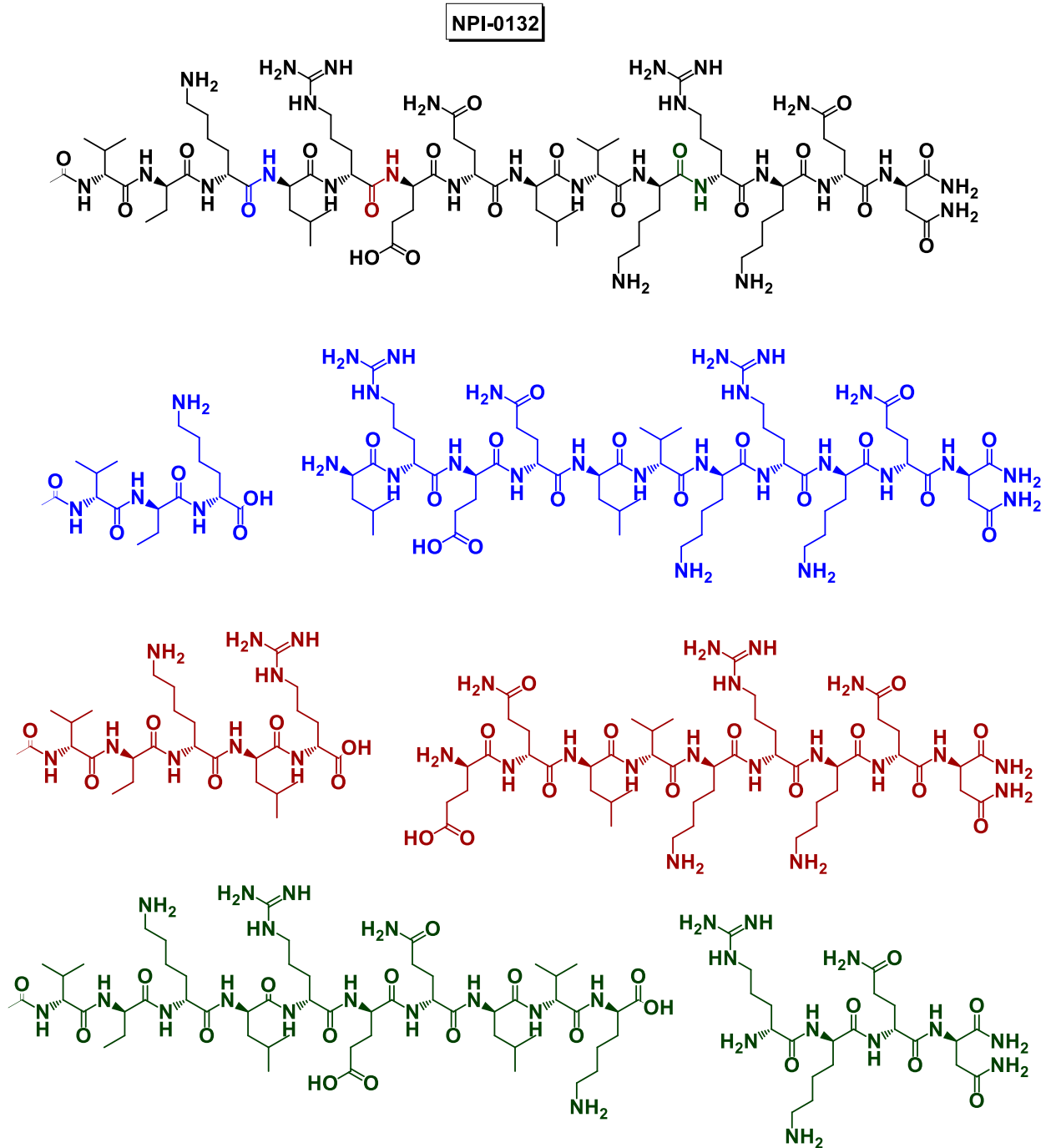
5.2.2   Trypsin Degradation Products of Compound 15
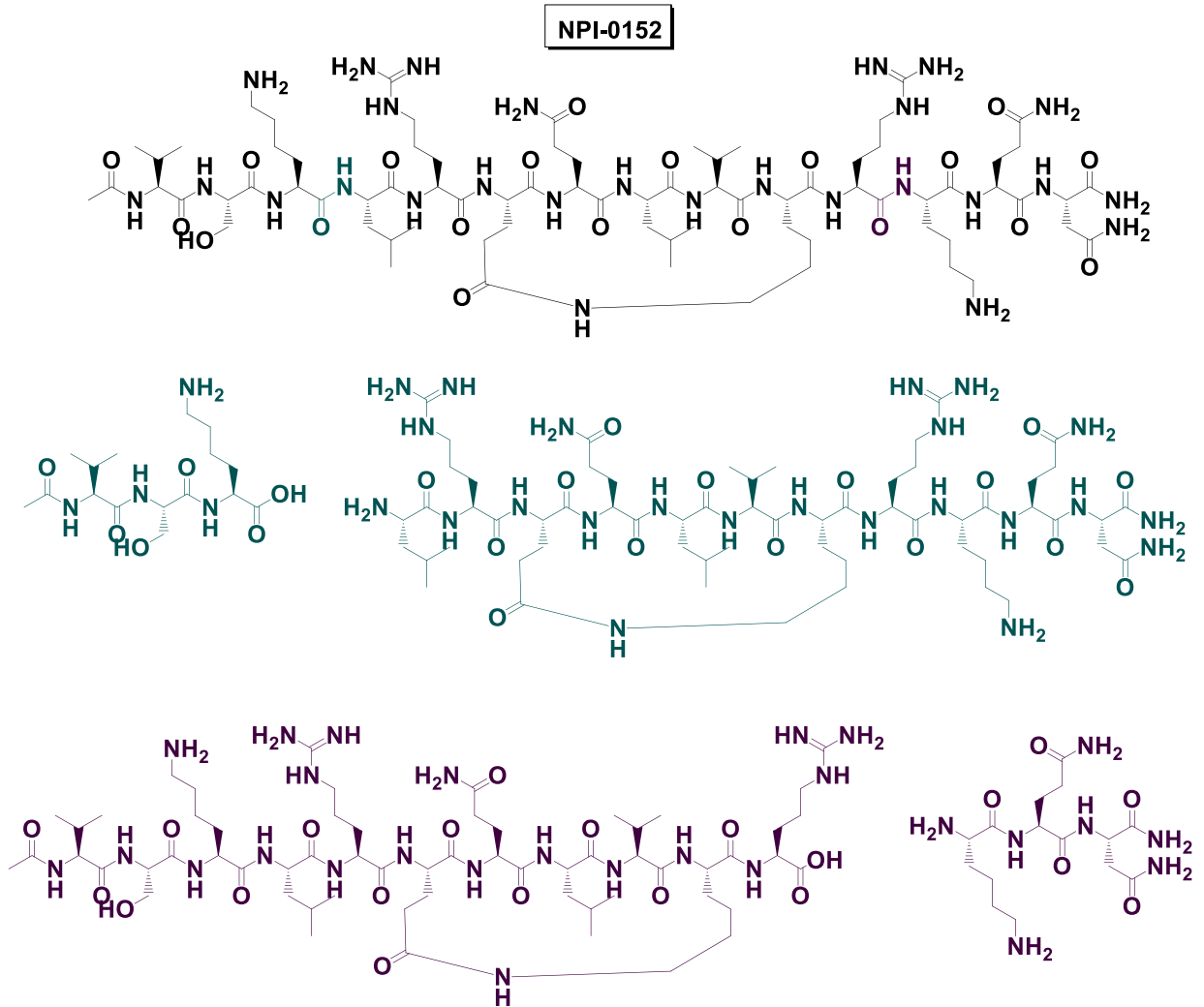
5.3   HPLC Traces

Compound 1

m/z
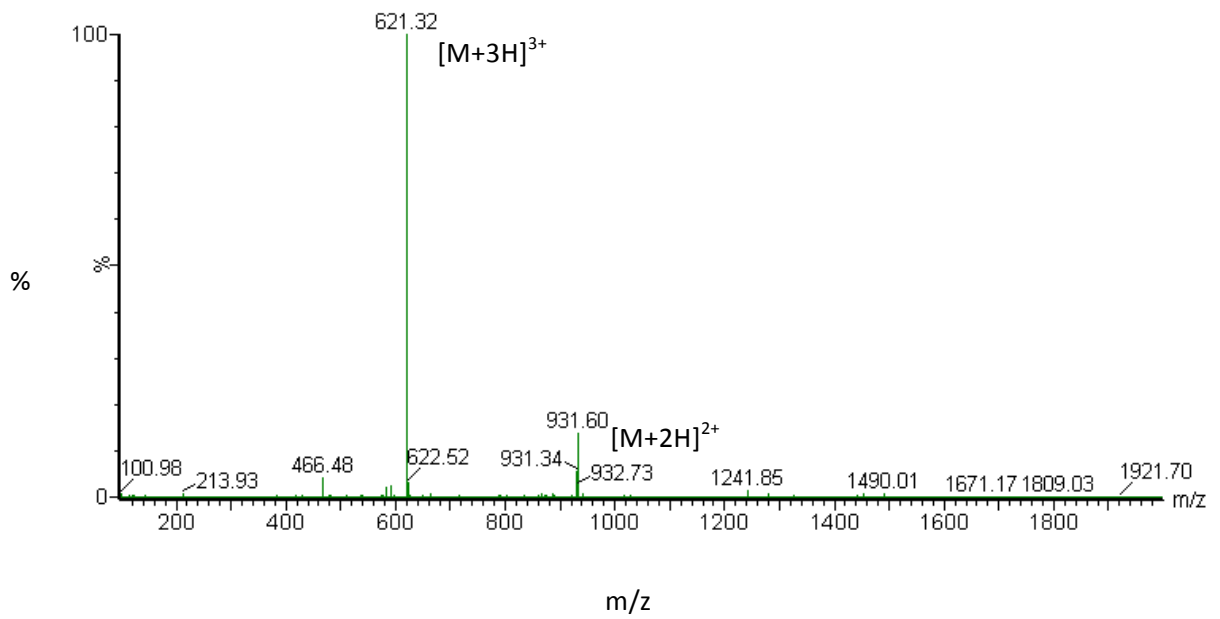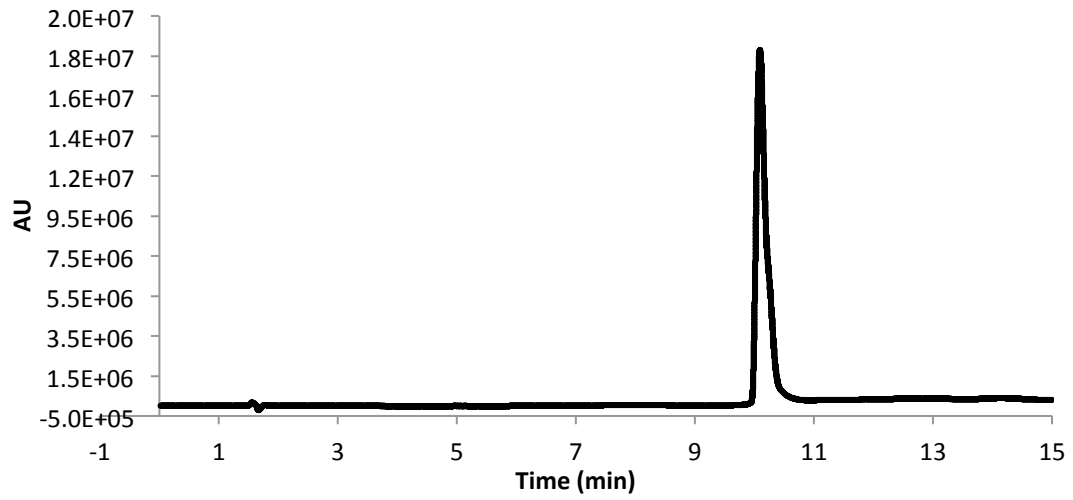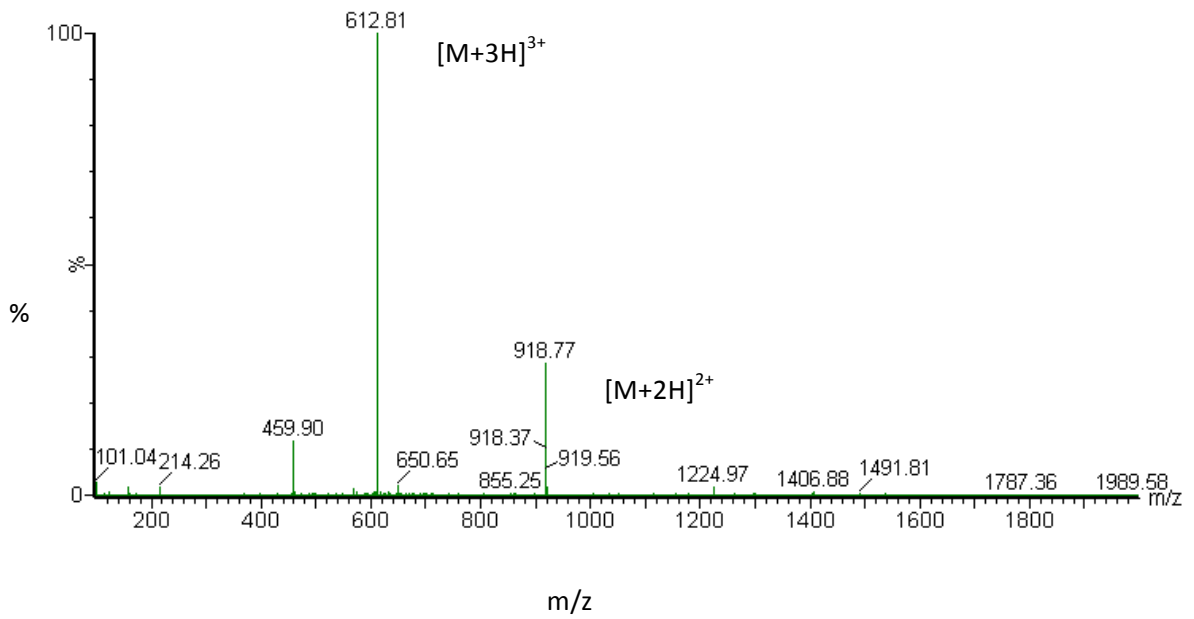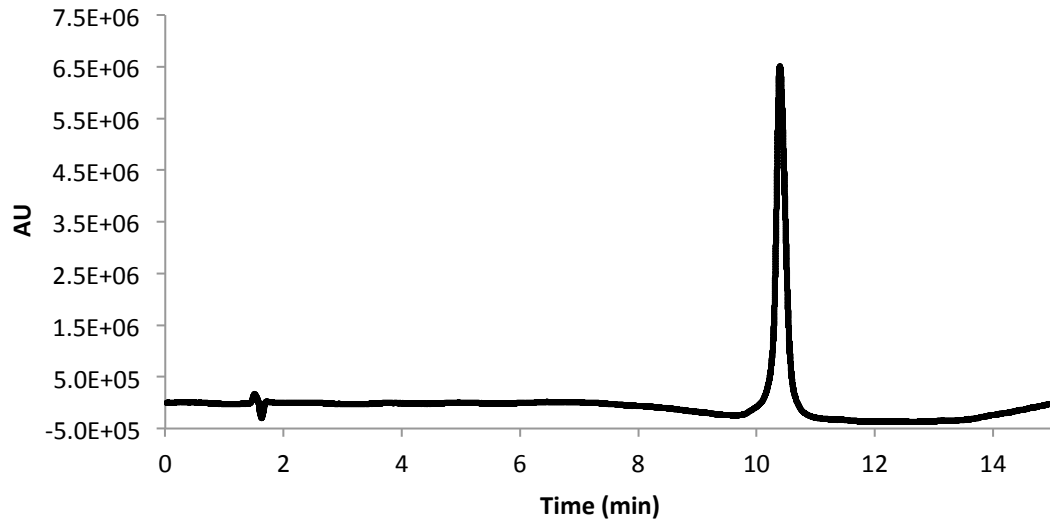
Compound 2

Compound 3
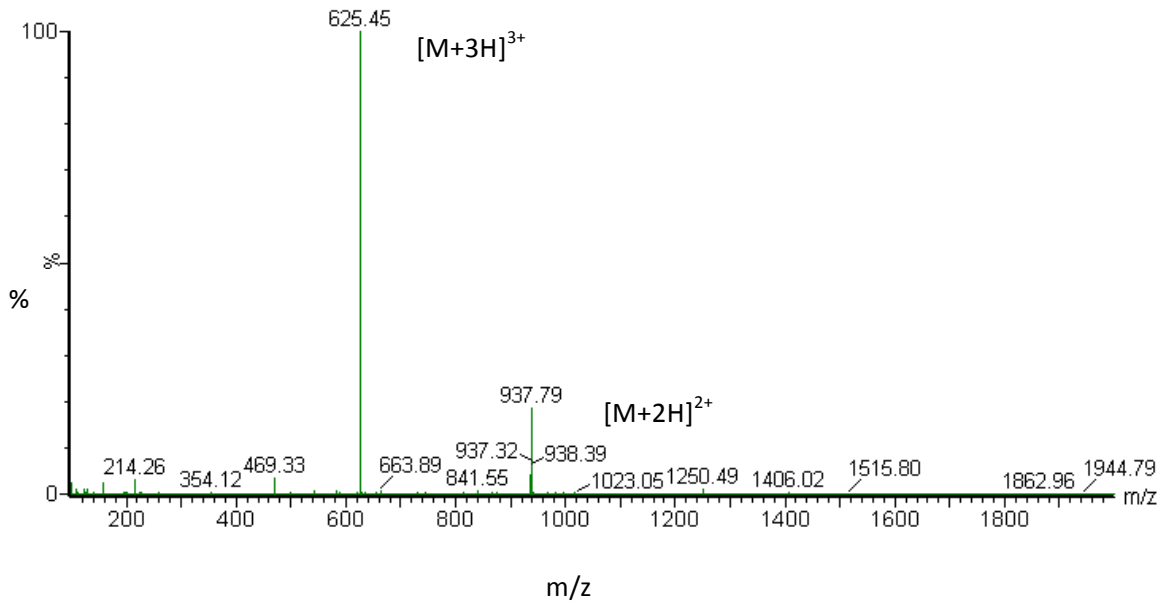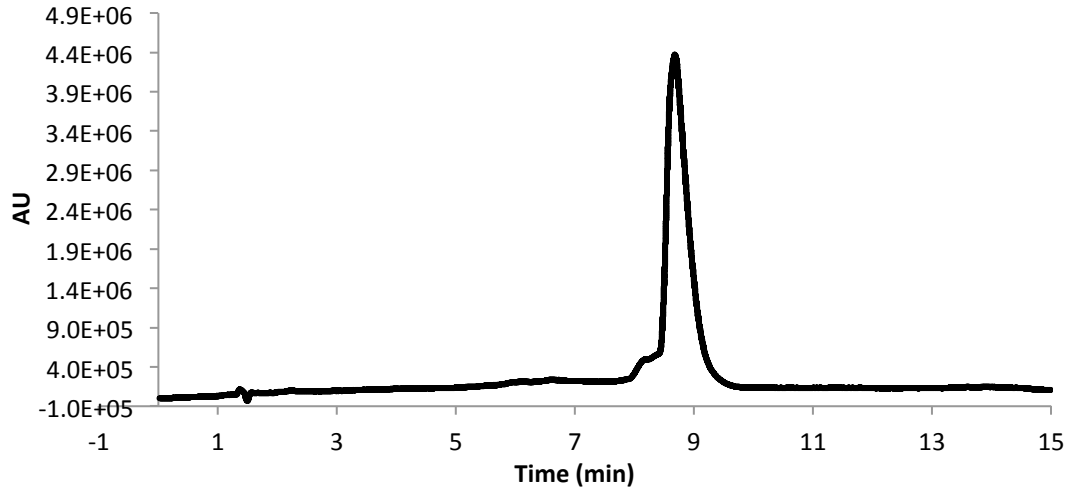
Compound 4

Compound 5

m/z

Compound 6

m/z
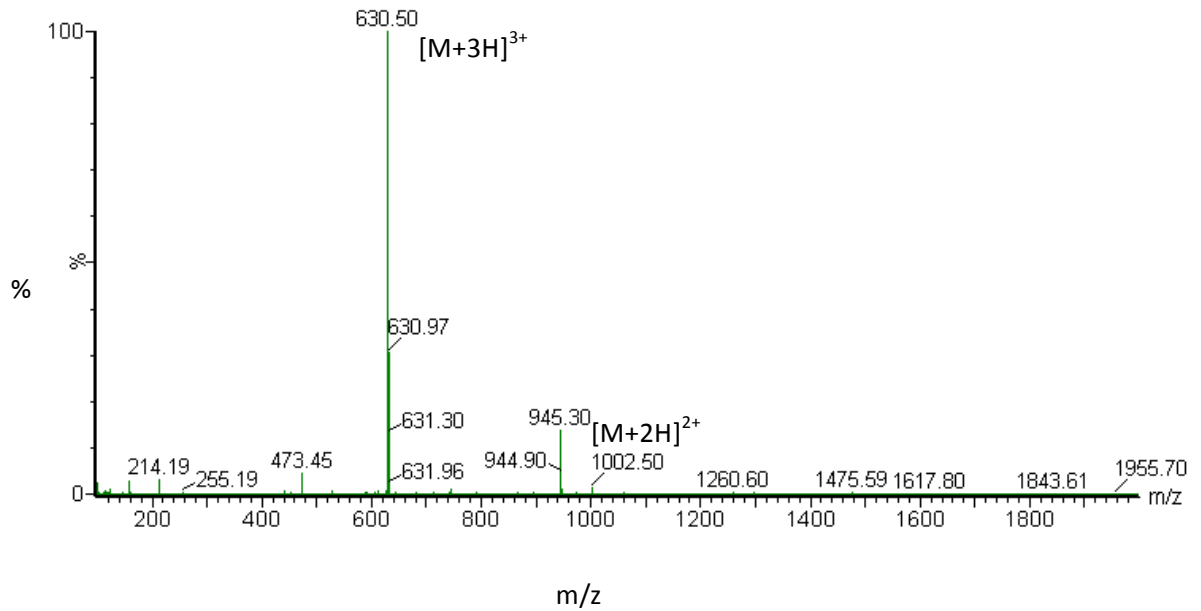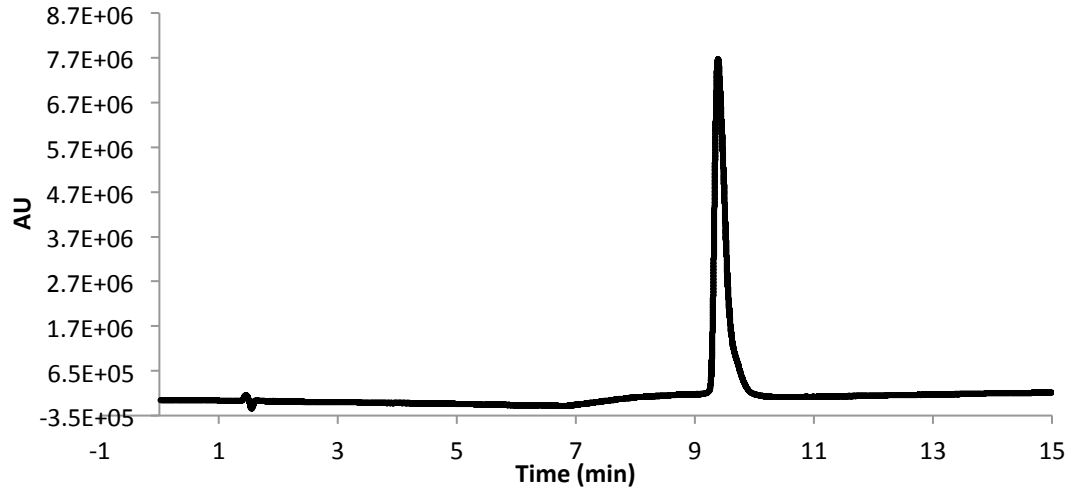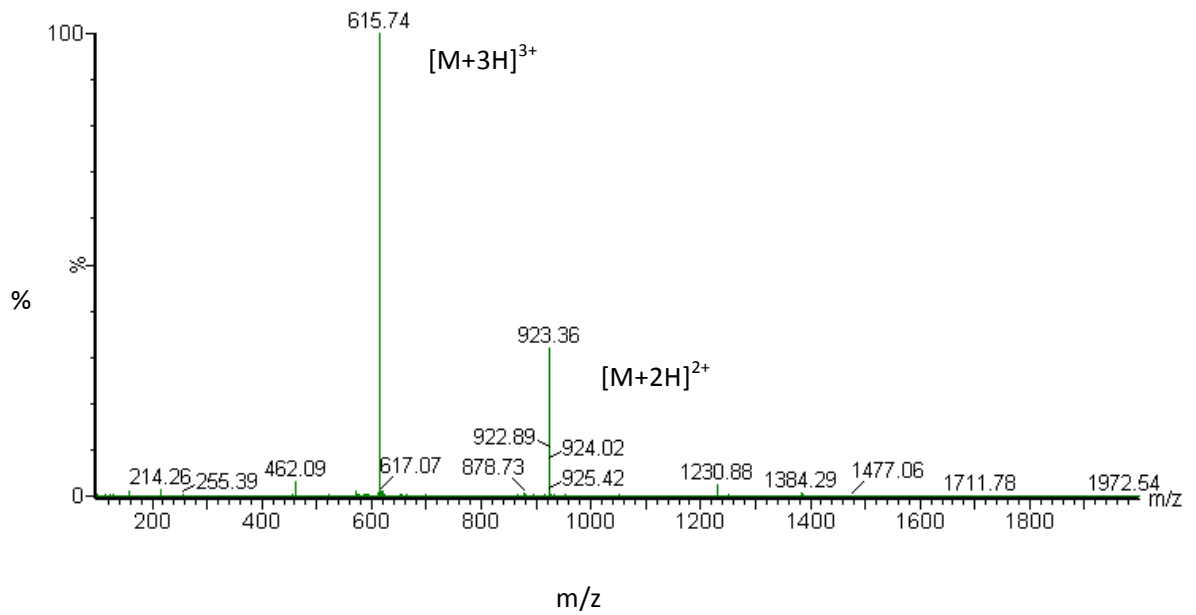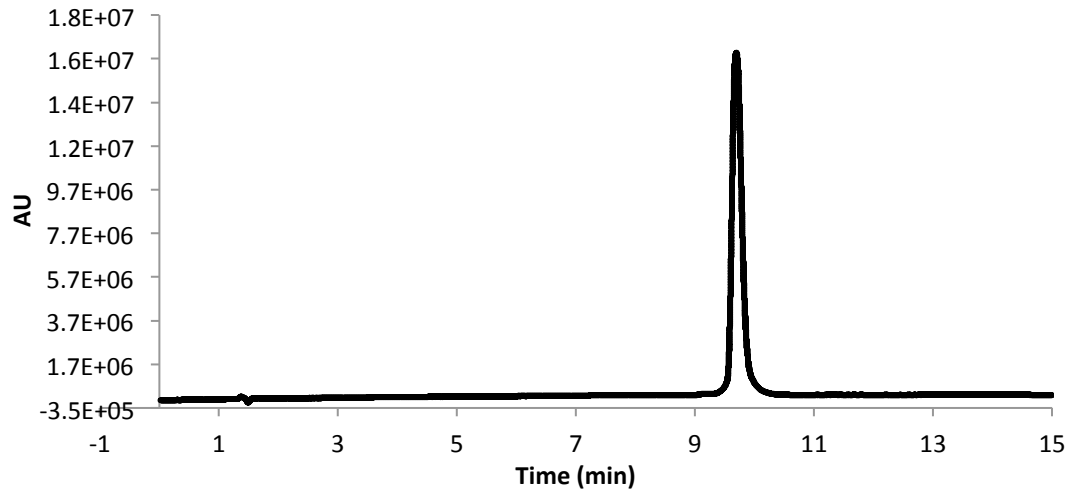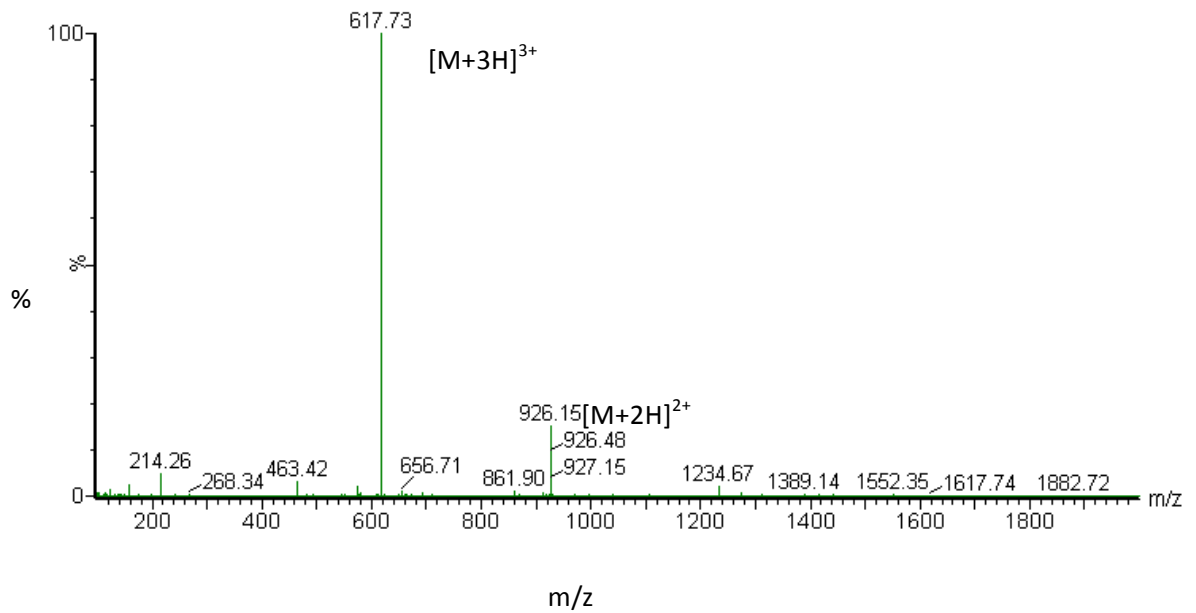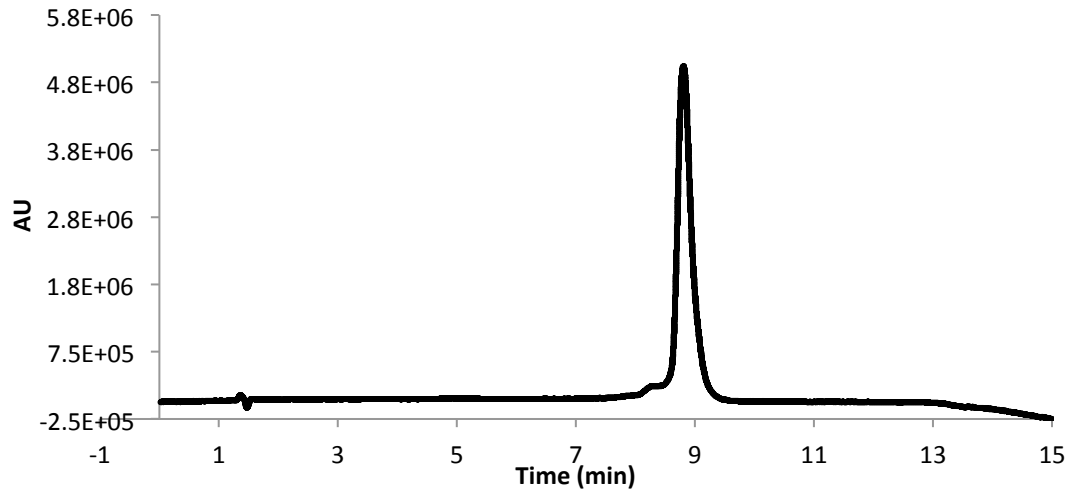
Compound 7

Compound 8

m/z
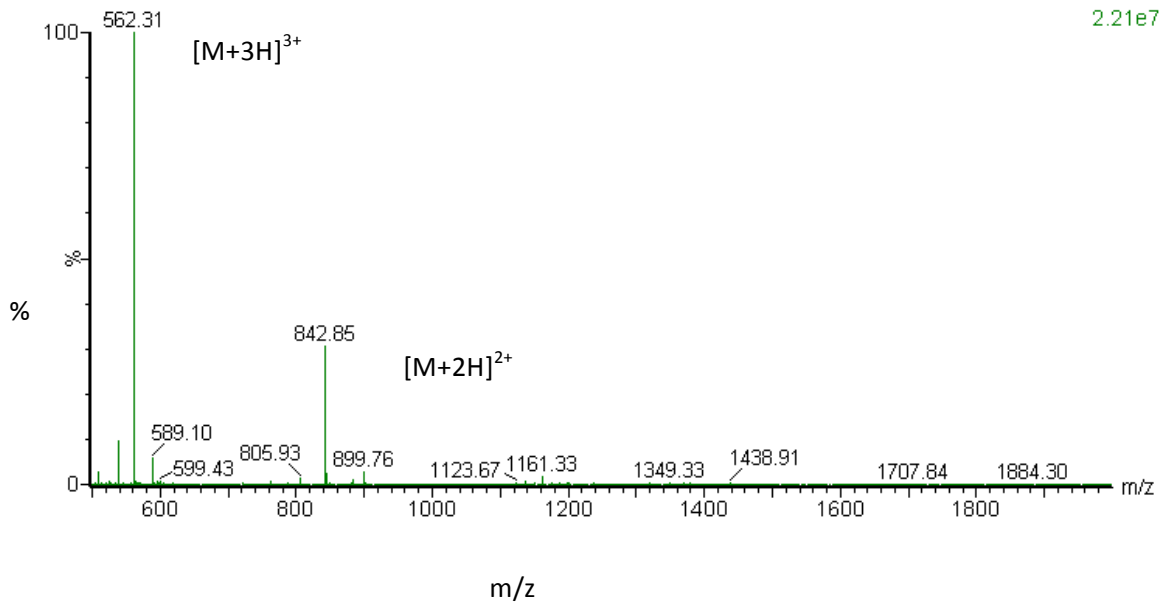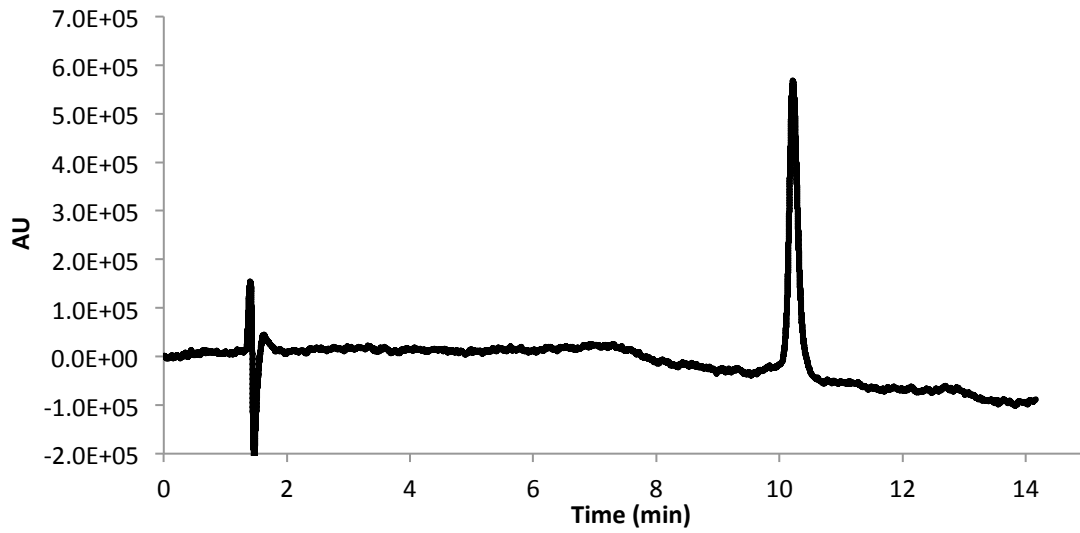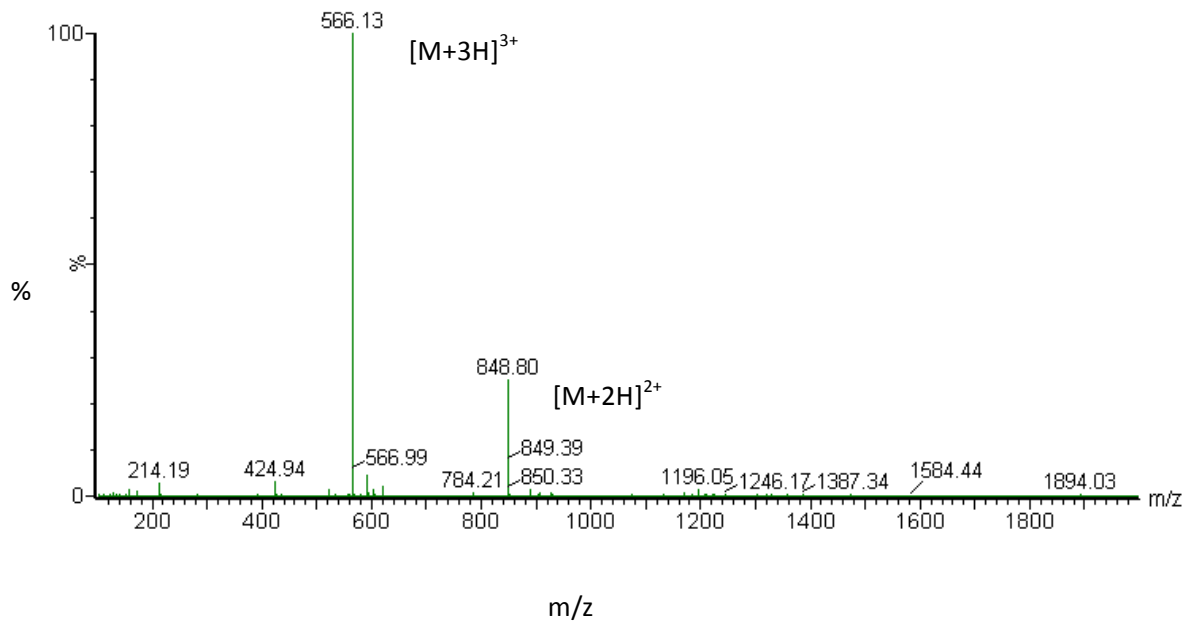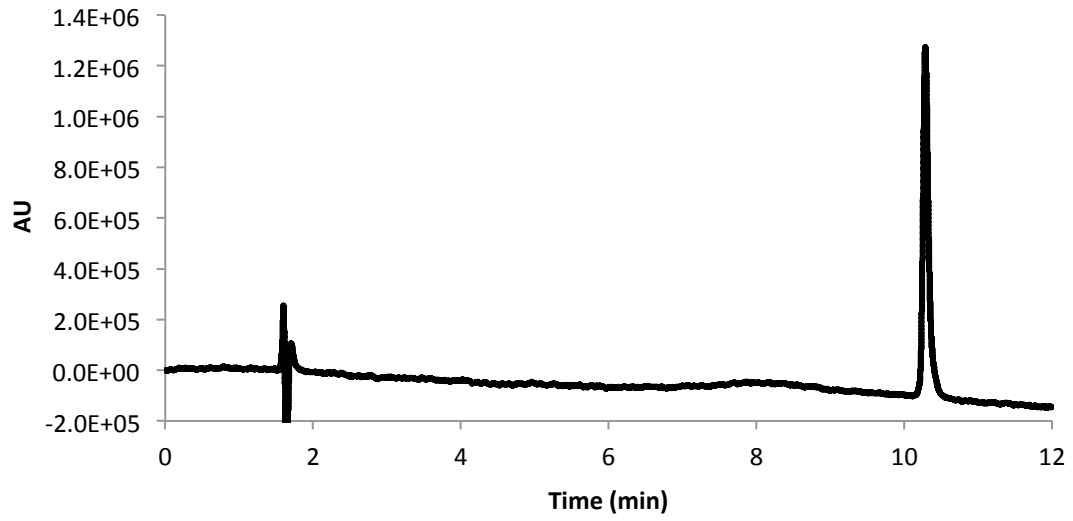
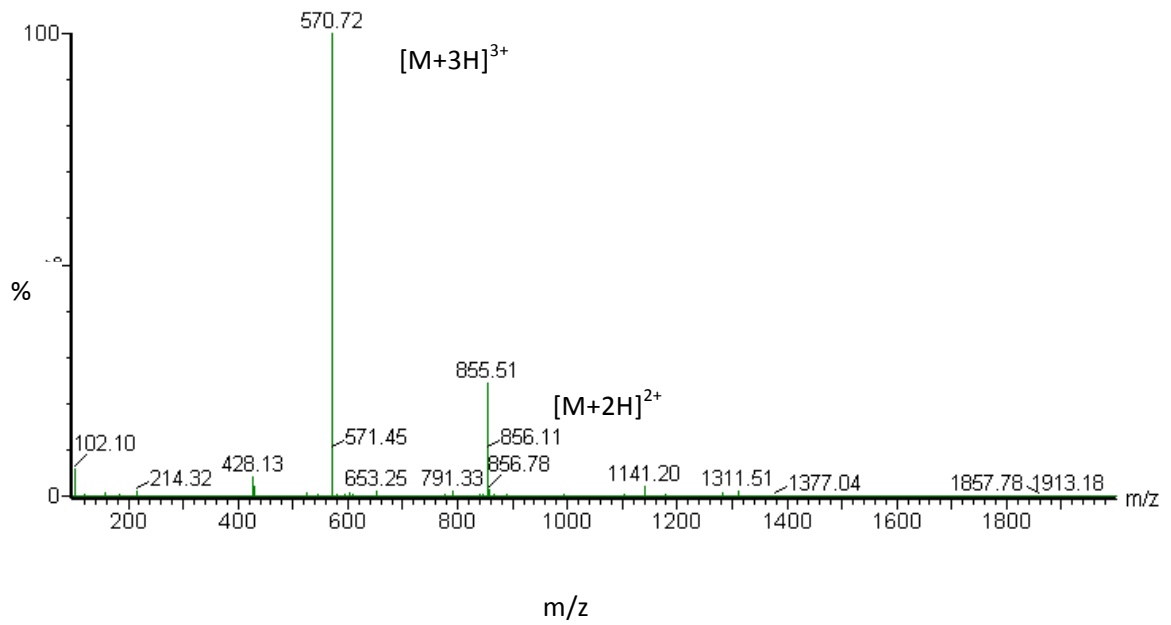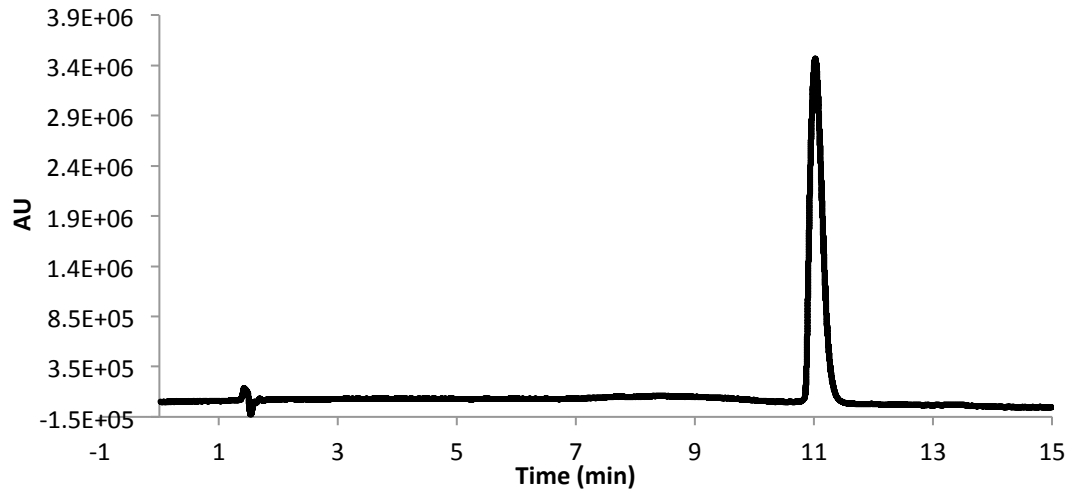Compound 9

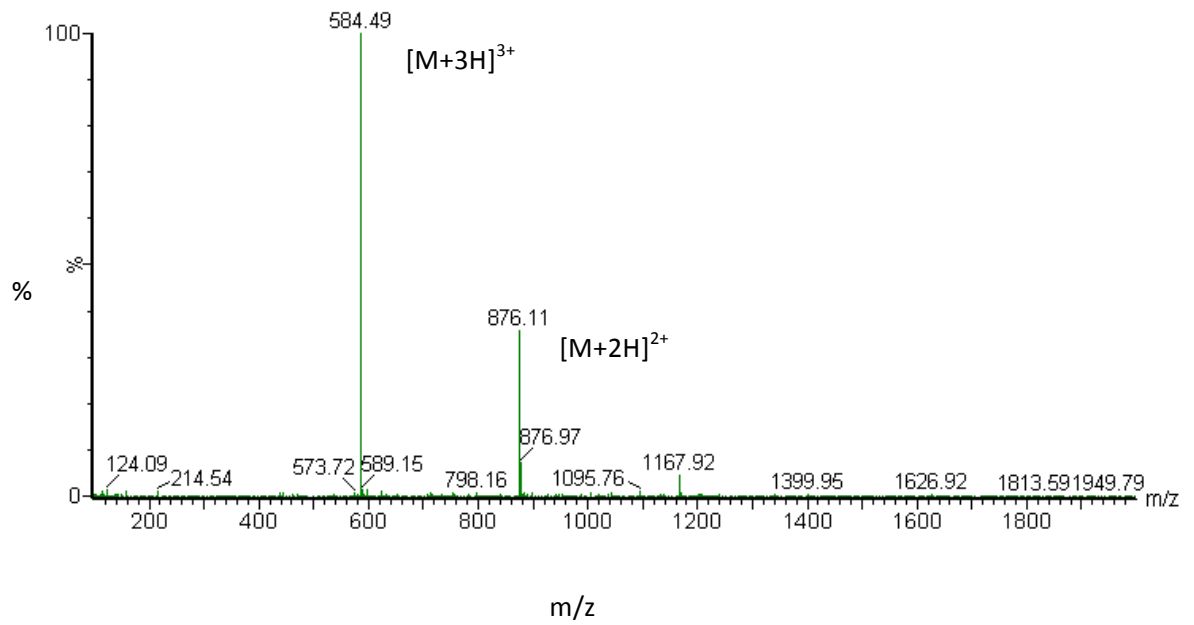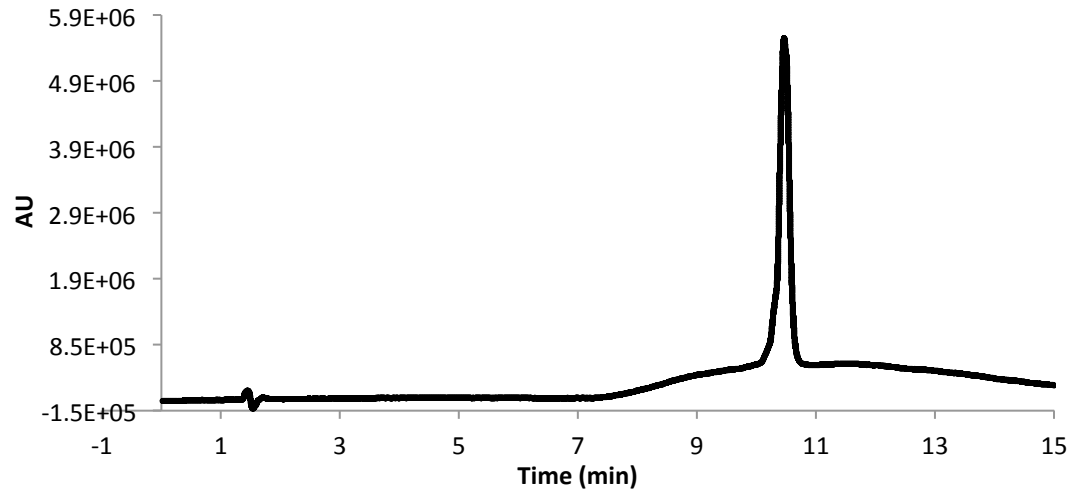Compound 10

m/z

Compound 11

m/z
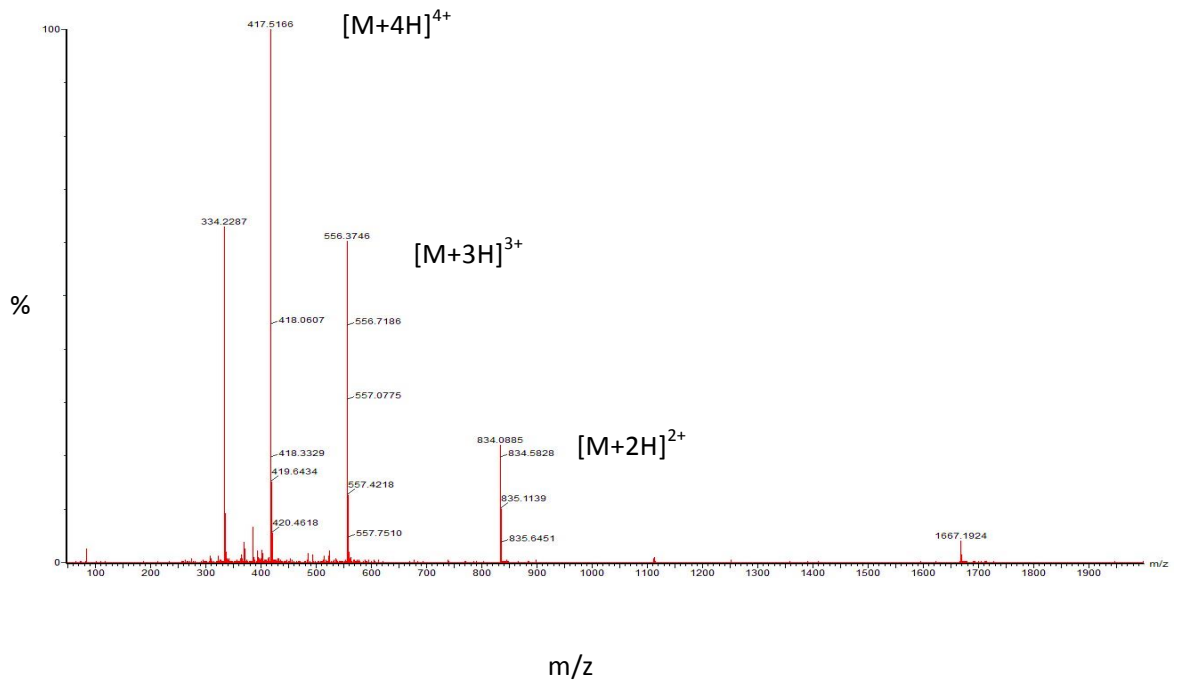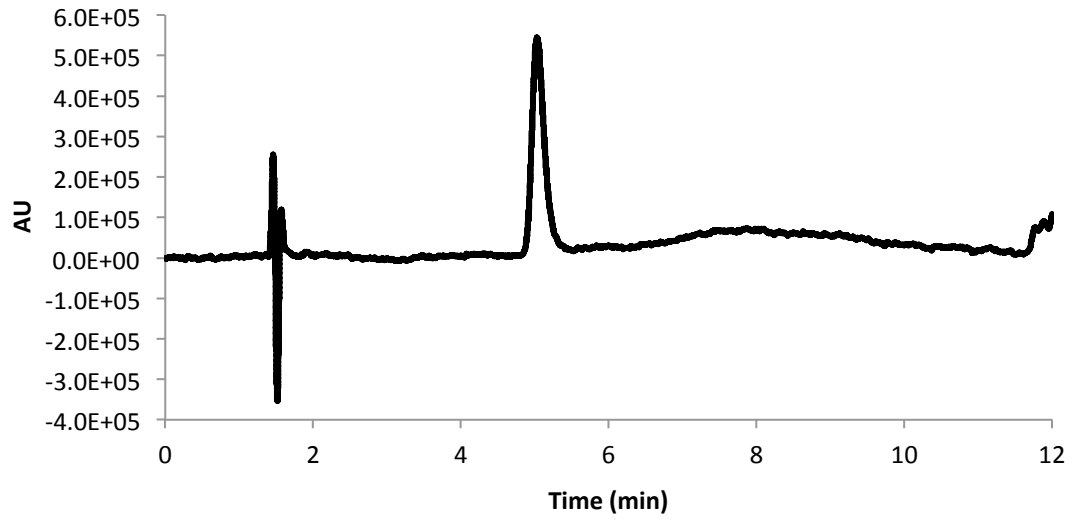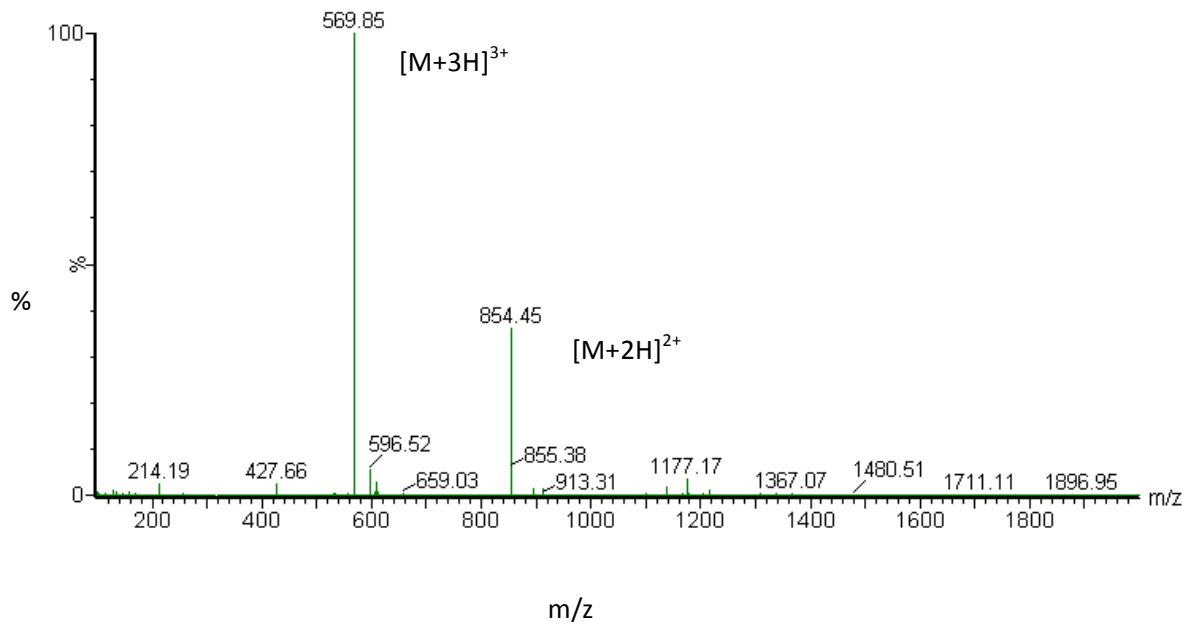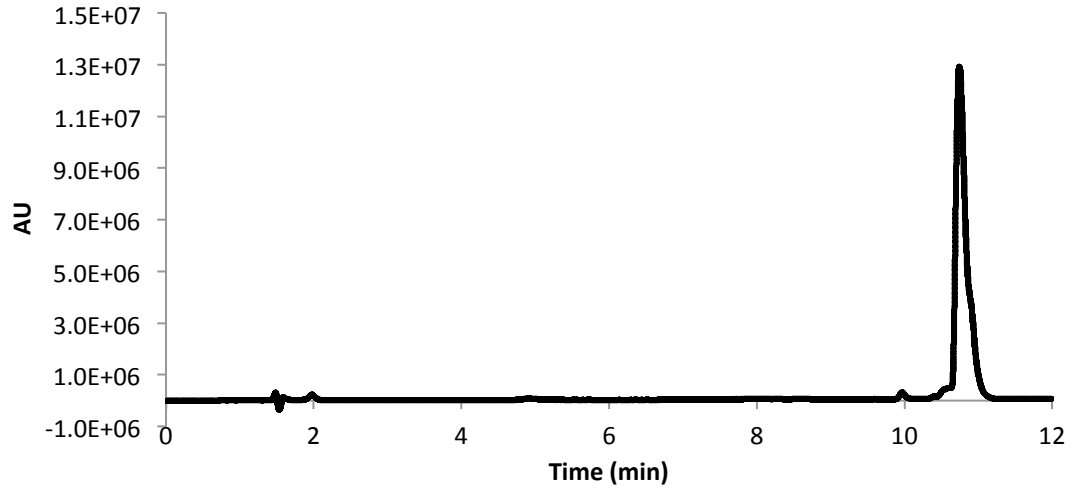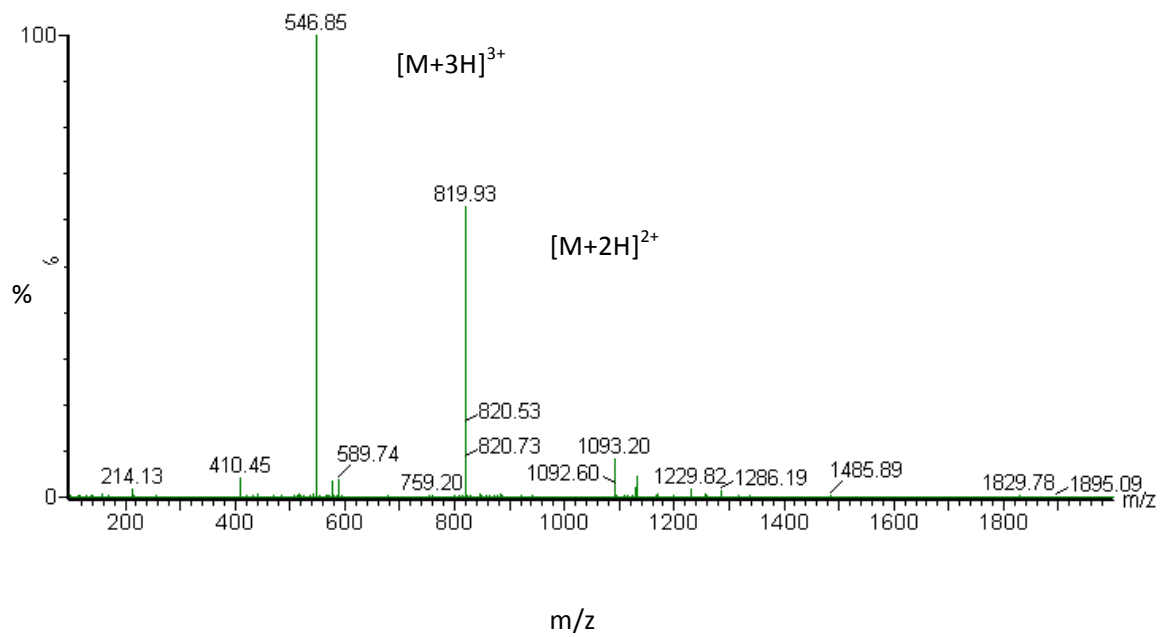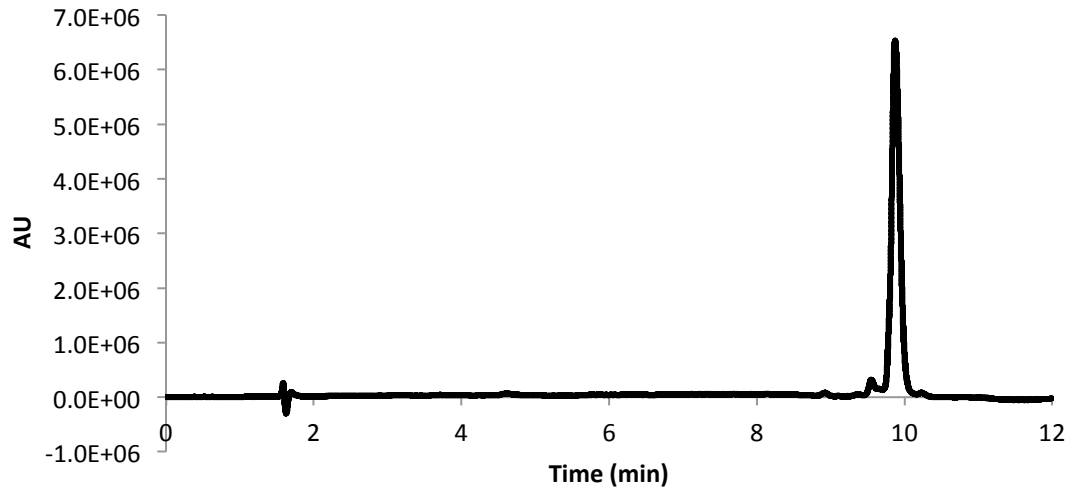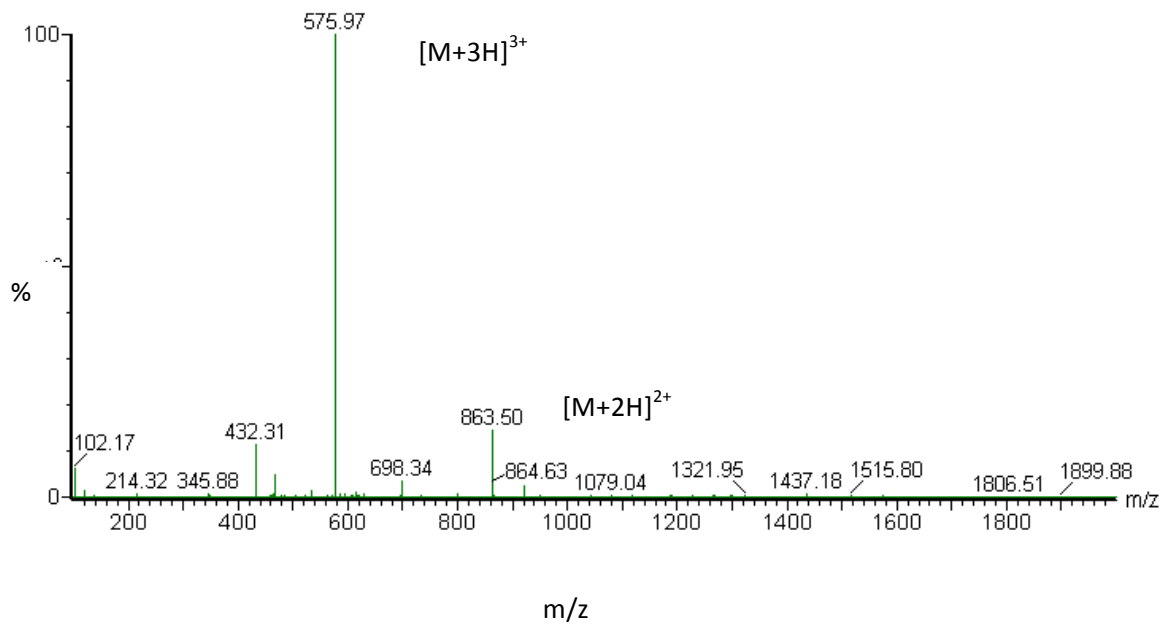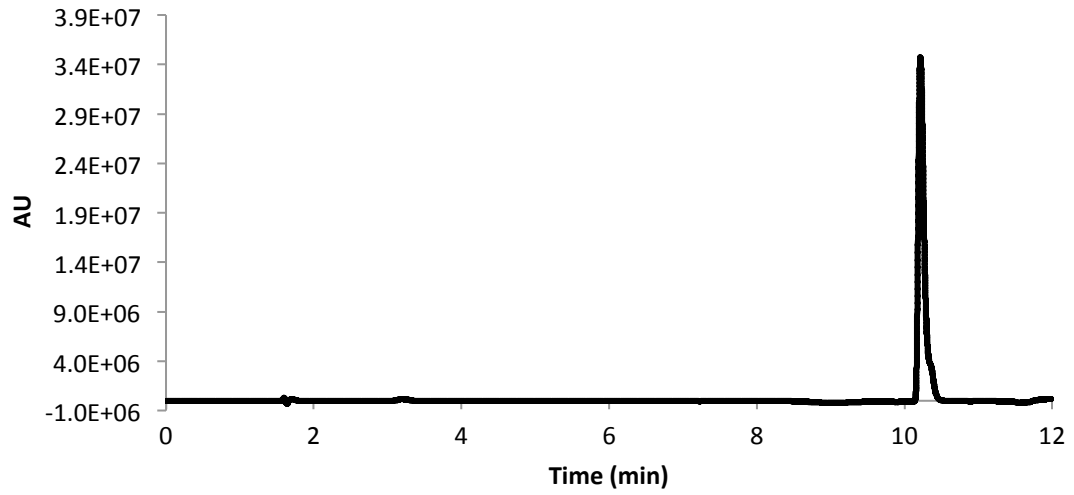
Compound 12

Compound 13

Compound 14
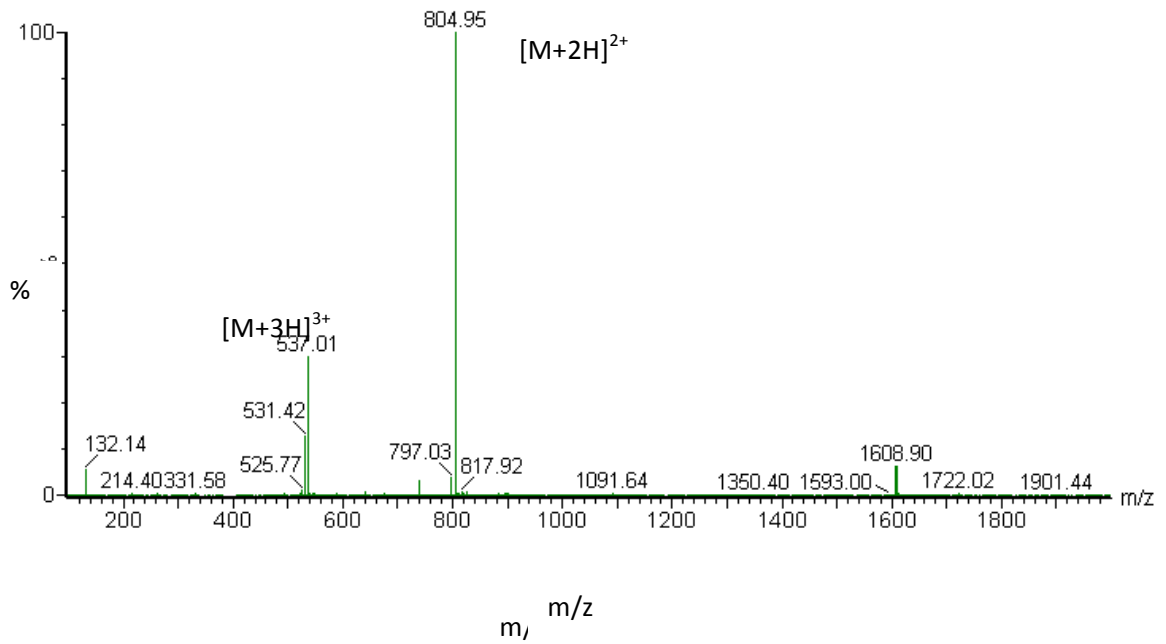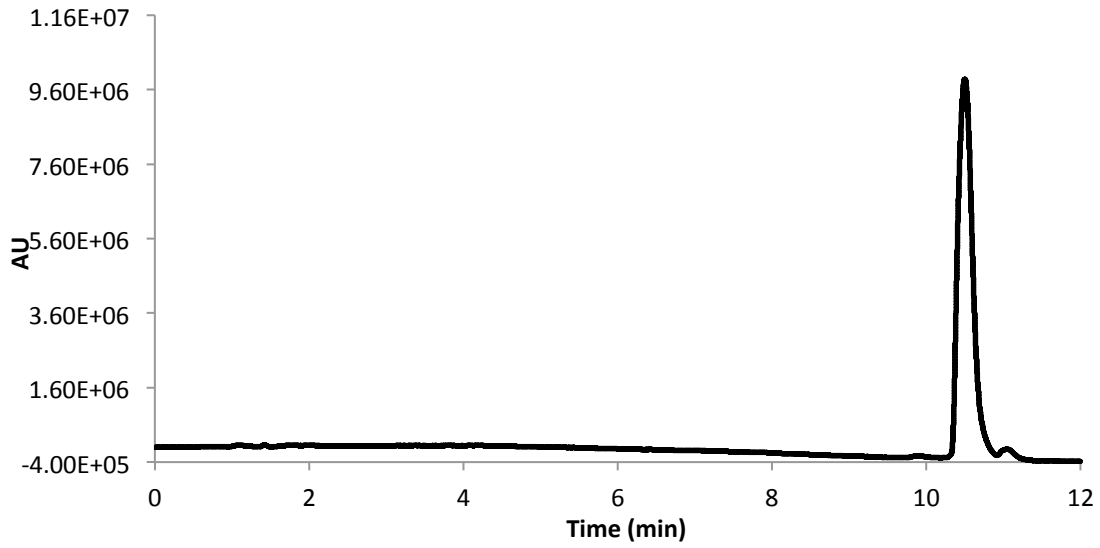

m/z

Compound 15

m/z
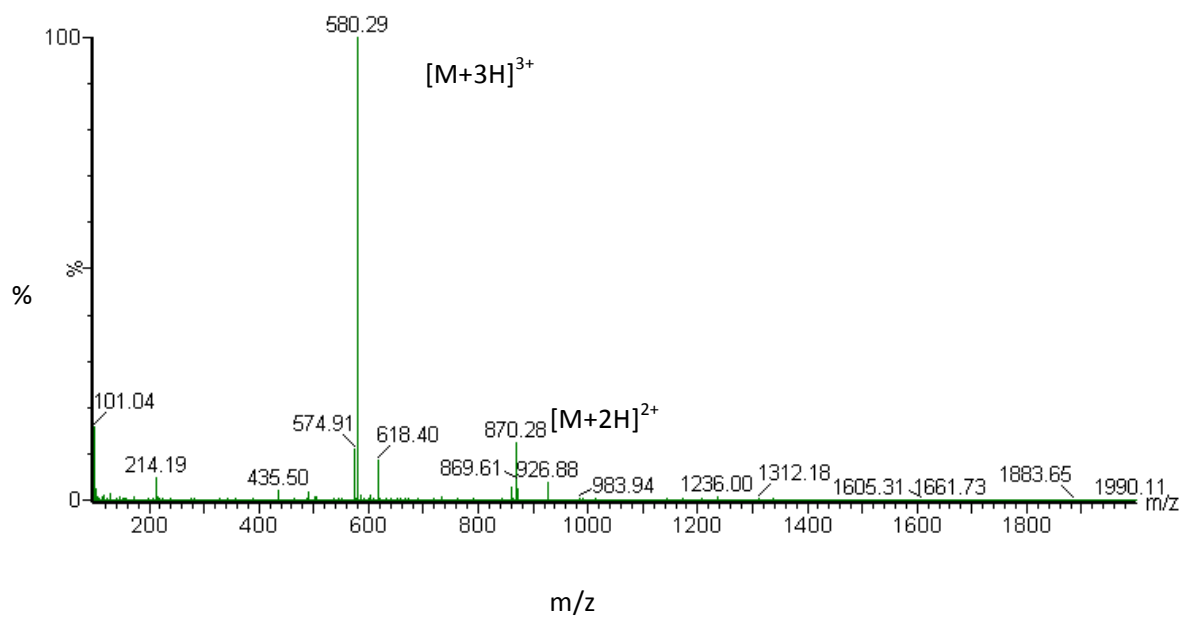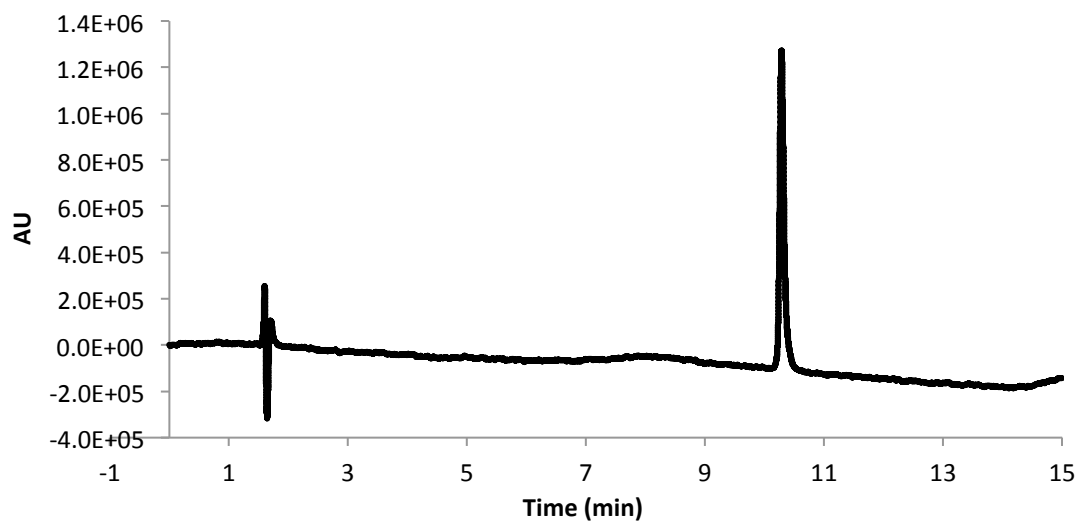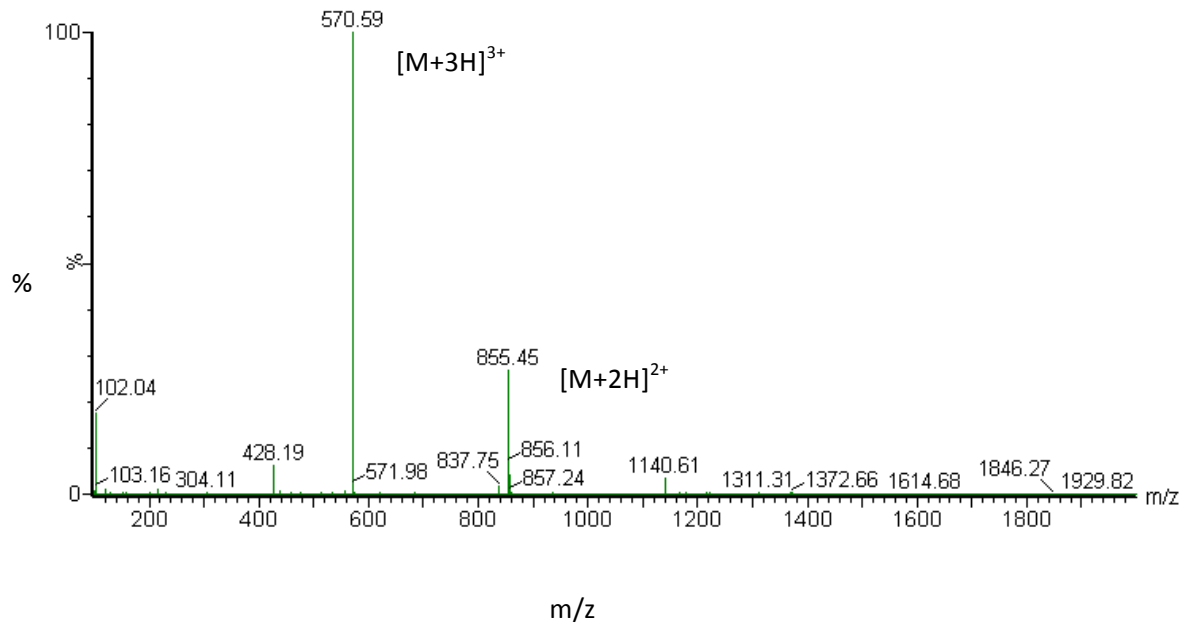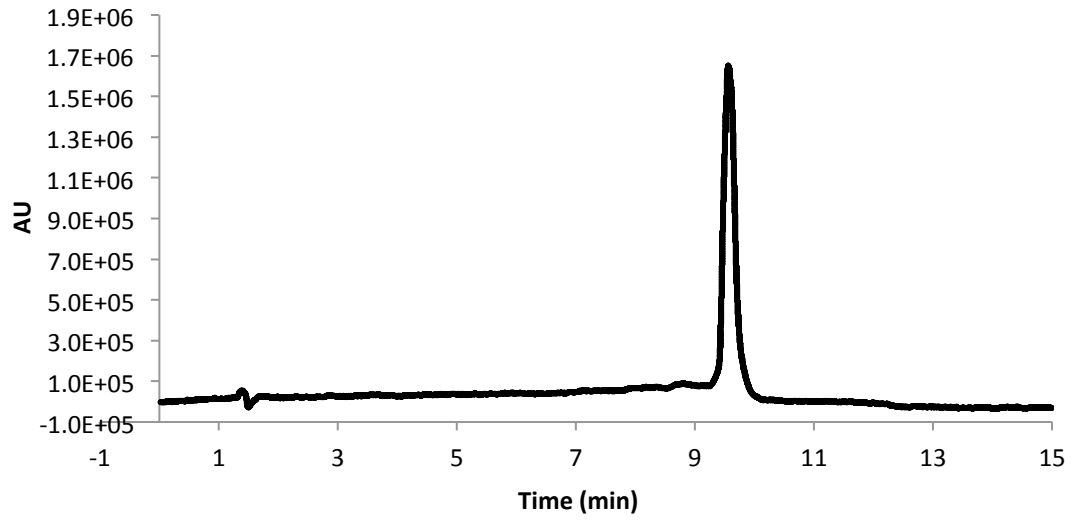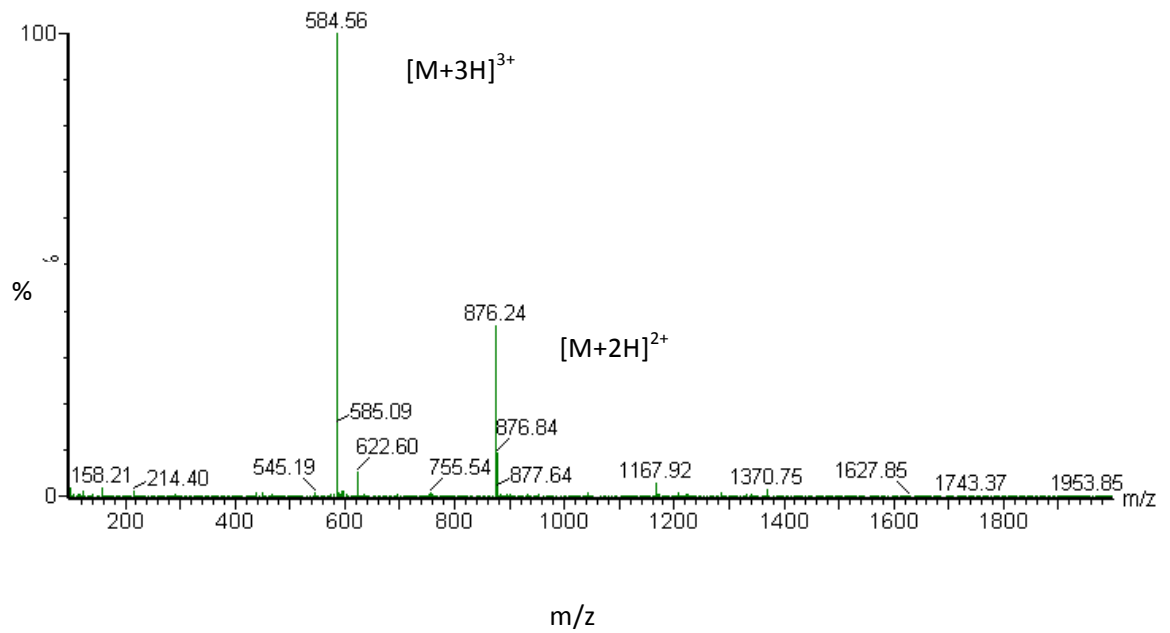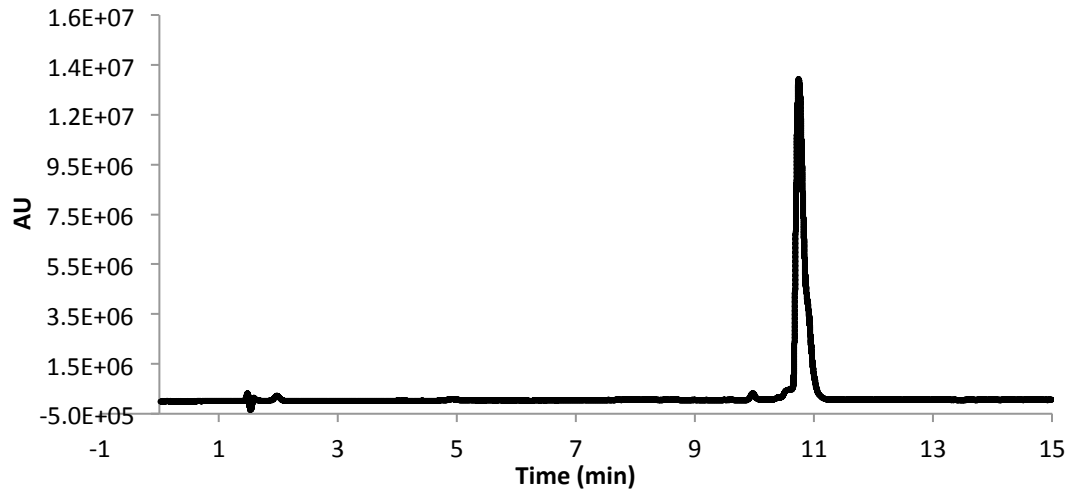
Compound 16
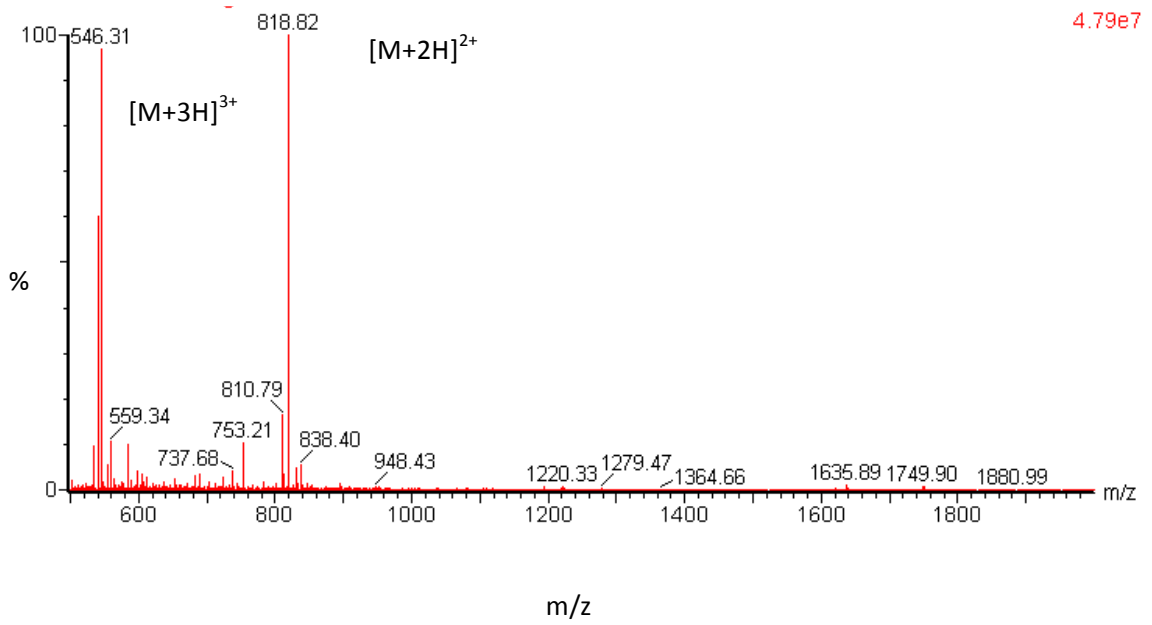
Compound 17

m/z
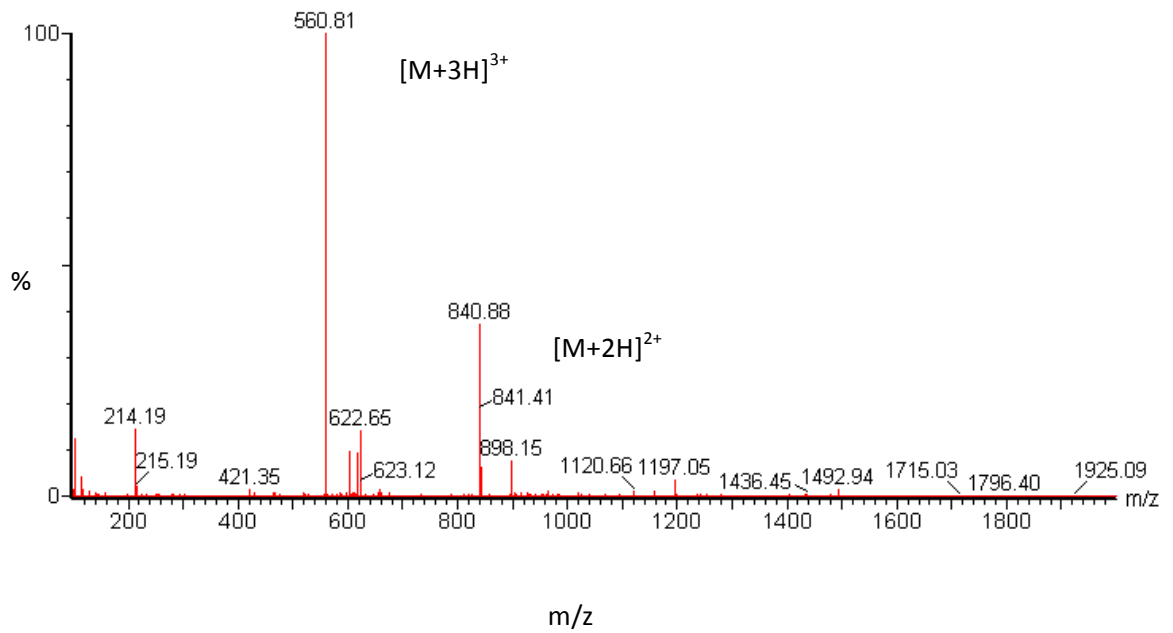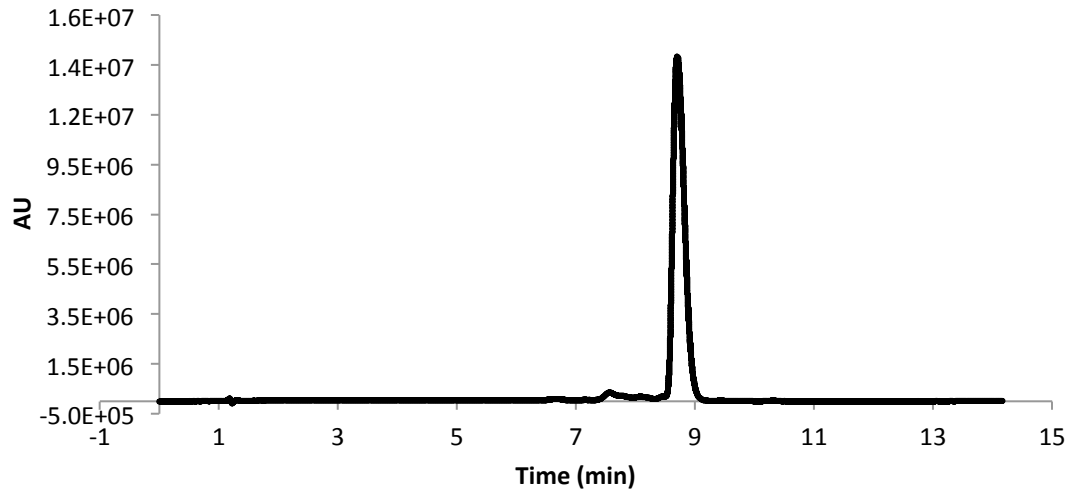
Compound 18

Compound 19

Compound 20
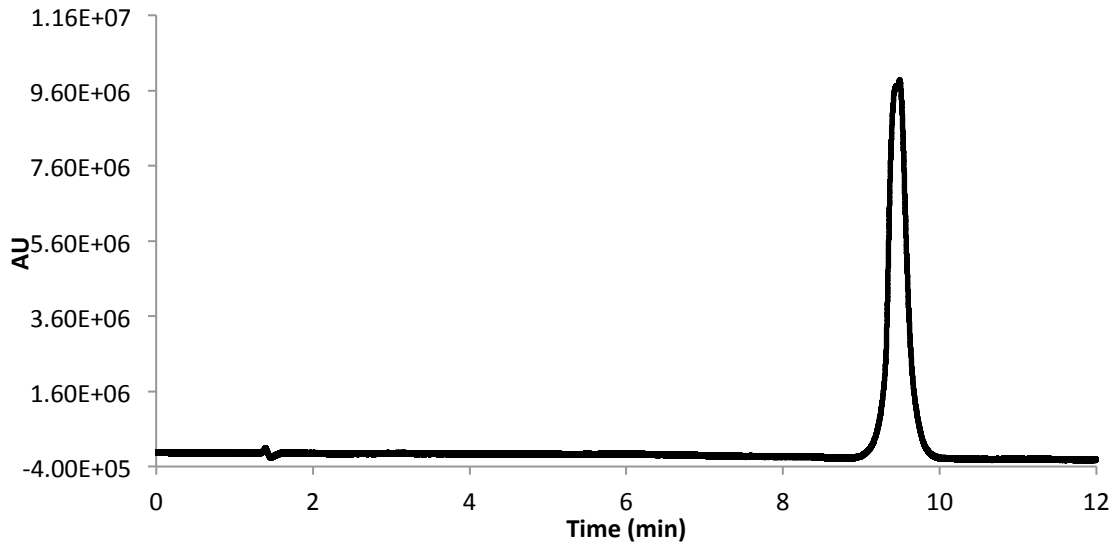

m/z
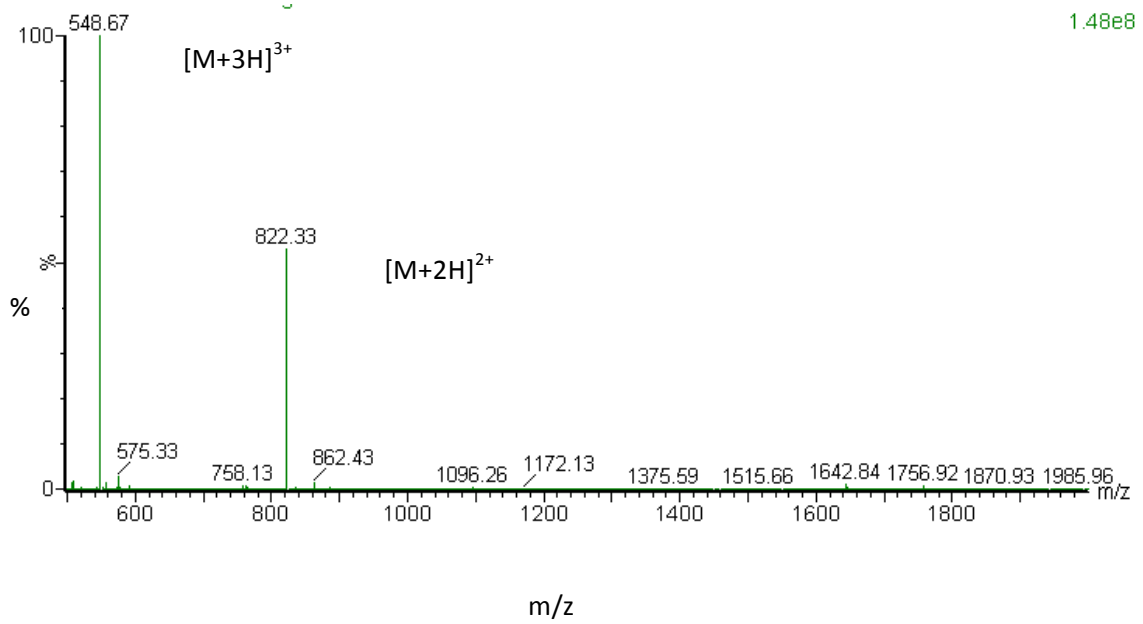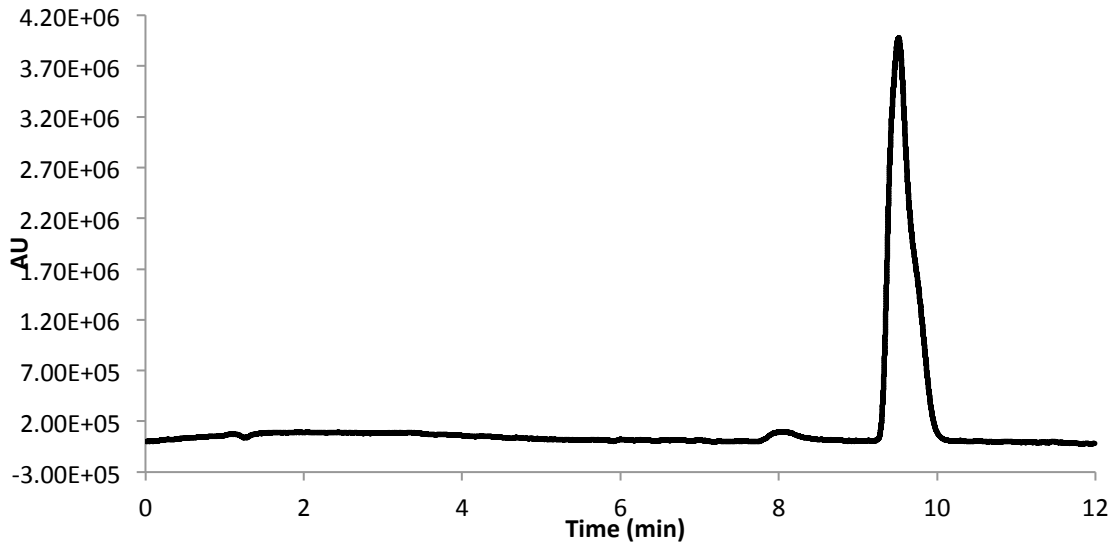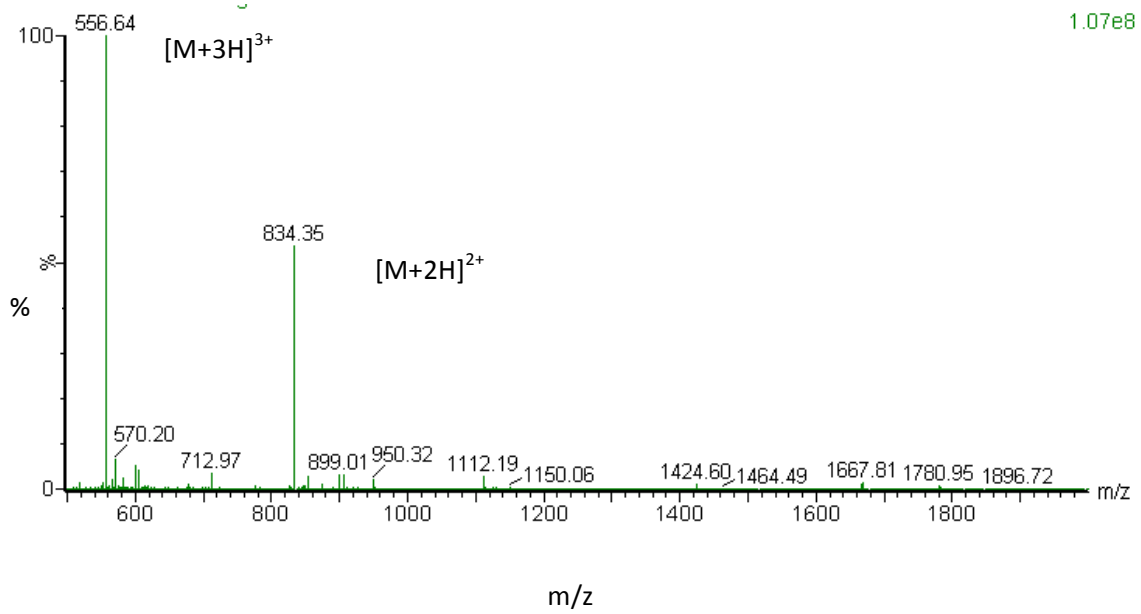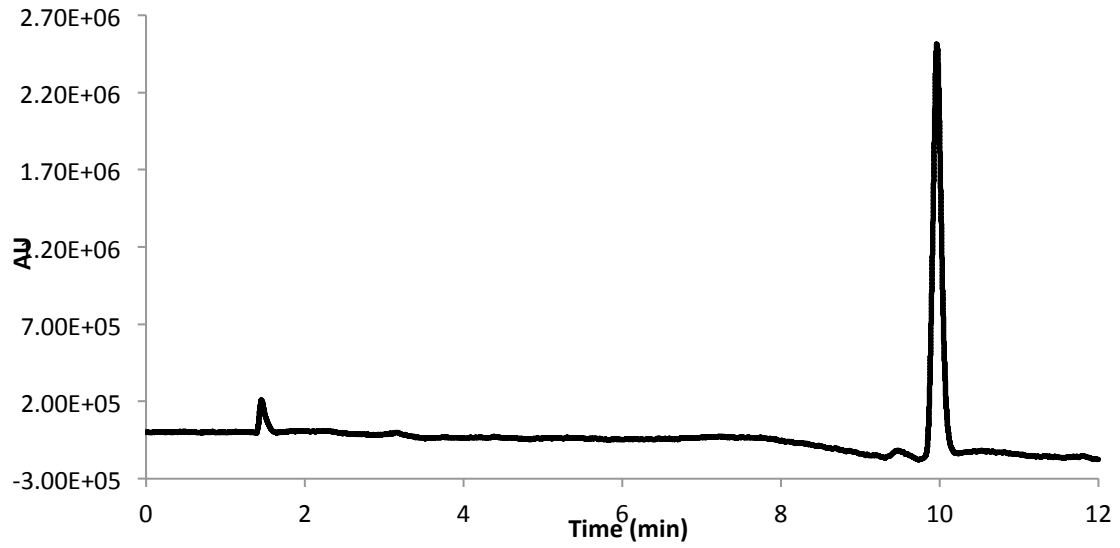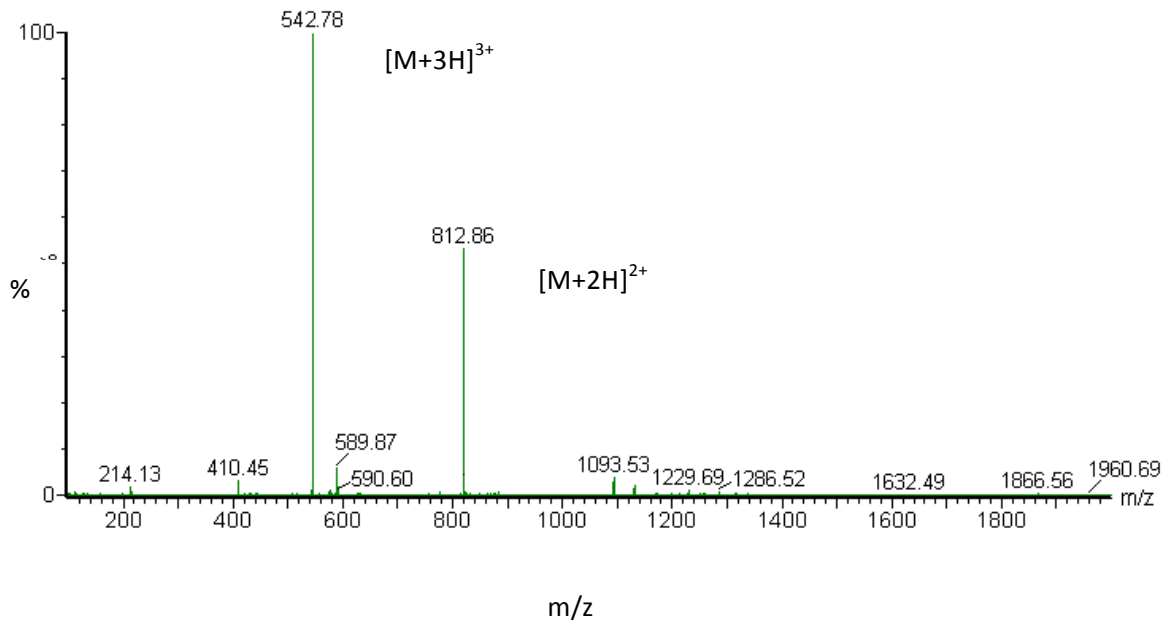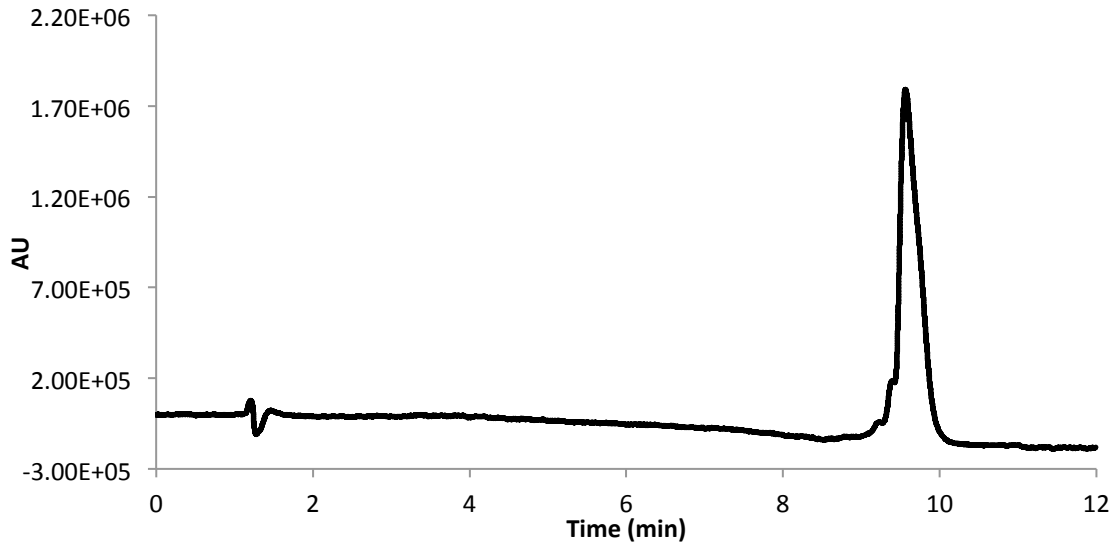
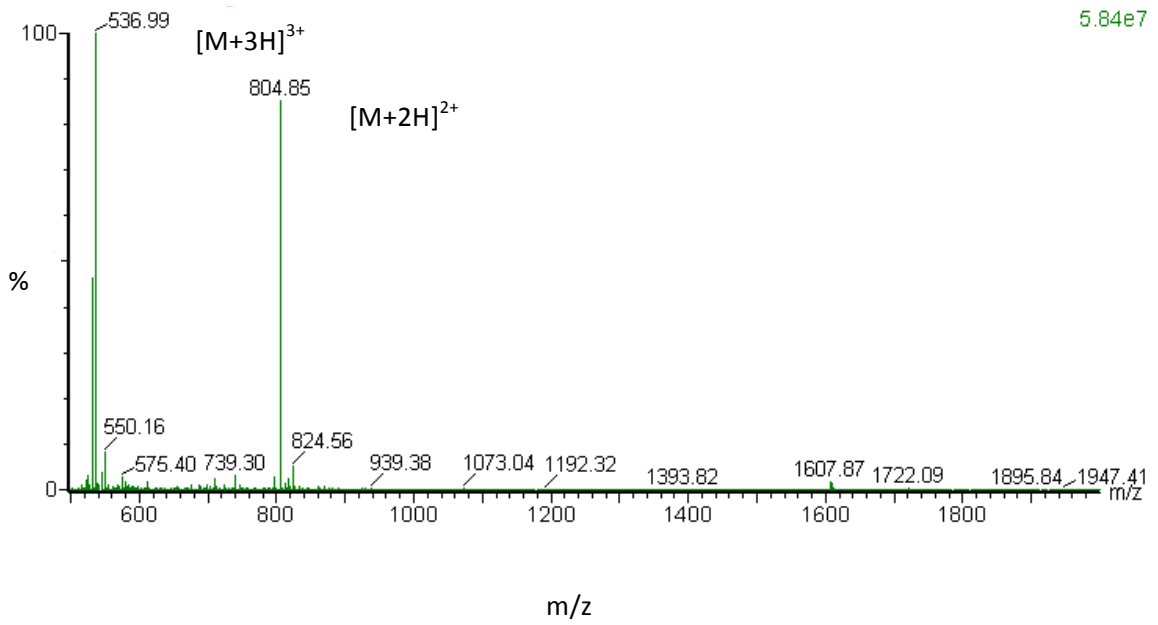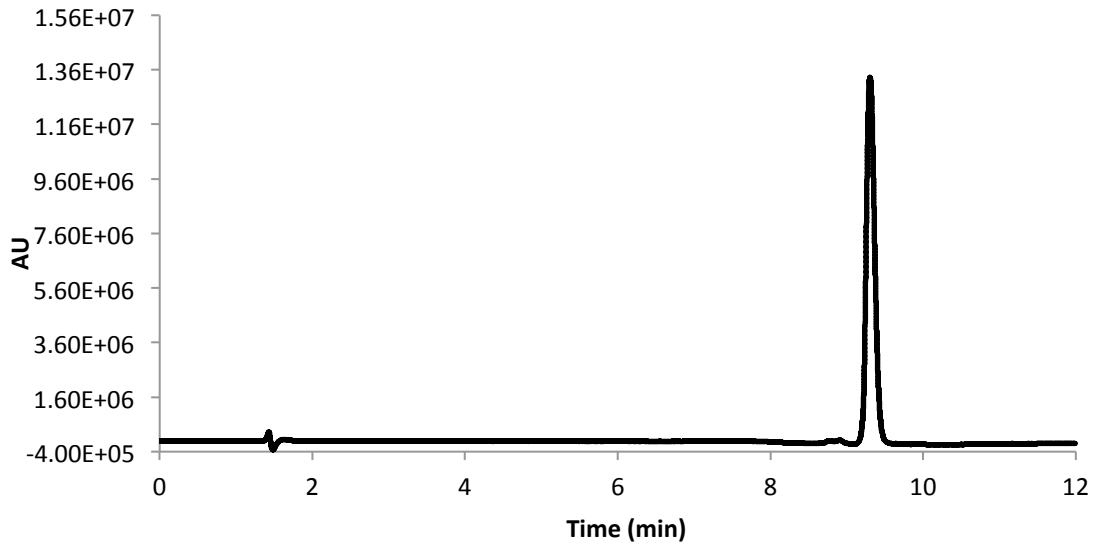Compound 21

Compound 22

Compound 23

Compound 24

Curriculum Vitae

Education/Academic Experience

Masters – Organic Chemistry   Sept. 2015- Aug. 2017
University of Western Ontario
London, ON
- Supervisor: <u>Prof. Len G. Luyt</u>
  Project: Stapled peptides as mimics of the hyaluronan binding domains of the receptor for hyaluronan mediated motility (RHAMM)

Honours Bachelor of Science   Sept. 2010- Apr. 2015
University of Western Ontario
London, ON
- Honors Specialization in Chemistry with Major in Medicinal Cell Biology
- International Exchange to Plymouth University in Plymouth, England (2012-2013)
- 4th Year Thesis Supervisor: <u>Prof. Len G. Luyt</u>,
  Project: Stapled peptides for the stabilization of the receptor for hyaluronan mediated motility

Awards
Dean's Honor List (2013-2015)
Aiming for the Top Tuition Scholarship (2010)

Teaching Experience
Integrated Science 1001X Teachers Assistant   Jan. 2017- Apr. 2017
Organic Chemistry 2213/2223 Teachers Assistant   Sept. 2014- Dec. 2016

Published Abstracts
1. **Rodrigues E**; Peart T; Ma J; Tolg C; Turley E; Luyt L. Stapled peptides as mimics of the hyaluronan binding domains of the receptor for hyaluronan mediated motility (RHAMM). 34th European Peptide Symposium / 8th International Peptide Symposium. *J. Pep. Sci.* 22(52). pp. S192.

Conference Presentations
1. **Rodrigues, E**.; Peart, T.; Tolg, C.; Ma, J.; Turley, E.; Luyt, L.G.; Design and synthesis of hyaluronan:RHAMM interaction inhibitors for cancer therapy. Oncology Research and Education Day. London, ON. June 16th, 2017. (Poster Presentation – Top poster presentation award).
2. **Rodrigues, E**.; Peart, T.; Tolg, C.; Ma, J.; Turley, E.; Luyt, L.G.; Stapled peptides as mimics of the hyaluronan binding domains of the receptor for hyaluronan mediated motility (RHAMM). 100th Canadian Chemistry Conference and Exhibition. Toronto, ON. May 28th- June 1st, 2017. (Oral Presentation).
3. **Rodrigues, E**.; Peart, T.; Tolg, C.; Ma, J.; Turley, E.; Luyt, L.G.; Stapled peptides as mimics of the hyaluronan binding domains of the receptor for hyaluronan mediated motility (RHAMM). Fallona Family Interdisciplinary Showcase. London, ON. January 16th, 2017. (Poster Presentation).
4. **Rodrigues, E**.; Peart, T.; Tolg, C.; Ma, J.; Turley, E.; Luyt, L.G.; Stapled peptides as mimics of the hyaluronan binding domains of the receptor for hyaluronan mediated motility (RHAMM). 34th European Peptide Symposium/8th International Peptide Symposium. Leipzig, Germany. September 4th-9th, 2016. (Poster presentation).

5. **Rodrigues, E**.; Tolg, C.; Turley, E.; Luyt, L.G.; Stapled peptides for the stabilization of the receptor for hyaluronan mediated motility (RHAMM). Fallona Family Interdisciplinary Showcase. London, ON. December 8th, 2015. (Poster Presentation)

6. **Rodrigues, E.;** Hauser-Kawaguchi, A.; Luyt, L.G.; Stapled peptides for the stabilization of the receptor for hyaluronan mediated motility (RHAMM). Southern Ontario Undergraduate Chemistry Conference. Mississauga, ON. March 21st, 2015. (Oral Presentation – 1st Prize Biochemistry Division)

Patents
Patent Provisional Applications
Luyt, LG; Turley, EA; Hauser-Kawaguchi, A; Rodrigues, E. Stapled peptides and uses thereof. WO2016151478. Filed 21Mar2016.